

Elsevier Editorial System(tm) for Journal of
Hydrology
Manuscript Draft

Manuscript Number: HYDROL20966R1

Title: Contributions of human activities to suspended sediment yield during storm events from a small, steep, tropical watershed

Article Type: Research Paper

Keywords: Sediment yield, volcanic islands, land use, storm events, coastal sediment load, American Samoa

Corresponding Author: Mr. Alex Messina, M.S.

Corresponding Author's Institution: San Diego State University

First Author: Alex Messina, M.S.

Order of Authors: Alex Messina, M.S.; Trent W Biggs, Phd

Abstract: Suspended sediment concentrations (SSC) and yields (SSY) were measured during storm and non-storm periods from undisturbed and human-disturbed portions of a small (1.8 km^2), mountainous watershed that drains to a sediment-stressed coral reef. Event-wise SSY (SSYEV) was calculated for 142 storms from measurements of water discharge (Q), turbidity (T), and SSC measured downstream of three key sediment sources: undisturbed forest, an aggregate quarry, and a village. SSC and SSYEV were significantly higher downstream of the quarry during both storm- and non-storm periods. The human-disturbed subwatershed accounted for an average of 71-87% of SSYEV from the total watershed, and has increased loads to the coast by 3.9x over natural background. Specific SSY (tons/area) from the disturbed quarry area was 49x higher than from natural forest compared with 8x higher from the village. The quarry, which covers 1.1% of the total watershed area, contributed 36% of total SSYEV at the outlet. Similar to mountainous watersheds in semi-arid and temperate climates, SSYEV from both the undisturbed and disturbed watersheds correlated closely with maximum event discharge (Q_{\max}), event total precipitation and event total Q, but not with a precipitation erosivity index. Best estimates of annual SSYEV varied from 41-61 tons/yr (45-68 tons/ km^2/yr) from the undisturbed subwatershed, 310-388 tons/yr (350-441 tons/ km^2/yr) from the human-disturbed subwatershed, and 360-439 tons/yr (200-247 tons/ km^2/yr) from the total watershed. Sediment yield was very sensitive to disturbance; only 5.2% of the watershed is disturbed by humans but sediment yield increased significantly (3.9x). While unpaved roads are often identified as a source of sediment in humid forested regions, field observations suggested that most roads in the urban area were paved or stabilized with aggregate. Repeated surface disturbance at the quarry is a key process maintaining high rates of sediment generation. Given the large distance to other sources of building material, aggregate mining and associated sediment disturbance may be a critical sediment source on remote islands in the Pacific and elsewhere. Identification of sediment hotspots like the quarry using rapid, event-wise measures of suspended sediment yield will help efforts to mitigate sediment loads and restore coral reefs.

Response to Reviewers:

Response to Editor's request for "Moderate Revision" of manuscript HYDROL20966, "Contributions of human activities to suspended sediment yield during storm events from a small, steep, tropical watershed"

1) Please don't use abbreviations (e.g., SSY) in the highlights, please expand in full. As you have 2 highlights spare this should be OK.

Done.

Common abbreviations were used to keep under the limit of 85 characters, including spaces. They have been rewritten.

2) L38 (and elsewhere), can you please number all heading, sub-headings etc.? This will enable reviewers to more easily navigate your manuscript when they are reviewing it.

Done.

My mistake leaving these out.

3) L128, rather than have 'questions addressed' it would be preferable to have specific objectives or aims for your study. In the last paragraph of your Introduction can you please explicitly state what your 'aim(s)' or 'objective(s)' or 'hypothesis (hypotheses)' is (are)? That is, specifically use one of these words. While you have a purpose, this is a little broader than having specific aims or objectives. Consider using a bulleted sentence structure to list these. Note the word 'question' is used in the following to generically mean aim / objective / hypothesis. It is common practice to list the aims/objectives at the very end of the last paragraph of the Introduction section.

Note the grammar of such a sentence follows (please pay careful attention to the use of colons and semi-colons):

- (i) question 1 is interesting;
- (ii) question 2 is really interesting; and
- (iii) my Mum thought I should write something about question 3.

Implementing this point makes it much easier for scientists from all language backgrounds to easily understand what you aim to do. This dove-tails into the comment directly below.

Done.

The word "Objectives" has been inserted to describe the numbered items in the last paragraph of the Introduction that summarize the two main objectives of the study.

We feel it is critical to explicitly state the research questions that the paper seeks to answer, as questions ending with a question mark. These questions are explicitly answered later in Results and Discussion, demonstrating that we have learned something about this hydrological system and our hypotheses were confirmed or not. We state the objectives of the data analysis (to quantify and model sediment yield) but more importantly we pose the questions that motivate this analysis, and structure key take-away messages of the paper.

4) Improved structure: once you've explicitly used one the following words to state what your 'aim(s)' or 'objective(s)' or 'hypothesis (hypotheses)' is (are), then, assuming you have objectives, use these objectives to provide structure to your revised MS. For example, let's assume you have three objectives, then use them to structure your Methods section, Results section and Discussion sections, as follows.

1 Introduction

2 Study Site and Materials (have as many sub-headings as needed to introduce all the datasets used, their pre-processing - or maybe this needs to be 2 main headings, noting you might also need a "2 Theoretical Background" section too, in which case this would be heading #3, and all others would increment by 1)

3 Methods

- 3.1 Objective 1 (4-8 words to summarise objective 1)
- 3.2 Objective 2 (4-8 words to summarise objective 2)
- 3.3 Objective 3 (and so on)

4 Results

- 4.1 Objective 1 (same words as 3.1)
- 4.2 Objective 2 (same words as 3.2 and so on)
- 4.3 Objective 3

5 Discussion

- 5.1 Objective 1
- 5.2 Objective 2
- 5.3 Objective 3

6 Conclusion

Currently I'm up to page 16 and given your structure and possible lack of numbered heading, I'm finding it very challenging to know what section of the (rather long) manuscript I'm reading.

Using the aims/objectives at end of your Introduction section to structure the rest of the paper makes it easy to read (and review).

Done.

The manuscript has been significantly shortened, and reorganized following the above template

5) L178, units of annual potential evapotranspiration need to be mm/yr, as you have correctly provided for the mean annual precipitation a few lines earlier.

Done.

6) As the JoH Guide for Authors is currently being updated and does not state the following can you please implement? Can you please provide all Figures in a WORD document with the figure captions directly following each figure? This means a reviewer only has to flick back-n-forth between 2 pages (text and figure).

Done.

The JoH and Elsevier Guide for Authors specifically calls for Figures and Tables to be submitted as separate files, with Figure Captions in separate document. This procedure required a fair bit of time to accomplish using the online submission system.

However, in the interest of making the review process as easy as possible, we have also compiled a new document including all figures, followed by the caption.

7) Plus you may wish to embed your figures and tables (and their captions) into the text directly following the paragraph where they are first mentioned. This will make it even easier for a reviewer. If you don't do this please put

< Figure 1 here please >

< Table 1 here please >

on new lines to highlight to reviewers (and the layout people) where the non-text elements should be located.

Done.

We added these tags in the appropriate places in the manuscript text, in addition to compiling a document with figures and captions, and uploading separately. We did not choose to embed figures in the text.

8) L749, what discharge metrics? It seems there is at least 1 word missing from this sentence.

Revised text:

Similar to other studies the highest correlations with SSY_{EV} at Faga'alu were observed for discharge metrics Qsum and Qmax (Basher et al., 2011; Duvert et al., 2012; Fahey et al., 2003; Hicks, 1990; Rankl, 2004; Rodrigues et al., 2013).

9) The submitted manuscript is long, very long. The PDF I see has 87 pages - that is big bordering on huge. As I've noticed that long manuscripts usually suffer harsh reviews I strongly urge you to seek to reduce the length of the submitted manuscript.

Can you move the Appendices into the Supplementary Material? If you can reduce the PDF that reviewers download to be 45 to 55 pages your manuscript will be much less likely to put reviewers offside from the start.

Appendices have been moved to Supplementary Material. We wanted to include these additional materials for an interested reviewer but they can be moved wherever you think is best. The manuscript text has also been shortened significantly.

This, and EC4, are the reasons I'm requesting moderate revision, as opposed to minor revision, as positively implementing these will take some time, however, it will be worth it as your manuscript will be clearer and much more likely to be viewed favourably by JoH reviewers.

***Highlights (3 to 5 bullet points (maximum 85 characters including spaces per bullet point)**

- 1 • Human disturbance increased suspended sediment yield to Faga'alu Bay by 3.9x
- 2 • Maximum event discharge was a good predictor of storm suspended sediment yield
- 3 • Rapidly developed an empirical suspended sediment yield model for remote watershed
- 4

1 TITLE:

2 Contributions of human activities to suspended sediment yield during storm events

3 from a small, steep, tropical watershed

4 Authors:

5 Messina, A.M.^{a*}, Biggs, T.W.^a

⁶ ^a San Diego State University, Department of Geography, San Diego, CA 92182,

7 amessina@rohan.sdsu.edu, +1-619-594-5437, tbiggs@mail.sdsu.edu, +1-619-594-0902

ABSTRACT

Suspended sediment concentrations (SSC) and yields (SSY) were measured during storm and non-storm periods from undisturbed and human-disturbed portions of a small (1.8 km^2), mountainous watershed that drains to a sediment-stressed coral reef. Event-wise SSY (SSY_{EV}) was calculated for 142 storms from measurements of water discharge (Q), turbidity (T), and suspended sediment concentration (SSC) measured downstream of three key sediment sources: undisturbed forest, an aggregate quarry, and a village. SSC and SSY_{EV} were significantly higher downstream of the quarry during both storm- and non-storm periods. The human-disturbed subwatershed accounted for an average of 71-87% of SSY_{EV} from the total watershed, and has increased loads to the coast by ~~1.7~~ 3.9x over natural background. Specific SSY (tons/area) from the disturbed quarry area was 49x higher than from natural forest compared with 8x higher from the village. The quarry, which covers 1.1% of the total watershed area, contributed 36% of total SSY_{EV} at the outlet. Similar to mountainous watersheds in semi-arid and temperate climates, SSY_{EV} from both the undisturbed and disturbed watersheds correlated closely with maximum event discharge (Q_{max}), event total precipitation and event total Q, but not with a precipitation

23 erosivity index. Best estimates of annual SSY_{EV} varied from 41-61 tons/yr (45-68 tons/km²/yr)
24 from the undisturbed subwatershed, 310-388 tons/yr (350-441 tons/km²/yr) from the human-
25 disturbed subwatershed, and 360-439 tons/yr (200-247 tons/km²/yr) from the total watershed.
26 Sediment yield was very sensitive to disturbance; only 5.2% of the watershed is disturbed by
27 humans but sediment yield increased significantly (3.9x). While unpaved roads are often
28 identified as a source of sediment in humid forested regions, field observations suggested that
29 most roads in the urban area were paved or stabilized with aggregate. Repeated surface
30 disturbance at the quarry is a key process maintaining high rates of sediment generation. Given
31 the large distance to other sources of building material, aggregate mining and associated
32 sediment disturbance may be a critical sediment source on remote islands in the Pacific and
33 elsewhere. Identification of sediment hotspots like the quarry using rapid, event-wise measures
34 of suspended sediment yield will help efforts to mitigate sediment loadloads and restore coral
35 reefs.

36 **Keywords:**

37 Sediment yield, volcanic islands, ~~mountainous catchments~~, land use, storm events, coastal
38 sediment load, American Samoa

39 **1. Introduction**
40 Human activities including deforestation, agriculture, road construction, mining, and
41 urbanization alter the timing, composition, and amount of sediment loads to downstream
42 ecosystems (Syvitski et al., 2005). Increased sediment loads can stress aquatic ecosystems,
43 including coral reefs that occur near the outlets of impacted watersheds. Sediment impacts coral
44 by decreasing light for photosynthesis and increasing sediment accumulation rates (~~Fabrieius~~,

45 | [2005; Storlazzi et al., 2015; West and van Woesik, 2004](#))-(Fabricius, 2005; Storlazzi et al.,
46 | [2015](#)). Anthropogenic sediment disturbance can be particularly high on volcanic islands in the
47 | humid tropics, which have a high potential for erosion due to high rainfall, extreme weather
48 | events, steep slopes, and erodible soils. Sediment yield in densely vegetated watersheds can be
49 | particularly sensitive to land clearing, which alters the fraction of exposed soil more than in
50 | sparsely-vegetated regions. The steep topography and small floodplains on small volcanic islands
51 | further limits sediment storage and the capacity of the watershed to buffer increased hillslope
52 | sediment supply. Such environments characterize many volcanic islands in the south Pacific
53 | where coral reefs are impacted by sediment.

54 | A large proportion of a watershed's sediment yield can originate from disturbed areas that
55 | cover a relatively small fraction of the watershed area. [In the Caribbean](#)-Unpaved roads covering
56 | 0.3-0.9% of the watershed area were the dominant sediment source in disturbed watersheds on
57 | St. John [in the Caribbean](#), and increased sediment yield to the coast by 5-9 times relative to
58 | undisturbed watersheds (Ramos-Scharrón and Macdonald, 2007). In the Pacific Northwest of the
59 | United States, several studies found most road-generated sediment can originate from just a
60 | small fraction of unpaved roads (Gomi et al., 2005; Henderson and Toews, 2001; Megahan et al.,
61 | 2001; Wemple et al., 1996), and heavily used roads could generate 130 times as much sediment
62 | as abandoned roads (Reid and Dunne, 1984). In a watershed disturbed by grazing on Molokai,
63 | Hawaii, less than 5% of the land produces most of the sediment, and only 1% produces
64 | approximately 50% of the sediment (Risk, 2014; Stock et al., 2010), suggesting that management
65 | should focus on identifying, quantifying, and mediating erosion hotspots.

66 | [Management of sediment](#)[Sediment management](#) requires linking land use changes and
67 | mitigation strategies to changes in sediment yields at the watershed outlet (Walling and Collins,

68 2008). A sediment budget quantifies sediment as it moves from key sources like hillslope
69 erosion, channel-bank erosion, and mass movements, to its eventual exit from a watershed
70 (Rapp, 1960). Walling (1999) used a sediment budget to show that sediment yield from
71 watersheds can be insensitive to both land use change and erosion management due to high
72 sediment storage capacity on hillslopes and in the channel. Sediment yield from disturbed areas
73 can be large but may not be important compared to naturally high yields from undisturbed areas.
74 While a full description of all sediment production and transport processes are of scientific
75 interest, the sediment budget needs to be simplified to be used as a management tool (Slaymaker,
76 2003). Most management applications require only that the order of magnitude or the relative
77 importance of process rates be known, so Reid and Dunne (1996) argue a management-focused
78 sediment budget can be developed quickly in situations where the management problem is
79 clearly defined and the management area can be divided into homogenous sub-units.

80 Knowledge of suspended sediment yield (SSY) under both natural and disturbed
81 conditions on most tropical, volcanic islands remains limited, due to the challenges of in situ
82 monitoring in these remote, challenging environments. The limited data has also made it difficult
83 to develop reliable sediment yield models for ungauged watersheds. Existing sediment yield
84 models are often designed for agricultural landscapes and are not well-calibrated to the climatic,
85 topographic, and geologic conditions found on steep, tropical islands. Most readily available
86 models also do not incorporate many of the important processes that generate sediment in steep
87 watersheds, including mass movements (Calhoun and Fletcher, 1999; Ramos-Scharrón and
88 Macdonald, 2005; Sadeghi et al., 2007). Developing models that predict SSY_{EV} from small,
89 mountainous catchments is a significant contribution for establishing baselines for change-

90 detection for sediment mitigation projects, and can also further improve models applied at the
91 regional scale (Duvert et al., 2012).

92 Traditional approaches to quantifying human impact on sediment budgets, including
93 comparison of total annual yields (Fahey et al., 2003) and sediment rating curves (Asselman,
94 2000; Walling, 1977), are complicated by interannual climatic variability and hysteresis in the
95 discharge-concentration relationship. Sediment yield can be highly variable over various time
96 scales, even under natural conditions. At geologic time scales, if an undisturbed watershed is not
97 in a steady-state condition, sediment yields may decrease over time as it reaches equilibrium, or
98 the sediment contributions from different subwatersheds may change with time (Ferrier et al.,
99 2013; Perroy et al., 2012). At decadal scales, cyclical climatic variability like El Nino-Southern
100 Oscillation (ENSO) events or Pacific Decadal Oscillation (PDO) patterns can significantly alter
101 sediment yield from undisturbed watersheds (Wulf et al., 2012).

102 As an alternative to comparing annual sediment loads, SSY generated by storm events of
103 the same magnitude can be compared to assess the contribution of individual subwatersheds to
104 total SSY (Zimmermann et al., 2012), determine changes in SSY from the same watershed over
105 time (Bonta, 2000), and compare the responses of different watersheds to various precipitation or
106 discharge variables ("storm metrics") (Basher et al., 2011; Duvert et al., 2012; Fahey et al., 2003;
107 Hicks, 1990). Event-wise SSY (SSY_{EV}) may correlate with storm metrics such as total
108 precipitation, the Erosivity Index (Kinnell, 2013), or total discharge, but the best correlation has
109 consistently been found with maximum event discharge (Qmax). Several researchers have
110 hypothesized that Qmax integrates the hydrological response of a watershed, making it a good
111 predictor of SSY_{EV} in diverse environments (Duvert et al., 2012; Rankl, 2004). High correlation
112 between SSY_{EV} and Qmax has been found in semi-arid, temperate, and sub-humid watersheds in

113 Wyoming (Rankl, 2004), Mexico, Italy, France (Duvert et al., 2012), and New Zealand (Basher
114 et al., 2011; Hicks, 1990), but this approach has not been attempted for steep, tropical watersheds
115 on volcanic islands.

116 The anthropogenic impact on SSY_{EV} may vary by storm magnitude, as documented in
117 Pacific Northwest forests (Lewis et al., 2001). As storm magnitude increases, water yield and/or
118 SSY_{EV} from natural areas may increase relative to human-disturbed areas, diminishing
119 anthropogenic impact relative to the natural baseline. While large storms account for most SSY
120 under undisturbed conditions, human-disturbed areas may show the largest disturbance,
121 expressed as a percentage increase above the natural background, for smaller storms (Lewis et
122 al., 2001). The disturbance ratio (DR) may be highest for small storms, when background SSY_{EV}
123 from the undisturbed forest is low and erodible sediment from disturbed surfaces is the dominant
124 source. For large storms, mass movements and bank erosion may contribute to naturally high
125 SSY_{EV} from undisturbed watersheds, increasing the background and reducing the DR for large
126 events.

127 This study uses in situ measurements of precipitation (P), stream discharge (Q), turbidity
128 (T) and suspended sediment concentration (SSC) to accomplish three objectives: Objective 1
129 Quantify suspended sediment yield concentrations (SSC) and yields (SSY) from undisturbed and
130 human-disturbed portions of a small watershed in the south Pacific ~~and 2) develop an empirical~~
131 ~~model of during~~ ~~storm-generated suspended sediment yield and non-storm periods.~~ The research
132 questions addressed under this objective include: How much has human disturbance increased
133 suspended sediment yield to the coast? during storm events? What human activities dominate the
134 anthropogenic contribution to ~~the suspended sediment load?~~ suspended sediment yield? How do
135 concentrations vary between storm and non-storm periods? Objective 2) Develop an empirical

136 model of SSY during storm events (SSY_{EV}). This objective will answer the questions: Which
137 storm metric is the best predictor of ~~storm event suspended sediment yield (SSY_{EV})~~:SSY_{EV}: total
138 event precipitation, Erosivity Index, total event discharge, or maximum event discharge? How do

139 sediment contributions from undisturbed areas and human-disturbed areas vary with storm size?

140 Objective 3) Estimate annual sediment yields and compare with other volcanic tropical islands.

141 This objective will use the results from Objective 2 to model annual sediment load from the
142 study watersheds, for comparison with other literature on volcanic tropical islands and disturbed
143 watersheds.

144 2. Study Area

145 The study watershed, Faga'alu, is located on Tutuila (14S, 170W), ~~the largest~~
146 ~~island in the Territory of~~ American Samoa (~~140 km²~~). ~~Like many volcanic islands in the Pacific,~~

147 Tutuila has steep, heavily forested mountains with villages and roads mostly confined to the flat
148 areas near the coast. The main stream in Faga'alu ~~runs the length of the watershed (~3 km)~~, and

149 drains an area of 1.78 km² into Faga'alu Bay (area draining to FG3 in Figure 1). ~~The main~~
150 ~~watershed includes Matafao Mountain, the highest point on Tutuila (653 m)~~. The mean slope of
151 the main Faga'alu watershed is 0.53 m/m and total relief is 653 m. The administrative boundary

152 of Faga'alu includes the watersheds of the main stream and several small ephemeral streams that
153 drain directly to the bay (0.63 km²) (grey dotted boundary in Figure 1). The coral reef in

154 Faga'alu Bay is highly degraded by sediment (Fenner et al., 2008). ~~Faga'alu watershed was~~
155 ~~identified by local environmental management agencies in the American Samoa Coral Reef~~
156 ~~Advisory Group (CRAG) as a heavily impacted watershed, and in August 2012, and Faga'alu~~
157 watershed was selected by the US Coral Reef Task Force (USCRTF) as a Priority Watershed for
158 conservation and remediation efforts (Holst-Rice et al., 2015).

159 <Figure 1 here please>

160 Faga'alu occurs on intracaldera Pago Volcanics where the K-Ar age for a sample in the
161 watershed is formed about 1.20 Mya (McDougall, 1985). Soil types in the steep uplands are
162 Fagasa family lithic hapludolls with rock outcrops in the steep uplands, and soil types in the
163 lowlands are Aua Leafu complex(15%) with well-drained Lithic Hapludolls ranging from silty
164 clay to clay loams 20-150 cm deep (Nakamura, 1984). In the uplands, an estimated 50% of soil
165 cover is Fagasa family soils which are moderately deep and well drained silty clay (50-150 cm)
166 overlying weathered igneous bedrock. An estimated 20% of soil cover is lithic hapludolls which
167 are well drained but shallower (10-50 cm) than Fagasa family soil, and composed of silty clay
168 and clay loam. The remaining 15% of soil in the uplands is rock outcrops. The lowlands are
169 composed of urban surfaces and a mix of Aua and Leafu soils, composed of colluvium and
170 alluvium derived from the weathered igneous rock and soil from the steep uplands. Aua soils in
171 the lowlands are deep (>150 cm), well drained accumulations of very stony silty clay loam with
172 only moderate runoff and erosion potential. Leafu soils in the lowlands are very deep (>150 cm),
173 poorly drained silty clay to fine sandy loam that are typically along streams and valley bottoms
174 where the high water table is typically 90-150 cm deep. Soils in the lowlands include a mix of
175 deep (>150 cm), well drained very stony silty clay loams, and poorly drained silty clay to fine
176 sandy loam along streams and valley bottoms.

177 2.1 Climate

178 Precipitation on Tutuila is caused by several mechanisms including cyclones and tropical
179 depressions, isolated thunderstorms, and orographic uplifting of trade wind squalls over the high
180 (300-600 m), mountainous ridge that runs the length of the island. The ridge runs parallel to the
181 predominant wind direction, and does not cause a significant windward/leeward rainfall gradient

182 like many other Pacific Islands (Ferrier et al., 2013; Menking et al., 2013). Average annual
183 specific discharge ($\text{m}^3/\text{yr}/\text{km}^2$) shows little spatial variation across the island, irrespective of
184 watershed location or orientation (Dames & Moore, 1981). Precipitation increases with
185 elevation, from an average 2,380 mm/yr at the shoreline to 6,350 mm/yr at the highest elevation
186 on the island, averaging 3,800 mm/yr over the island from 1903 to 1973 (Eyre, 1989; Izuka et al.,
187 2005). In Faga'alu watershed, rainfall records show average annual precipitation is 6,350 mm at
188 Matafao Mtn. Annual precipitation in Faga'alu watershed is 6,350 mm at Matafao Mtn. (653 m
189 m.a.s.l), 5,280 mm at Matafao Reservoir (249 m m.a.s.l.) and about 3,800 mm on the coastal
190 plain (Craig, 2009; Dames & Moore, 1981; Perreault, 2010; Tonkin & Taylor International Ltd.,
191 1989; Wong, 1996). Mean annual potential evapotranspiration follows the opposite trend,
192 varying from 890 mm at high elevation to 1,150 mm at sea level (Izuka et al., 2005). Tropical
193 cyclones are erratic but occurred on average every 1–13 years from 1981–2014 (Craig, 2009) and
194 bring intense rainfall, flooding, landslides, and high sediment yield (Buchanan Banks, 1979).

195 There are two subtle rainfall seasons: a drier winter season, from June through September
196 that accounts for 25% of annual precipitation and a wetter summer season, from October through
197 May (Izuka et al., 2005). During the drier winter season, the island is influenced by relatively
198 stronger, predominantly east to southeast trade winds, lower temperatures, lower humidity and
199 lower total rainfall. During the wetter summer season the Inter-Tropical Convergence Zone
200 (ITCZ) moves over the region, causing light to moderate Northerly winds, higher temperatures,
201 higher humidity, and higher total rainfall. While total rainfall is lower in the drier tradewind
202 season, large storm events are still observed. Analysis of 212 peak discharges at 11 continuous
203 record gaging sites 1959–1990 showed 65% of annual peak flows occurred during the wet season
204 and 35% of annual peak flows occurred during the drier Tradewind season (Wong, 1996).

205 ~~Analysis of mean monthly rainfall data for the period 1971–2000 showed that 75% of~~
206 ~~precipitation occurred in the wet season, which includes 67% of the year (October–May), and~~
207 ~~25% occurred in the dry season, which covers 33% of the year (June–September) (Perreault,~~
208 ~~2010 (Perreault, 2010); data from USGS rain gauges and Parameter-elevation Relationships on~~
209 ~~Independent Slopes Model (PRISM) Climate Group (Daly et al., 2008)). While total rainfall is~~
210 ~~lower in the drier season, large storm events are still observed. At 11 sites around the island, 35%~~
211 ~~of annual peak flows occurred during the drier season over 1959–1990 (Wong, 1996).~~

212 2.2 Land Cover and Land Use

213 2.2.1. Vegetation, agriculture, and urban areas

214 The predominant land cover in Faga'alu watershed is undisturbed vegetation (94.8%),
215 including forest (85.7%) and scrub/shrub (9.0%) on the steep hillsides (Table 1),~~based on a 1~~
~~m² resolution land cover map from NOAA's Ocean Service and Coastal Services Center~~
~~(2010). The upper watershed, draining to FG1 in Figure 1, is dominated by undisturbed~~
216 ~~rainforest on steep hillslopes. The lower subwatershed, draining areas between FG1 and FG3 in~~
217 ~~Figure 1, has steep vegetated hillslopes and a relatively small flat area in the valley bottom that is~~
218 ~~urbanized. This settlement pattern is typical in the South Pacific and other volcanic islands,~~
219 ~~where their small size and steep topography constrain development to valley bottoms near the~~
220 ~~coast (Bégin et al., 2014). Compared to other watersheds on Tutuila, a relatively large portion of~~
221 ~~Faga'alu watershed is urbanized (3.2% "High Intensity Developed" in Table 1), due to large areas~~
222 ~~of impervious surface associated with the hospital and the numerous residences and businesses.~~
223 ~~(3.2% of the watershed area "High Intensity Developed" in Table 1). A small portion of the~~
224 ~~watershed (0.9%) is developed open space, which includes landscaped lawns and parks. In~~
225 ~~addition to some small household gardens there are several small agricultural areas of banana~~

228 and taro on the steep hillsides. These agricultural plots were classified as grassland (0.2% GA,
229 Table 1) due to the high fractional grass cover in the plots. ~~Farmers of these plots receive~~
230 ~~technical assistance from the Natural Resource Conservation Service (NRCS) to mitigate~~
231 ~~erosion.~~ There are several small footpaths and unpaved driveways in the village, but most
232 unpaved roads are stabilized with compacted gravel and do not appear to be a major contributor
233 of sediment (Horsley-Witten, 2012). ~~Longitudinal sampling of Faga'alu stream during low flow~~
234 ~~conditions in 2011 showed significantly increased turbidity downstream of a bridge construction~~
235 ~~site on the village road approximately 200 m downstream of FG2 (Curtis et al., 2011).~~
236 ~~Construction of the bridge was completed in March 2012 and no longer increases turbidity.~~
237 <Table 1 here please>

238 2.2.2 Aggregate quarry and reservoirs

239 An open-pit aggregate quarry covers 1.6 ha and accounts for ~~the majority~~nearly all of the
240 bare land, ~~which covers~~ (1.1% of the Faga'alu watershed) (Table 1). The quarry has been in
241 continuous operation since the 1960's ~~by advancing into the steep hillside to quarry the~~
242 ~~underlying basalt formation~~ (Latinis et al., 1996). ~~The overburden of soil and weathered rock~~
243 ~~was either piled up on site where it was eroded by storms, or was manually rinsed from crushed~~
244 ~~aggregate.~~ With few sediment runoff controls in place, sediment ~~washas been~~ discharged directly
245 to Faga'alu stream. In 2011, the quarry operators installed some sediment runoff management
246 practices such as silt fences and small settling ponds (Horsley-Witten, 2011) but they were
247 unmaintained and inadequate to control the large amount of sediment mobilized during storm
248 events (Horsley-Witten, 2012). During the study period (2012-2014), additional sediment control
249 measures were installed and some large piles of overburden were ~~naturally~~ overgrown by
250 vegetation (Figure 2), altering the sediment availability. In late 2014, large sediment retention

251 ponds were installed to mitigate sediment runoff ~~and work is underway to document the~~
252 ~~reduction in sediment loading (Messina and Biggs, forthcoming, but these mitigation activities~~
253 ~~happened after the sample collection reported here.~~ See Holst-Rice et al. (2015) for a full
254 description of sediment mitigation efforts at the quarry~~).~~
255 <Figure 2 here please>

256 Three water impoundment structures were built in the early 20th century in the upper part
257 of the watershed for drinking water supply and hydropower ~~but only the highest, Matafao~~
258 ~~Reservoir, was ever connected to the municipal water system and has since fallen out of use~~
259 ~~(Tonkin & Taylor International Ltd., 1989) (Figure 1). The dam at point FG1 has filled with~~
260 ~~bedload sediment and flows over the spillway even at the lowest flows, but none are in use and~~
261 ~~the one at FG1 is filled with sediment.~~ We assume the other reservoirs are similarly filled with
262 coarse sediment and are not currently retaining fine suspended sediment. A full description of
263 stream impoundments is in Appendix 4A.

264 **3. Methods**

265 The equations used to accomplish Objectives 1-3 are described in sections 3.1-3.3, and
266 the field methods to measure precipitation, discharge, SSC and SSY are described in section 3.4.

267 **3.1 Objective 1: Compare SSC and SSY_{EV} for disturbed and undisturbed subwatersheds**

268 Stream discharge (Q) and suspended sediment yield concentrations (SSC) and yields
269 (SSY) in Faga'alu stream was ~~were~~ measured during both storm and interstorm periods at three
270 sampling points that drain key ~~define~~ three subwatersheds with different land covers ~~we~~
271 ~~hypothesized would have different SSY: FG1 drains undisturbed forest in~~ The UPPER
272 subwatershed ~~(watershed boundary to FG1), FG2~~ drains undisturbed forest and ~~the quarry is~~

273 sampled at point FG1; the LOWER_QUARRY subwatershed (is sampled at FG2 and includes
274 the forest and quarry between FG1 and FG2), and FG3; the LOWER_VILLAGE subwatershed is
275 sampled at FG3 and drains undisturbed forest and the village in the LOWER_VILLAGE
276 subwatershed (between FG2 and FG3) (Figure 1; Table 1). FG3 is also the watershed outlet for
277 the TOTAL watershed.

278 *Calculating suspended sediment yield from 3.1.1. Calculation of SSY_{EV}*

279 SSY during individual storm events (SSY_{EV})

280 SSY_{EV} at FG1, FG2, and FG3 were calculated for each sample location by integrating
281 continuous estimates of SSY, calculated from measured or modeled water discharge (Q) and
282 measured or modeled suspended sediment concentration (SSC) (Duvert et al., 2012):

$$SSY_{EV} = k \int_{t=0}^T Q(t) * SSC(t) * dt \quad \text{Equation 1}$$

where SSY_{EV} is suspended sediment yield (tons) for an event from t=0 at storm start to T=storm end, SSC is suspended sediment concentration (mg/L), and Q is water discharge (L/sec), and k converts from mg to tons (10⁻⁶).

283 Storm events can be defined by precipitation (Hicks, 1990) or discharge parameters
284 (Duvert et al., 2012), and the method used to identify storm events on the hydrograph can
285 significantly influence the analysis of SSY_{EV} (Gellis, 2013). Dunne and Leopold (1978) assert
286 that all hydrograph separation schemes are arbitrary and usually have little to do with the
287 processes that generate storm flow, but if a consistent method is used then at least the results of
288 different analyses can be compared. Graphical techniques may be implemented to separate the
289 hydrograph into baseflow and quickflow, using the start and end of quickflow as the start and
290 end of the storm event (Dunne and Leopold, 1978; Perreault, 2010). Storms can also be filtered

from the analysis by using various criteria such as minimum storm duration, time between discharge peaks, minimum peak discharge, or more complex schemes using statistical distributions of flow percentiles (Gellis, 2013; Lewis et al., 2001). More complex signal processing methods can also be used, including finding the inflection point of the second derivative of the hydrograph to determine the end of the storm event. However, complex events occur where subsequent precipitation generates stormflow before the stream has returned to baseflow. In these cases, the storm definition scheme can significantly affect the analysis of storm sediment yields by separating or combining multiple hydrograph peaks. Due to the high number of storm events and the prevalence of complex storm events recorded at the study site, an automated approach that robustly separated complex events was desirable. The storm definition approach used in this study performed baseflow separation with Due to the large number of storm events and the prevalence of complex storm events recorded at the study site, we used a digital filter signal processing technique (Nathan and McMahon, 1990) embedded in the R-statistical package EcoHydRology (Fuka et al., 2014). Spurious events were sometimes identified due to instrument noise, so only events with quickflow for at least one hour and peak flow greater than 10% of baseflow were included in the analysis. This approach was easily automated for application to a large number of events, and adequately separated complex storm events with multiple hydrograph peaks (See Appendix 3(See Appendix C for example).

3.1.2. SSY from disturbed and undisturbed portions of subwatersheds

Land cover in the LOWER subwatersheds includes both undisturbed and human-disturbed surfaces. SSY_{EV} from disturbed areas only was estimated as:

$$SSY_{EV_distrb} = SSY_{EV_subws} - (sSSY_{EV_UPPER} * Area_{undist}) \quad \text{Equation 3}$$

where SSY_{EV_distrb} is SSY_{EV} from disturbed areas only (tons), SSY_{EV_subws} is SSY_{EV} (tons) measured from the LOWER subwatershed (e.g. SSY_{EV_FG3}- SSY_{EV_FG2}), $sSSY_{EV_UPPER}$ is specific SSY_{EV} (tons/km²) from the UPPER subwatershed (SSY_{EV_FG1}), and $Area_{undist}$ is the area of undisturbed forest in the LOWER subwatershed (km²). Similar calculations were made for the LOWER_QUARRY and LOWER_VILLAGE subwatersheds to isolate the contributions from the disturbed quarry and village.

312 The disturbance ratio (DR) is the ratio of SSY_{EV} under current conditions to SSY_{EV} under
313 pre-disturbance conditions:

$$DR = \frac{SSY_{EV_subw}}{A_{subw} * sSSY_{EV_UPPER}} \quad \text{Equation 4}$$

where A_{subw} is the area of the subwatershed.

314 Both Equations 3 and 4 assume that sSSY_{EV} from forested areas in the LOWER subwatershed
315 equals sSSY_{EV} from the undisturbed UPPER watershed.

3.1.3. Relationship of sediment load to sediment budget

317 We use the measured sediment yield at three locations to quantify the in-stream
318 suspended sediment budget. Other components of sediment budgets include channel erosion and
319 or channel and floodplain deposition (Walling and Collins, 2008). Sediment storage and
320 remobilization can significantly complicate the interpretation of in-stream loads, and complicate
321 the identification of a land use signal. In Faga'alu, the channel bed is predominantly large
322 volcanic cobbles and coarse gravel, with no significant deposits of fine sediment. Upstream of
323 the village, the valley is very narrow with no floodplain. In the downstream reaches of the lower
324 watershed, where fines might deposit in the floodplain, the channel has been stabilized with
325 cobble reinforced by fencing, so overbank flows and sediment deposition on the floodplain are
326 not observed. We therefore assume that channel erosion and channel and floodplain deposition

327 are insignificant components of the sediment budget, so the measured sediment yields at the
328 three locations reflect differences in hillslope sediment supply. Minimal sediment storage also
329 reduces the lag time between landscape disturbance and observation of sediment at the watershed
330 outlet.

331 **3.2 Objective 2: Modeling SSY_{EV} with storm metrics**

332 The relationship between SSY_{EV} and storm metrics can be modelled by a power law
333 function:

$$SSY_{EV} = \alpha X^{\beta} \quad \text{Equation 5}$$

where X is a storm metric, and the regression coefficients α and β are obtained by ordinary least squares regression on the logarithms of SSY_{EV} and X (Basher et al., 2011; Duvert et al., 2012; Hicks, 1990). Model fits for each storm metric were compared using coefficients of determination (r^2) and Root Mean Square Error (RMSE). The correlation between storm metrics (X) and SSY_{EV} was also quantified using both parametric (Pearson) and non-parametric (Spearman) correlation coefficients.

Four storm metrics were tested as predictors of SSY_{EV} : total event precipitation (Psum), event Erosivity Index (EI30) (Hicks, 1990; Kinnell, 2013), total event water discharge (Qsum), and maximum event water discharge (Qmax) (Duvert et al., 2012; Rodrigues et al., 2013). SSY_{EV} and the discharge metrics (Qsum and Qmax) were normalized by watershed area to compare different sized subwatersheds.

334 The regression coefficients (α and β) for the UPPER and TOTAL watersheds were tested
335 for statistically significant differences using Analysis of Covariance (ANCOVA) (Lewis et al.,
336 2001). A higher intercept (α) for the human-disturbed watershed indicates higher sediment yield
337 for the same size storm event, compared to sediment yield from the undisturbed watershed. A

338 difference in slope (β) would indicate the relative sediment contributions from the subwatersheds
339 change with increasing storm size.

340 3.3. Objective 3: Estimation of annual SSY

341 Annual estimates of SSY and sSSY were estimated to compare Faga'alu with other
342 watersheds reported in the literature. A continuous annual time-series of SSY was not possible at
343 the study site due to the discontinuous field campaigns and failure of or damage to the
344 instruments during some months. Continuous records of P and Q were available for 2014, so the
345 Psum-SSY_{EV} and Qmax-SSY_{EV} models (Equation 5) were used to predict SSY_{EV} for all storms
346 in 2014 (Basher et al., 1997). Construction of sediment mitigation structures at the quarry began
347 in October 2014, greatly reducing SSY_{EV} from the LOWER QUARRY subwatershed
348 (unpublished data), so the Qmax-SSY_{EV} relationship developed prior to the mitigation was used
349 to calculate the annual pre-mitigation sediment yield. For storms missing Qmax data at FG3,
350 Qmax was predicted from a linear regression between Qmax at FG1 and Qmax at FG3 for the
351 study period ($R^2 = 0.88$).

352 Annual SSY and sSSY were also estimated by multiplying SSY_{EV} from measured storms
353 by the ratio of annual storm precipitation (P_{EVann}) to the precipitation measured during storms
354 where SSY_{EV} was measured (P_{EVmeas}):

$$SSY_{ann} = SSY_{EV_meas} * \frac{P_{EVann}}{P_{EVmeas}} \quad \text{Equation 6}$$

where SSY_{ann} is estimated annual SSY from storms, SSY_{EV_meas} is SSY_{EV} from sampled storms (all, Tables 2 and 4), P_{EVmeas} is precipitation measured during the sampled storms, and P_{EVann} is the precipitation during all storm events defined by the hydrograph separation.

355 Equation 6 assumes that the sediment yield per mm of storm precipitation is constant
356 over the year, and that the size distribution of storms has no effect on SSY_{EV}, though there is
357 some evidence that SSY_{EV} increases exponentially with storm size (Lewis et al., 2001; Rankl,
358 2004). Equation 6 also ignores sediment yield during non-storm periods, which is justified by the
359 low SSC and Q observed between storms.

360 **3.4. Field Data Collection Methods**

361 Data on precipitation (P), water discharge (Q), suspended sediment concentration (SSC)
362 and turbidity (T) were collected during four field campaigns: January-March~~5~~ 2012, February-
363 July 2013, January-March 2014, and October-December 2014, and several intervening periods of
364 unattended monitoring by instruments with data loggers. Field sampling campaigns were
365 scheduled to coincide with the period of most frequent storms in the November-May wet season,
366 though large storms were sampled throughout the year.

367 Precipitation

368 **3.4.1. Precipitation (P)**

369 P was measured at three locations in Faga'alu watershed using Rainwise RAINEW
370 tipping-bucket rain gages (RG1 and RG2) and a Vantage Pro Weather Station (Wx) (Figure 1).

371 Data at RG2 was only recorded January-March, 2012, ~~to determine a relationship between~~
372 ~~elevation and precipitation in the LOWER subwatershed. While previous data suggest that~~
373 ~~precipitation increases with elevation (Izuka et al., 2005), here we do not calculate watershed-~~
374 ~~mean precipitation, and instead use precipitation depth at RG1 to indicate the depth of rainfall~~
375 ~~during a storm event. Most sheetwash and rill erosion, which depends on rainfall intensity and~~
376 ~~erosivity, occurred at the quarry, near the location of RG1. Rainfall data from RG1 is therefore~~

377 most representative of rainfall at the quarry, to determine a relationship between elevation and
378 precipitation in the LOWER subwatershed. The total event precipitation (Psum) and event
379 Erosivity Index (EI30) were calculated using data from RG1, with data gaps filled by 15
380 min minute interval precipitation data from Wx.

381 3.4.2. Water Discharge (Q)

382 Stream gaging sites were chosen to take advantage of an existing control structure (FG1)
383 and a stabilized stream cross section (FG3) (Duvert et al, 2010). At FG1 and FG3, Q was
384 calculated from stream stage measurements taken at 15 minute intervals using HOBO pressure
385 transducers (PT) and a stage-Q rating curve calibrated to manual Q measurements. Q was
386 measured manually in the field under both baseflow and stormflow conditions by the area-
387 velocity method (AV) using a Marsh-McBirney flowmeter ~~to measure flow velocity and channel~~
388 ~~surveys of cross-sectional area~~ (Harrelson et al., 1994; Turnipseed and Sauer, 2010). The
389 highest PTs recorded ~~stage was higher than stages that exceeded~~ the highest stage with manually-
390 measured Q, so the stage-Q rating at FG3 was extrapolated using Manning's equation, calibrating
391 Manning's n (0.067) to the Q measurements. At FG1, the flow control structure is a masonry
392 ~~egee~~ spillway crest of a defunct stream capture. ~~Since~~ The highest stage recorded ~~stage by the PT~~
393 (120 cm) ~~was higher than exceeded~~ the highest stage with manually-measured Q (17 cm), and the
394 flow structure did not meet the assumptions for using Manning's equation to predict flow, so the
395 HEC-RAS model was used to create the stage-Q relationship (Brunner, 2010). See Appendix 2B
396 for details of the cross sections and rating curves.

397 A suitable site for stream gaging was not present at the outlet of the LOWER_QUARRY
398 subwatershed (FG2), so water discharge at FG2 was calculated as the product of the specific
399 water discharge from FG1 ($m^3/0.9\ km^2$) and the watershed area draining to FG2 ($1.17\ km^2$). This

400 assumes that specific water discharge from the subwatershed above FG2 is similar to above FG1.
401 Discharge may be higher from the quarry surface, which represents 5.7% of the
402 LOWER_QUARRY subwatershed, so Q_5 and ~~thus SSY from the quarry at FG2~~ are a
403 conservative, lower bound ~~estimateestimates~~, particularly during small events when specific
404 discharge from the UPPER watershed was small relative to specific discharge from the quarry.
405 The quarry surface is continually being disturbed, sometimes with large pits excavated and
406 refilled in the course of weeks, as well as intentional water control structures implemented over
407 time. Given the changes in the contributing area of the quarry, estimates of water yield from the
408 quarry were uncertain, so we assumed a uniform specific discharge for the whole
409 LOWER_QUARRY subwatershed.

410 *Continuous3.4.3. Suspended Sediment Concentration*
411 *Continuous-(SSC)*
412 *SSC was estimated at 15 minute intervals ~~was estimated~~ from either 1) linear
413 interpolation of SSC measured from water samples, ~~and/or~~ 2) ~~15 min interval~~-turbidity data (T)
414 recorded at 15 minute intervals and a T-SSC relationship calibrated to stream water samples
415 collected over a range of Q and SSC. Stream water samples were collected by grab sampling
416 with 500 mL HDPE bottles at FG1, FG2, and FG3. At FG2, water samples were also collected at
417 30 min intervals during storm events by an ISCO 3700 Autosampler triggered by a stage height
418 sensor. Samples were analyzed for SSC on-island using gravimetric methods (Gray, 2014; Gray
419 et al., 2000). Water samples were vacuum filtered on pre-weighed 47mm diameter, 0.7 um
420 Millipore AP40 glass fiber filters, oven dried at 100 C for one hour, cooled and weighed to
421 determine SSC (mg/L).*

422 Interpolation of SSC values from grab samples ~~could only be~~ was performed if at least
423 three stream water samples were collected during a storm event (Nearing et al., 2007), and if an
424 SSC sample was collected within 30 minutes of peak Q. SSC was assumed to be zero at the
425 beginning and end of each storm if no grab sample data was available for those times (Lewis et
426 al., 2001).

427 Turbidity (T) was measured at FG1 and FG3 using three types of turbidimeters: 1)
428 Greenspan TS3000 (TS), 2) YSI 600OMS with 6136 turbidity probe (YSI), and 3) Campbell
429 Scientific OBS500 (OBS). All turbidimeters were permanently installed in protective PVC
430 housings near the streambed where the turbidity probe would be submerged at all flow
431 conditions, with the turbidity probe oriented downstream. Despite regular maintenance, debris
432 fouling during storm and baseflows was common and caused data loss during several storm
433 events (Lewis et al., 2001).

434 The T-SSC relationship can be unique to each region, stream, instrument or even each
435 storm event (Lewis et al., 2001), and can be influenced by water color, dissolved solids and
436 organic matter, temperature, and the shape, size, and composition of sediment. However, T has
437 proved to be a robust surrogate measure of SSC in streams (Gippel, 1995), and is most accurate
438 when a unique T-SSC relationship is developed for each instrument separately, using in situ grab
439 samples under storm conditions (Lewis, 1996). A unique T-SSC relationship was developed for
440 each turbidimeter, at each location, using T data and SSC samples from storm periods only (r^2
441 values 0.79-0.99). See Appendix [4D](#) for details on the T-SSC relationships.

442 [3.4.4. Cumulative Probable Error \(PE\)](#)

443 Uncertainty in SSY_{EV} estimates arises from both measurement and model errors,
444 including stage-Q and T-SSC (Harmel et al., 2006). The Root Mean Square Error (RMSE)

445 method estimates the "most probable value" of the cumulative or combined error by propagating
446 the error from each measurement and modeling procedure to the final SSY_{EV} calculation
447 (Topping, 1972). The resulting cumulative probable error (PE) is the square root of the sum of
448 the squares of the maximum values of the separate errors:

$$PE = \sqrt{(E_{Qmeas}^2 + E_{SSCmeas}^2) + (E_{Qmod}^2 + E_{SSCmod}^2)} \quad \text{Equation 2}$$

where PE is the cumulative probable error for individual measured values ($\pm\%$), E_{Qmeas} is uncertainty in Q measurements ($\pm\%$), $E_{SSCmeas}$ is uncertainty in SSC measurements ($\pm\%$), E_{Qmod} is uncertainty in Q modeled by the Stage-Q relationship (RMSE, as $\pm\%$ of the mean observed Q), E_{SSCmod} is uncertainty in SSC modeled by the T-SSC relationship (RMSE, as $\pm\%$ of the mean observed SSC) (Harmel et al., 2009).

449 E_{Qmeas} and $E_{SSCmeas}$ were estimated using lookup tables from the DUET-H/WQ software
450 tool (Harmel et al., 2009). The effect of uncertain SSY_{EV} estimates may complicate conclusions
451 about contributions from subwatersheds, anthropogenic impacts, and SSY_{EV}-Storm Metric
452 relationships. This is common in sediment yield studies where successful models estimate SSY
453 with ± 50 -100% accuracy (Duvert et al., 2012) but the difference in SSY from undisturbed and
454 disturbed areas was expected to be much larger than the cumulative uncertainty. PE was
455 calculated for SSY_{EV} from the UPPER and TOTAL watersheds, but not calculated for SSY_{EV}
456 from the LOWER subwatershed since it was calculated as the difference of SSY_{EV_UPPER} and
457 SSY_{EV_TOTAL}.

458 ~~Relationship of sediment load to sediment budget~~

459 ~~We use the measured sediment yield at three locations to quantify the in-stream~~
460 ~~suspended sediment budget. Other components of sediment budgets include channel erosion and~~
461 ~~or channel and floodplain deposition (Walling and Collins, 2008). Sediment storage and~~

462 remobilization can significantly complicate the interpretation of in-stream loads, and complicate
463 the identification of a land-use signal. In Faga'alu, the channel bed is predominantly large
464 volcanic cobbles and coarse gravel, with no significant deposits of fine sediment. Upstream of
465 the village, the valley is very narrow with no floodplain. In the downstream reaches of the lower
466 watershed, where fines might deposit in the floodplain, the channel has been stabilized with
467 cobble reinforced by fencing, so overbank flows and sediment deposition on the floodplain are
468 not observed. We therefore assume that channel erosion and channel and floodplain deposition
469 are insignificant components of the sediment budget, so the measured sediment yields at the
470 three locations reflect differences in hillslope sediment supply. Minimal sediment storage also
471 reduces the lag time between landscape disturbance and observation of sediment at the watershed
472 outlet.

473 Quantifying SSY from disturbed and undisturbed subwatersheds

474 A main objective for this study was to quantify anthropogenic changes in SSY_{EV_TOTAL}
475 as measured at FG3. Relative contributions to SSY_{EV_TOTAL} from undisturbed and human-
476 disturbed areas were assessed using two approaches: 1) comparing SSY_{EV} contributions from
477 subwatersheds for each storm and the average of all storms, and 2) the Disturbance Ratio (DR).

478 The percent contributions of subwatersheds to SSY_{EV_TOTAL} were calculated from SSY_{EV}
479 measured at FG1, FG2, and FG3 (Figure 1). SSY_{EV} from the UPPER subwatershed was
480 measured at FG1 ($SSY_{EV_UPPER} = SSY_{EV_FG1}$). SSY_{EV} from the LOWER subwatershed was
481 calculated as $SSY_{EV_LOWER} = SSY_{EV_FG3} - SSY_{EV_FG1}$. Where SSY_{EV} data at FG2 were also
482 available, the contributions from the quarry subwatershed ($SSY_{EV_LOWER_QUARRY} = SSY_{EV_FG2} -$
483 SSY_{EV_FG1}), and village subwatershed ($SSY_{EV_LOWER_VILLAGE} = SSY_{EV_FG3} - SSY_{EV_FG2}$) were
484 calculated separately.

485 Land cover in the LOWER subwatershed includes both undisturbed and human disturbed
486 surfaces. To calculate SSY_{EV} from disturbed areas, SSY_{EV} from undisturbed areas was estimated
487 using the specific SSY_{EV} ($sSSY_{EV}$ tons/km²) from the UPPER subwatershed multiplied by the
488 undisturbed area in the LOWER subwatershed:

489 The disturbance ratio (DR) is the ratio of SSY_{EV} from the watershed under current
490 conditions to SSY_{EV} under pre-disturbance conditions, estimated using $sSSY_{UPPER}$:

491 Both Equation 3 and 4 assume that the whole watershed was originally covered in forest,
492 and $sSSY_{EV}$ from forested areas in the LOWER subwatershed equals $sSSY_{EV}$ from the
493 undisturbed UPPER watershed. SSY_{EV} from the disturbed portions of the LOWER subwatershed
494 (Equation 3) was used to calculate a DR for just the disturbed areas in the LOWER
495 subwatershed.

496 Predicting event suspended sediment yield (SSY_{EV})

497 Four storm metrics were tested as predictors of SSY_{EV}: total event precipitation (Psum),
498 event Erosivity Index (EI30) (Hicks, 1990; Kinnell, 2013), total event water discharge (Qsum),
499 and maximum event water discharge (Qmax) (Duvert et al., 2012; Rodrigues et al., 2013).
500 SSY_{EV} and the discharge metrics (Qsum and Qmax) were normalized by watershed area to
501 compare different sized watersheds.

502 The relationship between SSY_{EV} and storm metrics is often best fit by a power law
503 function:

504 The regression coefficients (α and β) for the UPPER and TOTAL watersheds were tested
505 for statistically significant differences using Analysis of Covariance (ANCOVA) (Lewis et al.,
506 2001). A higher intercept (α) for the human disturbed watershed indicates higher sediment yield
507 for the same size storm event, compared to sediment yield from undisturbed areas. A difference

508 ~~in slope (β) would indicate the relative sediment contributions from the subwatersheds change~~
509 ~~with increasing storm size. If regression slopes for the UPPER and TOTAL watersheds are~~
510 ~~significantly different, it supports the conclusion that the effect of human disturbance changes~~
511 ~~with storm size.~~

512 ~~Annual estimates of SSY and sSSY~~

513 ~~Annual estimates of SSY and sSSY were calculated to compare Faga'alu with other~~
514 ~~watersheds reported in the literature. A continuous annual time series of SSY was not possible at~~
515 ~~the study site due to the discontinuous field campaigns and failure of or damage to the~~
516 ~~turbidimeters during some months. Continuous records of P and Q were available for 2014, so~~
517 ~~the Psum SSY_{EV} and Qmax SSY_{EV} models (Equation 5) were used to predict SSY_{EV} for all~~
518 ~~storms in 2014 (Basher et al., 1997). Construction of sediment mitigation structures at the quarry~~
519 ~~began in October 2014, greatly reducing SSY_{EV} from the LOWER_QUARRY subwatershed~~
520 ~~(unpublished data), so the Qmax SSY_{EV} relationship developed prior to the mitigation was used~~
521 ~~to calculate the annual pre-mitigation sediment yield. For storms with no Qmax data at FG3,~~
522 ~~Qmax was predicted from a linear regression between Qmax at FG1 and Qmax at FG3 for the~~
523 ~~study period ($R^2=0.88$).~~

524 ~~Annual SSY and sSSY were also estimated by multiplying SSY_{EV} from measured storms~~
525 ~~by the ratio of annual storm precipitation (P_{sann}) to the precipitation measured during storms~~
526 ~~where SSY_{EV} was measured (P_{smeas}):~~

527 ~~Equation 6 assumes that the sediment yield per mm of storm precipitation is constant~~
528 ~~over the year, and that the size distribution of storms has no effect on SSY_{EV}, though there is~~
529 ~~some evidence that SSY_{EV} increases exponentially with storm size (Lewis et al., 2001; Rankl,~~

530 ~~2004). Equation 6 also ignores sediment yield during non-storm periods, which is justified by the~~
531 ~~low SSC and Q observed between storms.~~

532 **4. Results**

533 **Field Data Collection**

534 **4.1 Precipitation and discharge**

535 Annual precipitation (P) measured at RG1, ~~with gaps filled with data from Wx~~, was
536 3,502 mm, 3,529 mm, and 3,709 mm in 2012, 2013, and 2014, respectively, which averages 94%
537 of long-term precipitation (=3,800 mm) from PRISM data (Craig, 2009). No difference in
538 measured P was found between RG1 and Wx, or between RG1 and RG2, so P was assumed to be
539 homogenous over the watershed for all analyses. Rain gauges could only be placed as high as
540 ~300 m (RG2), though the highest point in the watershed is ~600 m. Long-term rain gage
541 records show a strong precipitation gradient with increasing elevation, with average
542 ~~precipitation annual P~~ of 3,000-4,000 mm on the lowlands, increasing to more than 6,350 mm at
543 high elevations (>400 m.a.s.l.) (Craig, 2009; Dames & Moore, 1981; Wong, 1996).

544 ~~Precipitation P~~ data measured at higher elevations would be useful to determine ~~a more robust the~~
545 orographic ~~precipitation relationship effect~~. For this analysis, however, the absolute values of
546 ~~total precipitation P~~ in each subwatershed are not ~~as~~ important since ~~precipitation P~~ and the
547 erosivity index are only used as predictive storm metrics for Objective 2.

548 **Water Discharge**

549 ~~Discharge (Q)~~ at both FG1 and FG3 was characterized by periods of low but perennial
550 baseflow, punctuated by short, flashy hydrograph peaks (~~FG1: max 8,356 L/sec, FG3: max~~
551 ~~13,071 L/sec~~) (Figure 3). Though Q data was unavailable for some periods, storm events were

552 generally smaller but more frequent in the October-April wet season compared to the May-
553 September dry season. The largest event in the three year monitoring period was observed in the
554 dry season (August 2014).

555 ***Storm Events***

556 ~~A total of 210 storm events were identified using hydrograph separation on the Q data at~~
557 ~~FG1 and FG3 between January, 2012, and December 2014. 169 events had simultaneous Q data~~
558 ~~at FG1 and FG3 (Appendix 3, Table 1). SSC data from T or interpolated grab samples were~~
559 ~~recorded during 112 events at FG1, and 74 events at FG3. Of those storms, 42 events had data~~
560 ~~for P, Q, and SSC at both FG1 and FG3 to calculate SSY_{EV} from the LOWER subwatershed.~~
561 ~~SSY data from interpolated grab samples were collected at FG2 for 8 storms to calculate SSY_{EV}~~
562 ~~from the LOWER_QUARRY and LOWER_VILLAGE subwatersheds separately. Storm event~~
563 ~~durations ranged from 1 hour to 2 days, with mean duration of 13 hours.~~

564 ~~Most storm events showed a typical pattern, where a short period of intense rainfall~~
565 ~~caused a rapid increase in SSC downstream of the quarry (FG2) while SSC remained low at the~~
566 ~~undisturbed forest site (FG1) (Figure 4). The highest SSC was typically observed at FG2, with~~
567 ~~slightly lower and later peak SSC observed at FG3. SSC downstream of the undisturbed forest~~
568 ~~(FG1) typically increased more slowly, remained lower, and peaked later than the disturbed sites~~
569 ~~downstream of the quarry (FG2) and the village (FG3). Though peak SSC was highest at FG2,~~
570 ~~the highest SSY was measured at FG3 due to the addition of storm runoff and sediment from the~~
571 ~~larger subwatershed draining to FG3.~~

572 <Figure 3 here please>

573 4.2 Objective 1: Compare SSC and SSY_{EV} for disturbed and undisturbed subwatersheds

574 4.2.1 Suspended sediment Concentration

575 ~~From January 6, 2012, to October 1, 2014, 506 water samples were collected at FG1 (n=59), FG2~~

576 ~~(n=90 grab samples, n=198 from the Autosampler), and FG3 (n=159). Mean (μ) and maximum~~

577 ~~SSC of water samples, collected during concentrations (SSC) during storm and non stormflow and~~

578 ~~stormflow storm periods by grab and autosampler~~

579 <Figure 4 here please>

580 SSC was consistently lowest downstream of the forested watershed (FG1), highest

581 downstream of the quarry (FG2), and intermediate downstream of the village (FG3), during both

582 storm and non-storm periods (Figure 5a, 5b). A single storm event from 2/14/2014 (Figure 4)

583 shows that SSC was highest at FG2 on the rising limb of the hydrograph, and that turbidity and

584 SSC at FG3 were always higher than at FG1 throughout the storm event. Mean (μ) and

585 maximum SSC of all water samples, including those collected during both storm and non-storm

586 periods, were lowest at FG1 ($\mu=28$ mg/L, max=500 mg/L, n=59), highest at FG2 ($\mu=337$ mg/L,

587 ~~max=12,600 mg/L), and in between, n=90 grab samples, n=198 from the Autosampler), and~~

588 intermediate at FG3 ($\mu=148$ mg/L, max=3,500 mg/L). At FG1, 24% of grab samples (n=14) were

589 ~~collected during non-stormflow, $\mu=8$ mg/L (Figure 5a); 76% of grab samples (n=45) were~~

590 ~~collected during stormflow, $\mu=35$ mg/L (Figure 8b). At FG2, 23% of grab samples (n=21) were~~

591 ~~collected during non-stormflow, $\mu=105$ mg/L; 77% of grab samples (n=69) were collected~~

592 ~~during stormflow, $\mu=409$ mg/L. At FG3, 25% of samples (n=39) were, n=159). SSC collected~~

593 ~~during non-stormflow, $\mu=52$ mg/L; 75% of samples storm periods were lowest at FG1, highest at~~

594 FG2 (n=21), and in between at FG3 (n=45) (Figure 5a). Similarly, SSC during storms was

595 highest at FG1 (n=45), highest at FG 2, (n=69) and intermediate at FG3 (n=120) were collected
596 during stormflow, $\mu = 179 \text{ mg/L}$. This pattern of SSC values suggests that little sediment is
597 contributed from the forest upstream of FG1, followed by a large input of sediment between FG1
598 and FG2, and then SSC is diluted by addition of stormflow with lower SSC between FG2 and
599 FG3.

600 Probability plots of the). SSC data collected at FG1, FG2 and FG3 showed they were
601 highly non-normal, so non-parametric tests for statistical significance were applied. The results
602 of the Kruskall-Wallis test were significant for non-stormflow ($p < 10^{-4}$) and stormflow ($p < 10^{-4}$);
603 means of SSC samples were SSC was statistically significantly different among all the three
604 locations. The results of the sampled site during non-storms ($p < 10^{-4}$) and storms ($p < 10^{-4}$). Pair-
605 wise Mann-Whitney test tests between FG1 and FG2 were significant (non-stormflow, $p < 10^{-4}$;
606 stormflow, $p < 10^{-4}$ for both storms and non-storms), but between FG2 and FG3 were significant
607 for non-stormflow storm periods ($p < 0.05$) but not for stormflow storms ($p > 0.10$); means of SSC
608 samples at FG1 and FG2 were significantly different, but FG2 and FG3 were not.).

609 <Figure 5 here please>

610 SSC varied by several orders of magnitude for a given Q at FG1, FG2, and FG3 due to
611 significant hysteresis observed during storm periods (Figure 4, 6). At FG1, variability of SSC
612 during stormflow was assumed to be caused by randomly occurring landslides or mobilization of
613 sediment stored in the watershed during large storm events. The maximum SSC sampled
614 downstream of the undisturbed forest, at FG1 (500 mg/L), was sampled on 04/23/2013 at high
615 discharge ($Q_{FG1} = 3,724 \text{ L/sec}$) (Figure 6a). Anecdotal and field observations reported higher than
616 normal SSC upstream of the quarry during the 2013 field season, possibly due to landsliding
617 from previous large storms (G. Poysky, pers. comm.).

618 | [<Figure 6 here please>](#)
619 | At FG2 and FG3, additional variability in the Q-SSC relationship was due to the
620 | changing sediment availability associated with quarrying operations and construction in the
621 | village. The high SSC values observed downstream of the quarry (FG2) during low Q were
622 | caused by two mechanisms: 1) precipitation events that did not result in stormflow as defined by
623 | the hydrograph separation algorithm, but generated runoff from the quarry with high SSC and 2)
624 | washing fine sediment into the stream during rock crushing operations at the quarry.

625 | The maximum SSC sampled at FG2 (12,600 mg/L) and FG3 (3,500 mg/L) were sampled
626 | during the same rainfall event (03/05/2012), but during low Q (~~Q_{FG3}=287 L/sec)~~) (Figure 6b-c).
627 | During this event, brief but intense precipitation caused high sediment runoff from the quarry.
628 | SSC was diluted further downstream of the quarry at FG3 by the addition of runoff with lower
629 | SSC from the village.

630 | Given the close proximity of the quarry to the stream, SSC downstream of the quarry can
631 | be highly influenced by mining activity like rock extraction, crushing, and/or hauling operations.
632 | During 2012, a common practice for removing fine sediment from crushed aggregate was to
633 | rinse it with water pumped from the stream. In the absence of retention structures the fine
634 | sediment was ~~then~~ discharged directly into the Faga'alu stream, causing high SSC during
635 | baseflow non-storm periods with no precipitationP in the preceding 24 hours (solid symbols,
636 | Figure 6b-c). Riverine discharge of fine sediment rinsed from aggregate was discontinued in
637 | 2013. In 2013 and 2014, waste sediment was piled on-site and severe erosion of these changing
638 | stockpiles caused high SSC Riverine discharge of fine sediment rinsed from aggregate was
639 | discontinued in 2013. In 2013 and 2014, waste sediment was piled on site and severe erosion of
640 | these changing stockpiles caused high SSC only during storm events.

641 *4.2.2. Suspended sediment yield during storm events (SSYEV)*

642 A total of 210 storm events were identified using hydrograph separation on the Q data at
643 FG1 and FG3 between January, 2012, and December 2014. A total of 169 events had
644 simultaneous Q data at FG1 and FG3 (Appendix C, Table 1). SSC data from T or interpolated
645 grab samples were recorded during 112 (FG1) and 74 events (FG3). Of those storms, 42 events
646 had data for P, Q, and SSC at both FG1 and FG3. SSY data from interpolated grab samples were
647 collected at FG2 for 8 storms to calculate SSY_{EV} from the LOWER_QUARRY and
648 LOWER_VILLAGE subwatersheds separately. Storm event durations ranged from 1 hour to 2
649 days, with mean duration of 13 hours.

650 For the 42 storms with complete data at both FG1 and FG3 (Table 2), SSY_{EV_TOTAL} was
651 129±121 tons, with 17±7 tons from the UPPER subwatershed and 112 tons from the LOWER
652 subwatershed. The UPPER and LOWER subwatersheds are similar in size (0.90 km² and 0.88
653 km²) but SSY_{EV_LOWER} accounted for 87% of SSY_{EV} at the watershed outlet (Table 2). The DR
654 estimated using Equation 4, with sSSY_{EV_UPPER} = 18.8 tons/km², suggests sSSY_{EV} has increased
655 by 6.8x in the LOWER subwatershed, and 3.9x for the TOTAL watershed compared with
656 undisturbed forest.

657 <Table 2 here please>

658 Disturbed areas accounted for 10% of the LOWER subwatershed area but approximately
659 87% of the SSY_{EV} from the LOWER subwatershed. Only 5.2% of the TOTAL watershed area
660 was disturbed, but SSY from disturbed areas accounted for 75% of SSY_{EV_TOTAL}. sSSY from
661 disturbed areas in the LOWER subwatershed was 1,095 tons/km², or 58x the sSSY of
662 undisturbed forest (Table 3).

663 <Table 3 here please>

664 The separate contributions to SSY from the quarry and village were determined for eight
665 storm events (Table 4), where 29% of SSY_{EV} came from the UPPER subwatershed, 36% from
666 the LOWER_QUARRY subwatershed, and 35% from the LOWER_VILLAGE subwatershed.
667 sSSY from the UPPER, LOWER_QUARRY, and LOWER_VILLAGE subwatersheds, and the
668 TOTAL watershed was 15, 61, 27, and 26 tons/km², respectively. The storms in Table 4 show a
669 smaller increase in SSY from the TOTAL watershed (1.7x SSY_{UPPER}) compared with the 42
670 storms with data at FG1 and FG3 (3.9x SSY_{UPPER} Table 2), so these storms may underrepresent
671 the contributions of the quarry and village to SSY. sSSY increased by 4.1x in the
672 LOWER_QUARRY subwatershed and 1.8x in the LOWER_VILLAGE subwatershed compared
673 with the undisturbed UPPER watershed.

674 <Table 4 here please>

675 Very small fractions of the subwatershed areas are disturbed, yet roughly 77% of SSY
676 EV LOWER_QUARRY (6.5% disturbed) and 51% of SSY_{EV LOWER_VILLAGE} (11.7% disturbed)
677 subwatersheds was from disturbed areas. Similarly, 5.2% of the TOTAL watershed was
678 disturbed but 75-45% of SSY_{EV TOTAL} was from disturbed areas (Tables 3 and 5). The quarry
679 significantly increased SSY and contributed the majority of SSY from disturbed areas in Faga'alu
680 watershed. sSSY from disturbed areas in the UPPER (37 tons/km²), LOWER_QUARRY (722
681 tons/km²), and LOWER_VILLAGE subwatersheds (116 tons/km²) suggested that disturbed areas
682 increase sSSY over forested conditions by 49x and 8x in the LOWER_QUARRY and
683 LOWER_VILLAGE subwatersheds, respectively. Human disturbance in the
684 LOWER_VILLAGE subwatershed also increased SSY above natural levels but the magnitude of
685 disturbance was much lower than the quarry.

686 <Table 5 here please>

687 | [4.2.3 Cumulative Probable Error \(PE\)](#)

688 | Cumulative Probable Error (RMSE %) for SSY_{EV} estimates at FG1 and FG3 were
689 | calculated from the measurement errors for Q (8.5%) and SSC grab samples (16.3%), and the
690 | model errors of the respective stage-Q and T-SSC relationships for that location. Cumulative
691 | Probable Errors (PE) in SSY_{EV} were 28-49% ($\mu=43\%$) at FG1 and 36-118% ($\mu=94\%$) at FG3.

692 | The measurement error (RMSE) for Q at FG1 and FG3 was 8.5 %, which included error
693 | in the area-velocity measurements (6%), continuous Q measurement in a natural channel (6%),
694 | pressure transducer error (0.1%), and streambed condition (firm, stable bed=0%) (DUET-H/WQ
695 | look-up table (Harmel et al., 2006)). The model errors (RMSE) were 32% for the stage-Q rating
696 | curve using Manning's equation at FG3, and 22% using HEC-RAS at FG1.

697 | The measurement error (RMSE) for SSC was 16.3%, which included errors for sample
698 | collection and analysis. Sample collection error consisted of interpolating over a 30 min interval
699 | (5%) and sampling during stormflows (3%). Sample analysis error was from measuring SSC by
700 | filtration (3.9%). The model errors (RMSE) of the T-SSC relationships were 16% (4 mg/L) for
701 | the YSI and TS turbidimeters at FG1, 113% (348 mg/L) for the YSI turbidimeter at FG3, and
702 | 46% (48 mg/L) for the OBS turbidimeter at FG3.

703 | [Comparing 4.3 Objective 2: Modeling SSY_{EV} from disturbed and undisturbed subwatersheds](#)

704 | SSY_{EV} was measured simultaneously at FG1 and FG3 for 42 storms (Table 2).
705 | SSY_{EV_TOTAL} was 129.2±121.4 tons (72.6±68.2 tons/km²), with 17.0±7.3 tons (18.8±8.1
706 | tons/km²) from the UPPER subwatershed and 112.2 tons (127.5 tons/km²) from the LOWER
707 | subwatershed. The UPPER and LOWER subwatersheds are similar in size (0.90 km² and 0.88
708 | km²) but SSY_{EV_UPPER} accounted for an average of just 13% and SSY_{EV_LOWER} for 87% of SSY_{EV}
709 | at the watershed outlet (Table 2). The DR estimated from sSSY_{EV_UPPER} (=18.8 tons/km²) and

710 ~~sSSY_{EV_LOWER}~~ (Equation 4) suggests ~~sSSY_{EV}~~ has increased by 6.8x in the LOWER
711 subwatershed, and 3.9x for the TOTAL watershed.

712 ~~SSY_{EV}~~ from the undisturbed forest areas in the LOWER watershed was estimated to be
713 14.9 tons for the 42 events in Table 2 (Equation 3), so ~~SSY_{EV}~~ from the disturbed areas was 97.3
714 tons (Table 3). Approximately 87% of ~~SSY_{EV_LOWER}~~ was from disturbed areas, despite the
715 disturbed areas only accounting for 10.1% of the LOWER subwatershed area (0.089 km²).
716 Similarly, despite only 5.2% of the TOTAL watershed being disturbed, ~~SSY~~ from disturbed
717 areas accounted for 75% of ~~SSY_{EV_TOTAL}~~. ~~SSY~~ from disturbed areas in the LOWER
718 subwatershed was 1,095 tons/km², or 58x the ~~sSSY~~ of undisturbed forest.

719 It was hypothesized the quarry was a key sediment source, but ~~SSY_{EV}~~ was measured
720 simultaneously at FG1, FG2, and FG3 for only 8 of the storms in Table 2. ~~SSY_{EV}~~ was calculated
721 separately from the LOWER subwatershed containing the quarry (~~SSY_{EV_LOWER_QUARRY}~~) and
722 LOWER subwatershed containing the village below the quarry (~~SSY_{EV_LOWER_VILLAGE}~~) for those
723 8 storms (Table 4). For the 8 storms in Table 4, ~~SSY_{EV_TOTAL}~~ was 46 tons with an average of
724 29% from the UPPER subwatershed, 36% from the LOWER_QUARRY subwatershed, and 35%
725 from the LOWER_VILLAGE subwatershed. ~~SSY~~ from the UPPER, LOWER_QUARRY, and
726 LOWER_VILLAGE subwatersheds, and the TOTAL watershed was 15, 61, 27, and 26 tons/km²,
727 respectively. The results from the smaller sample of storms in Table 4, show a slightly lower
728 increase in ~~SSY~~ from the TOTAL watershed, 1.7x, but show the ~~sSSY~~ has increased by 4.08x in
729 the LOWER_QUARRY subwatershed and 1.8x in the LOWER_VILLAGE subwatershed.

730 Very small fractions of the subwatershed areas are disturbed, yet roughly 77% of ~~SSY~~
731 ~~EV_LOWER_QUARRY~~ (6.5% disturbed) and 51% of ~~SSY_{EV_LOWER_VILLAGE}~~ (11.7% disturbed)
732 subwatersheds was from disturbed areas. Similarly, despite only 5.2% of the TOTAL watershed

733 being disturbed, 75–45% of SSY_{EV TOTAL} was from disturbed areas (Tables 3 and 5). Bare land
734 in the LOWER QUARRY subwatershed significantly increased SSY_{LOWER QUARRY} and
735 SSY_{TOTAL}, and contributed the majority of SSY from disturbed areas in Faga'alu watershed.
736 SSY from disturbed areas in the UPPER (37.0 tons/km²), LOWER QUARRY (721.6 tons/km²),
737 and LOWER VILLAGE subwatersheds (116.2 tons/km²) suggested that disturbed areas increase
738 SSY over forested conditions by 49x and 8x in the LOWER QUARRY and
739 LOWER VILLAGE subwatersheds, respectively. Human disturbance in the
740 LOWER VILLAGE subwatershed also increased SSY above natural levels but the magnitude of
741 disturbance was much lower than the quarry.

742 Predicting SSY_{EV} from storm metrics

743 SSY_{EV} from the UPPER and TOTAL watersheds was correlated with each of the four
744 storm metrics tested (Figure 7), though the correlations with precipitation metrics were poor in
745 the heavily forested UPPER watershed (Table 6). Pearson and Spearman correlation coefficients
746 were similar, meaning the relationships were mostly linear in log-log space. Significant scatter
747 was observed around all models, which reflects the changing sediment availability at the quarry
748 and village, and the natural variability in the watershed response for different storm events.

749 Qsum was 4.3.1. Selecting the best predictor of SSY_{EV} for the

750 Qsum and Qmax were the best predictors of SSY_{EV} for the forested UPPER watershed,
751 and Psum ~~was~~ and Qmax were the best predictor~~predictors~~ for the TOTAL watershed, ~~though~~
752 ~~Qmax was nearly as good a predictor for both watersheds~~. SSY_{EV} is calculated from Q so it is
753 expected that Qsum should correlate closely with SSY_{EV}, ~~as observed in other studies~~ (Duvert et
754 al., 2012; Rankl, 2004). ~~Indeed the Qsum model for the UPPER watershed showed the highest~~
755 ~~coefficient of determination (r^2), lowest RMSE, and highest Pearson and Spearman correlation~~

756 coefficients (Table 6). Psum showed an equally high r^2 and a lower RMSE, but only for the
757 TOTAL subwatershed. This suggests that sediment production is more related to discharge
758 processes in the UPPER subwatershed, and more related to precipitation processes in the
759 LOWER subwatershed. Discharge metrics were also highly correlated with SSY_{EV} in the
760 TOTAL watershed, suggesting discharge metrics are good predictors in both disturbed and
761 undisturbed watersheds. Qmax was not the best predictor in either watershed, but performed well
762 in both watersheds, with similar correlation statistics to both Qsum and Psum models. Most of
763 the scatter in the Qmax-SSY_{EV} relationship is observed for small events, and Qmax correlated
764 strongly with the largest SSY_{EV} values, when most of the annual sediment load is generated.
765 (Table 6).

766 <Table 6 here please>

767 Precipitation was measured at the quarry, which may reflect precipitation characteristics
768 more accurately in the LOWER than the UPPER watershed, and account for the lower
769 correlation coefficients between precipitation and SSY_{EV_UPPER}. SSY from the LOWER
770 subwatershed is hypothesized to be mostly generated by hillslope erosion by sheetwash and rill
771 formation at the quarry and on dirt roads, and agricultural plots, whereas SSY from the UPPER
772 subwatershed is hypothesized to be mainly from channel processes and mass wasting. Mass
773 wasting can contribute large pulses of sediment which can be deposited near or in the streams
774 and entrained at high discharges during later storm events. Given the high correlation
775 coefficients between SSY_{EV} and Qmax in both watersheds, Qmax may be a promising predictor
776 that integrates both precipitation and discharge processes.

777 | ~~In all models,~~ 4.3.2. Effect of event size and watershed disturbance

778 | SSY_{EV} from the TOTAL watershed was higher than from the UPPER watershed for the

779 | full range of measured storms with the exception of a few events that are considered outliers.

780 | ~~These~~The outlier events could be attributed to measurement error or to landslides or other mass

781 | movements in the UPPER subwatershed ~~and the increased sediment supply for that specific~~

782 | ~~event~~. The separation of multi-peak storm events, storm sequence, and antecedent conditions

783 | may also play a role. While the climate on Tutuila is tropical, without strong seasonality, periods

784 | of low rainfall can persist for several weeks, perhaps altering the water and sediment dynamics in

785 | the subsequent storm events.

786 | All model intercepts (α) were significantly different ($p < 0.01$), but only the Qsum-SSY_{EV}

787 | model showed significantly different ($p < 0.01$) slopes (β , $p < 0.01$). The Qsum-SSY_{EV} models

788 | indicate that SSY_{EV} from the UPPER and TOTAL watersheds converge at higher Qsum values.

789 | Conversely, the Psum- and Qmax-SSY_{EV} models show no change in relative contributions of

790 | SSY over the range of storm sizes (Figure 7).

791 | <Figure 7 here please>

792 | The relative contribution of SSY from the human-disturbed watershed was hypothesized

793 | to diminish with increasing storm size. The results from precipitation metrics and discharge

794 | metrics were contradictory. The relative contribution of SSY_{EV} from the human-disturbed

795 | watershed decreases with storm size in the Qsum-SSY_{EV} model, but the Psum- and Qmax-SSY_{EV}

796 | models show no change in relative contributions over increasing storm size (Figure 7). It was

797 | hypothesized that SSY_{EV} from natural undisturbed forest areas would become the dominant

798 | source for larger storm events, but the DR remains high for large storm events due to the

799 naturally low SSY_{EV} from natural forest areas in Faga'alu watershed. This suggests that disturbed
800 areas were not supply limited for the range of sampled storms.

801 **Annual estimates****4.4 Objective 3: Estimation of annual SSY and sSSY**

802 Estimates of annual sSSY depended on which predictor was used to estimate SSY_{EV}.

803 ~~Annual sSSY from the UPPER and TOTAL watersheds was 14 tons/km²/yr and 75 tons/km²/yr,~~
804 ~~respectively, as predicted by The Psum-SSY_{EV} relationship, and 68 tons/km²/yr and 247~~
805 ~~tons/km²/yr, respectively using model resulted in a much lower estimate of sSSY than the Qmax-~~
806 ~~SSY_{EV} relationship model~~ (Table 7). The large difference in sSSY between the two methods was
807 due to higher scatter about the Psum-SSY_{EV} relationship for large events compared with the
808 Qmax-SSY_{EV}. These results suggest the UPPER watershed contributed 14%, and the LOWER
809 subwatershed contributed 86% of annual SSY from the TOTAL watershed.

810 ~~In order to compare with SSY estimated from the Psum-SSY_{EV} and Qmax-SSY_{EV}~~
811 ~~relationships, model is likely more robust.~~ Annual SSY was also calculated for 2014 using
812 Equation 6 for three sets of storm events: a) all events with SSY_{EV} data, including those where
813 SSY_{EV} data were only available for a single site; b) only events where data was available for
814 both UPPER (FG1) and TOTAL (FG3) and c) only events where data was available for UPPER
815 (FG1), LOWER_QUARRY (FG2), and TOTAL (FG3). Including all storms (method a) will
816 provide the best estimate at a given location, while b) and c) allow more direct comparison of
817 different subwatersheds. Continuous records of Q and precipitation in 2014 showed
818 <Table 7 here please>

819 Annual storm precipitation (P_{ann}) P_{EVann} in 2014 was 2,770 mm, representing 69% of
820 total annual precipitation (3,709 mm). The remaining 31% of precipitation did not result in a rise
821 in stream level sufficient to be classified as an event with the hydrograph separation method used

822 here. All storms with measured SSY_{EV} at FG1 from 2012-2014 included 3,457 mm of
823 precipitation ($P_{smeas}P_{EVmeas}$), or 125% of $P_{sann}P_{EVann}$, so estimated annual SSY from the UPPER
824 subwatershed from Equation 6 was 41 tons/yr (45 tons/km²/yr). All storms with measured SSY_{EV}
825 at FG3 from 2012-2014 included 2,628 mm of precipitation, or 95% of expected annual storm
826 precipitation so estimated annual SSY from the TOTAL watershed was 428 tons/yr (241
827 tons/km²/yr). ~~These results suggest the UPPER watershed contributed 10%, and the LOWER~~
828 ~~subwatershed contributed 90% of annual SSY from the TOTAL watershed.~~

829 For storms with measured SSY_{EV} at both FG1 and FG3 (Table 2), P_{EVmeas} was 1,004 mm,
830 or 36% of P_{EVann} . From Equation 6, annual SSY increased from the UPPER (46 tons/yr),
831 LOWER (310 tons/yr), and TOTAL watershed (360 tons/yr). Annual sSSY increased from the
832 UPPER (51 tons/km²/yr), LOWER (350 tons/km²/yr), and TOTAL watershed (200 tons/km²/yr),
833 and, respectively.

834 For storms with measured SSY_{EV} at FG1, FG2, and FG3 (Table 4), P_{EVmeas} was 299 mm,
835 or 11% of P_{EVann} . Annual SSY increased from the UPPER (120 tons/yr), LOWER_QUARRY
836 subwatershed (150 tons/yr), LOWER_VILLAGE subwatershed (150 tons/yr), LOWER
837 subwatershed (300 tons/yr), and TOTAL watershed (420 tons/yr). Annual sSSY increased from
838 the UPPER (140 tons/km²/yr), LOWER_QUARRY (560 tons/km²/yr), LOWER_VILLAGE (250
839 tons/km²/yr), LOWER (340 tons/km²/yr), and TOTAL watershed 240 tons/km²/yr.

840 Overall, the Qmax model and Equation 6 using all events gave similar estimates of
841 annual SSY at both the UPPER watershed (41-61 tons/yr) and the TOTAL watershed (428-439
842 tons/yr). The accuracy of the Psum model was compromised by significant scatter for large
843 events, while the Qsum model had significantly less scatter for large events. The eight storms
844 sampled at all three locations (Table 4) had unusually high loads from the UPPER watershed but

845 similar SSY from the LOWER watershed, likely resulting in a low estimate of sediment loading
846 and DR from the quarry.

847 5. Discussion

848 ~~Methods for quantifying human impact~~

849 ~~Event wise measurement of SSY_{EV} allowed rapid quantification of sediment loading from~~
850 ~~natural~~5.1 Objective 1: Compare SSC and human-SSY_{EV} for disturbed areas and undisturbed
851 subwatersheds

852 Event wise analysis of SSY_{EV} was useful because hysteresis and interstorm variability
853 caused significant scatter in the instantaneous Q-SSC relationship. While the instantaneous Q-
854 SSC relationship illustrated large increases in SSC downstream of the quarry, the hysteresis and
855 interstorm variability meant that a single Q-SSC relationship could not be used to estimate ~~of~~
856 sediment loading, which complicated detection of human impact on sediment concentrations and
857 ~~yield. yields.~~

858 Measurement of SSY_{EV} allows comparison of similar size storms to determine change
859 over space and time without problems of interannual variability in precipitation totals, ~~and~~. The
860 simple regression models that predict annual sediment load from either precipitation or
861 stormflow measurements eliminate the need for long-term field work to estimate annual total
862 yields. From a management perspective, the event-wise approach to estimating human impacts
863 on sediment is less expensive than efforts to measure annual yields since it does not require a
864 ~~full complete~~ year of monitoring, and can be rapidly conducted if mitigation or disturbance
865 activities are already planned. With predictive models of SSY_{EV} that are based on an easily-

866 monitored storm metric like maximum event discharge, SSY_{EV} can be modeled ~~in the future~~ to
867 compare with either post-mitigation or post-disturbance SSY_{EV}.

868 ~~The estimation of human impact on sediment loads was facilitated by the spatial~~
869 ~~arrangement of disturbances and by the lack of significant sediment storage in the watershed. In~~
870 ~~Faga'alu watershed, and other similar steep watersheds, human disturbance is often constrained~~
871 ~~to the lower watershed, and sediment yields from these key sources can be measured separately~~
872 ~~from the undisturbed forest upstream. Reid and Dunne (1996) argue that in cases where there is a~~
873 ~~clear management question and the study area can be divided into sub-units, a sediment budget~~
874 ~~can be rapidly developed with only a few field measurements and limited periods of field~~
875 ~~monitoring. The use of event wise sampling in subwatersheds with specific land uses allowed for~~
876 ~~separation of different sources to the sediment budget.~~

877 ~~Interpreting slope and intercept of the Qmax-SSY_{EV}-relationship~~

878 [5.2 Objective 2: Modeling SSY_{EV} with storm metrics](#)

879 Several researchers have attempted to explain values of the intercept (α) and slope (β)
880 coefficients of the sediment rating curve as a function of watershed characteristics. A traditional
881 sediment rating curve (Q-SSC) is considered a 'black box' model, and though the slope and
882 intercept have no physical meaning, some physical interpretation has been ascribed to them
883 (Asselman, 2000). Rankl (2004) hypothesized that the intercept in the Qmax-SSY_{EV} relationship

884 varied with sediment availability and erodibility in watersheds. ~~Duvert et al. (2012) found that~~
885 ~~intercepts of the Qmax-SSY_{EV}-relationship are also dependent on the regression fitting method.~~

886 While slopes in log-log space can be compared directly (Duvert et al., 2012), intercepts must be
887 plotted in similar units, and normalized by watershed area. In five semi-arid to arid watersheds
888 (2.1-1,538 km²) in Wyoming, United States (Rankl, 2004), intercepts of the SSY_{EV}-Qmax

889 relationship ranged from 111-4,320 (Qmax in $\text{m}^3/\text{s}/\text{km}^2$, SSY_{EV} in Mg/km²). In eight sub-humid
890 to semi-arid watersheds (0.45-22 km²) (Duvert et al., 2012), the intercepts ranged from 25-5,039.
891 In Faga'alu, the intercept in the undisturbed, UPPER subwatershed was 0.35, and in the
892 disturbed, TOTAL watershed the intercept was 1.38, which are an order of magnitude or two
893 lower than the lowest intercepts in Rankl (2004) and Duvert et al. (2012). This suggests that
894 sediment availability is relatively low in Faga'alu, under natural and human-disturbed conditions,
895 likely due to the dense forest cover.

896 High slope values in the log-log plots (β coefficient) suggest that small changes in stream
897 discharge lead to large increases in sediment load due to the erosive power of the river or the
898 availability of new sediment sources at high Q (Asselman, 2000). Rankl (2004) assumed that the
899 slope was a function of rainfall intensity on hillslopes, and found that the slopes ranged from
900 1.07-1.29 in five semi-arid to arid watersheds in Wyoming, and were not statistically different
901 among watersheds. In the watersheds in Duvert et al. (2012), slopes ranged from 0.95-1.82, and
902 from 1.06-2.45 in eighteen other watersheds (0.60-1,538 km²) in diverse geographical settings
903 (Basher et al., 1997; Fahey and Marden, 2000; Hicks et al., 2009; Rankl, 2004; Tropeano, 1991)
904 compiled by Duvert et al. (2012). In Faga'alu, slopes were 1.51 and 1.40 in the UPPER and
905 TOTAL Faga'alu watersheds, respectively, ~~which~~. These slopes are very consistent with the
906 slopes presented in Rankl (2004) and Duvert et al. (2012), despite large differences in climate
907 and land cover.

908 In Faga'alu, SSY_{EV} was least correlated with the Erosivity Index (EI30). Duvert et al.
909 (2012) also found low correlation coefficients with 5 min rainfall intensity for 8 watersheds in
910 France and Mexico. Rodrigues et al. (2013) hypothesized that EI30 is poorly correlated with
911 SSY_{EV} due to the effect of previous events on antecedent moisture conditions and in-channel

912 sediment storage. Cox et al. (2006) found EI30 was more correlated with soil loss in an
913 agricultural watershed than a forested watershed, and Faga'alu is mainly covered in dense forest.

914 Similar to other studies, the highest correlations with SSY_{EV} at Faga'alu were observed for
915 discharge metrics Qsum and Qmax (Basher et al., 2011; Duvert et al., 2012; Fahey et al., 2003;
916 Hicks, 1990; Rankl, 2004; Rodrigues et al., 2013) ~~the highest correlations with SSY_{EV} at~~
917 ~~Faga'alu were observed for discharge metrics.~~ While Qsum and Psum had higher correlations in
918 individual watersheds, Qmax was a good predictor of SSY_{EV} in both the disturbed and
919 undisturbed watershed.

920 ~~Comparing sSSY~~5.3 Objective 3: Estimation of annual SSY and SSC in comparison with other small
921 ~~Pacific Island watershedstropical islands~~

922 Sediment yield is highly variable among individual watersheds, but is generally
923 controlled by climate, vegetation cover, and geology, with human disturbance playing an
924 increasing role in the 20th century (Syvitski et al., 2005). Sediment yields in tropical Southeast
925 Asia and high-standing islands between Asia and Australia range from ~10 tons/km²/yr in the
926 granitic Malaysian Peninsula to ~10,000 tons/km²/yr in the tectonically active, steeply sloped
927 island of Papua New Guinea (Douglas, 1996). Sediment yields from Faga'alu are on the lower
928 end of the range, with sSSY of 45-68 tons/km²/yr from the undisturbed UPPER watershed, and
929 241-247 tons/km²/yr from the disturbed TOTAL watershed.

930 Milliman and Syvitski (1992) report high average sSSY (1,000-3,000 tons/km²/yr) from
931 watersheds (10-100,000 km²) in tropical Asia and Oceania, though their regional models of sSSY
932 as a function of basin size and maximum elevation predict only 13 tons/km²/yr from watersheds
933 with peak elevation 500-1,000 m (highest point of UPPER Faga'alu subwatershed is 653 m), and
934 68 tons/km²/yr for max elevations of 1,000-3,000. Given the high vegetation cover and lack of

935 human activity in the UPPER Faga'alu subwatershed, its sSSY should be lower than sSSY from
936 watersheds presented in Milliman and Syvitski (1992), which included watersheds with human
937 disturbance. sSSY from the forested UPPER Faga'alu subwatershed (45-68 tons/km²/yr) was
938 approximately three to five times higher than the prediction from the Milliman and Syvitski
939 | (1992) model (13 tons/km²/yr)., though the scatter around their model is large for smaller
940 watersheds, and the Faga'alu data fall within the range of scatter (Figures 5e and 6e in Milliman
941 and Syvitski (1992)).

942 Sediment yield has been measured using modern fluvial measurements similar to ours for
943 two Hawaiian watersheds: Hanalei watershed on Kauai ("Hanalei"), and Kawela watershed on
944 Molokai ("Kawela") (Table 8) (Ferrier et al., 2013; Stock and Tribble, 2010). Hanalei (54 km²)
945 has steep relief and mean areal precipitation of 3,866 mm/yr (Ferrier et al., 2013), which is
946 | slightly higher than rainfall at Faga'alu during the ~~observationmonitoring~~ period (3,247 mm/yr).
947 Over a four year period, SSC at Hanalei averaged 63 mg/L and reached a maximum of 2,750
948 mg/L (Stock and Tribble, 2010), which is slightly lower than observations at the outlet of
949 Faga'alu (mean 148 mg/L, maximum 3,500 mg/L). Calhoun and Fletcher (1999) estimated sSSY
950 from Hanalei as 140±55 tons/km²/yr, but had fewer data than Stock and Tribble (2010), who
951 estimated sSSY as 525 tons/km²/yr. Ferrier et al., (2013) reported annual suspended sediment
952 yield at Hanalei as 369 ± 114 tons/km²/yr. These values are ~~all~~ higher than observed ~~at Faga'alu~~
953 ~~under bothfrom the~~ undisturbed subwatershed in Faga'alu (45-68 tons/km²/yr) ~~andbut similar to~~
954 the disturbed (430-441 tons/km²/yr) subwatersheds. Rocks at Hanalei are of similar age (1.5
955 Mya) or older (3.95-4.43 Mya) (Ferrier et al., 2013) compared with Faga'alu (1.2 Mya)
956 (McDougall, 1985), so landscape age does not explain the difference in observed SSY between
957 Hanalei and Faga'alu. Kawela (14 km²) is disturbed by grazing and is in a sub-humid climate,

958 where precipitation varies with elevation from 500-3,000 mm. Stock and Tribble (2010)
959 estimated sSSY from Kawela ~~as was~~ 459 tons/km²/yr, which is similar to the disturbed
960 subwatershed in Faga'alu, but nearly twice as high as the TOTAL Faga'alu watershed. In
961 Kawela, SSC (mean 3,490 mg/L, maximum 54,000 mg/L) was much higher than measured in
962 Faga'alu TOTAL watershed, so the difference in SSY is due in part to higher SSC rather than to
963 higher observed runoff. Overall, both Hawaiian watersheds have higher SSY than Faga'alu,
964 which is consistent with the low intercepts of Faga'alu in the Qmax-SSY_{EV} relationships, and
965 suggests that Faga'alu may have uniquely low erosion rates for a steep volcanic watershed.
966 Precipitation variability may contribute to the difference in SSY, so a more thorough comparison
967 between Hanalei and Faga'alu would require a storm-wise analysis of the type performed here.

968 <Table 8 here please>
969 Annual sSSY from the quarry was estimated from Equation 6 to be approximately 2,800
970 tons/km²/yr. The quarry surfaces are comprised of haul roads, piles of overburden, and steep rock
971 faces which can be described as a mix of unpaved roads and cut-slopes. ~~Literature values show~~
972 ~~measured~~ sSSY from cutslopes ~~varying varies~~ from 0.01 tons/km²/yr in Idaho (Megahan, 1980) to
973 105,000 tons/km²/yr in Papua New Guinea (Blong and Humphreys, 1982), so the sSSY ranges
974 measured in this study are well within the ranges found in the literature.

975 5.4 Comparison with other kinds of sediment disturbance

976 SSY at Faga'alu was increased by 3.9x compared with the natural background. Other
977 studies in small, mountainous watersheds have documented one to several orders of magnitude
978 increases in SSY from land use that disturbs a small fraction of the watershed area. Urbanization
979 and mining can increase sediment yield by two to three orders of magnitudes in catchments of
980 several km². Yields from construction sites can exceed those from the most unstable, tectonically

981 active natural environments of Southeast Asia (Douglas, 1996). In Kawela watershed on
982 Molokai, less than 5% of the land produces most of the sediment, and only 1% produces ~50%
983 of the sediment (Risk, 2014; Stock et al., 2010). In three basins on St. John, US Virgin Islands
984 unpaved roads increased sediment delivery rates by 3-9 times (Ramos-Scharrón and Macdonald,
985 2005).

986 Disturbances at larger scales have resulted in ~~similar~~-increases in total SSY to coral
987 environments-, similar to Faga'alu. The development of the Great Barrier Reef (GBR) catchment
988 ($423,000 \text{ km}^2$) ~~sineesince~~ European settlement (ca.1830) led to increases in SSY by an estimated
989 factor of 5.5x (Kroon et al., 2012). Mining has been a major contributor of sediment in other
990 watersheds on volcanic islands with steep topography and high precipitation, increasing sediment
991 yields by 5-10 times in a watershed in Papua New Guinea (Hettler et al., 1997; Thomas et al.,
992 2003). In contrast to other land disturbances like fire, logging, or urbanization where sediment
993 disturbance decreases over time, the disturbance from mining is persistently high. Disturbance
994 magnitudes are similar to the construction phase of urbanization (Wolman and Schick, 1967), or
995 high-traffic unpaved roads (Reid and Dunne, 1984), but persist or even increase over time.

996 While unpaved roads are often identified as a source of sediment in humid forested
997 regions (Lewis et al., 2001; Ramos-Scharrón and Macdonald, 2005; Reid and Dunne, 1984),
998 field observations at Faga'alu suggested that most roads in the urban area were stabilized with
999 aggregate and not generating significant amounts of sediment. Other disturbances in Faga'alu
1000 included a few small agricultural plots, small construction sites and bare dirt on roadsides-
1001 ~~Repeated. Repeated~~ surface disturbance at the quarry is a key process maintaining high rates of
1002 sediment generation. Given the large distance to other sources of building material, aggregate

1003 mining and associated sediment disturbance may be a critical sediment source on remote islands
1004 in the Pacific and elsewhere.

1005 **6. Conclusion**

1006 Human disturbance has increased sediment yield to Faga'alu Bay by 3.9x over pre-
1007 disturbance levels. The human-disturbed subwatershed accounted for the majority (87%) of total
1008 sediment yield, and the quarry (1.1% of watershed area) contributed about a third of total SSY to
1009 the Bay. Qmax was a good predictor of SSY_{EV} in both the disturbed and undisturbed
1010 ~~watershed~~watersheds, making it a promising predictor in diverse environments. The slopes of the
1011 Qmax-SSY_{EV} relationships were comparable with other studies, but the model intercepts were an
1012 order of magnitude lower than intercepts from watersheds in semi-arid to semi-humid climates.
1013 This suggests that sediment availability is relatively low in the Faga'alu watershed, either
1014 because of the heavy forest cover or volcanic rock type. The event-wise approach did not require
1015 continuous in situ monitoring for a single or multiple years, which would not have been
1016 logistically possible in this remote study area. This study presents an innovative method to
1017 combine sampling and analysis strategies to measure sediment contributions from key sources,
1018 estimate baseline annual sediment yields prior to management, and rapidly develop an empirical
1019 sediment yield model for a remote, data-poor watershed.

1020 **Acknowledgements**

1021 Funding for this project was provided by NOAA Coral Reef Conservation Program
1022 (CRCP) through the American Samoa Coral Reef Advisory Group (CRAG). Kristine
1023 Buccianeri at CRAG and Susie Holst at NOAA CRCP provided necessary and significant
1024 support. Christianera Tuitele, Phil Wiles, and Tim Bodell at American Samoa Environmental

1025 Protection Agency (ASEPA), and Fatima Sauafea-Leau and Hideyo Hattori at NOAA, provided
1026 on-island coordination with traditional local authorities. Dr. Mike Favazza provided critical
1027 logistical assistance in American Samoa. Robert Koch at the American Samoa Coastal Zone
1028 Management Program (ASCMP) and Travis Bock at ASEPA assisted in accessing historical
1029 geospatial and water quality data. Many others helped and supported the field and laboratory
1030 work including Professor Jameson Newson, Rocco Tinitali, and Valentine Vaeoso at American
1031 Samoa Community College (ASCC), Meagan Curtis and Domingo Ochavillo at American
1032 Samoa Department of Marine and Wildlife Resources (DMWR), Don and Agnes Vargo at
1033 American Samoa Land Grant, Christina Hammock at NOAA American Samoa Climate
1034 Observatory, and Greg McCormick at San Diego State University. George Poysky, Jr., George
1035 Poysky III, and Mitch Shimisaki at Samoa Maritime Ltd. provided unrestricted access to the
1036 Faga'alu quarry site, and historical operation information. Faafetai tele lava.

1037 **References**

- 1038 Asselman, N.E.M., 2000. Fitting and interpretation of sediment rating curves. *J. Hydrol.* 234,
1039 228–248. doi:10.1016/S0022-1694(00)00253-5
- 1040 Basher, L., Hicks, D., Clapp, B., Hewitt, T., 2011. Sediment yield response to large storm events
1041 and forest harvesting, Motueka River, New Zealand. *New Zeal. J. Mar. Freshw. Res.* 45,
1042 333–356. doi:10.1080/00288330.2011.570350
- 1043 Basher, L.R., Hicks, D.M., Handyside, B., Ross, C.W., 1997. Erosion and sediment transport
1044 from the market gardening lands at Pukekohe, Auckland, New Zealand. *J. Hydrol.* 36, 73–
1045 95.

- 1046 Bégin, C., Brooks, G., Larson, R. a., Dragićević, S., Ramos Scharrón, C.E., Coté, I.M., 2014.
1047 Increased sediment loads over coral reefs in Saint Lucia in relation to land use change in
1048 contributing watersheds. *Ocean Coast. Manag.* 95, 35–45.
1049 doi:10.1016/j.ocecoaman.2014.03.018
- 1050 Blong, R.J., Humphreys, G.S., 1982. Erosion of road batters in Chim Shale, Papua New Guinea.
1051 Civ. Eng. Trans. Inst. Eng. Aust. CE24 1, 62–68.
- 1052 Bonta, J. V, 2000. Impact of Coal Surface Mining and Reclamation on Suspended Sediment in
1053 Three Ohio Watersheds. *JAWRA J. Am. Water Resour. Assoc.* 36, 869–887.
- 1054 Brunner, G., 2010. HEC-RAS River Analysis System.
- 1055 Buchanan Banks, J., 1979. *The October 28, 1979 Landsliding on Tutuila. Open-File Report 81-81*.
1056 U.S. Geological Survey.
- 1057 Calhoun, R.S., Fletcher, C.H., 1999. Measured and predicted sediment yield from a subtropical,
1058 heavy rainfall, steep-sided river basin: Hanalei, Kauai, Hawaiian Islands. *Geomorphology*
1059 30, 213–226.
- 1060 Cox, C.A., Sarangi, A., Madramootoo, C.A., 2006. Effect of land management on runoff and soil
1061 losses from two small watersheds in St Lucia. *L. Degrad. Dev.* 17, 55–72.
1062 doi:10.1002/lde.694
- 1063 Craig, P., 2009. Natural History Guide to American Samoa. National Park of American Samoa,
1064 Pago Pago, American Samoa.

- 1065 ~~Curtis, S., Wetzel, L., Wiles, P., Tinitili, R., 2011. Turbidity in Faga'alu Stream: The Sources,~~
1066 ~~Impacts, and Solutions.~~
- 1067 Daly, C., Halbleib, M., Smith, J.I., Gibson, W.P., Doggett, M.K., Taylor, G.H., Curtis, J.,
1068 Passteris, P.P., 2008. Physiographically sensitive mapping of climatological temperature
1069 and precipitation across the conterminous United States. Int. J. Climatol. 28, 2031.
1070 doi:10.1002/joc
- 1071 Dames & Moore, 1981. Hydrologic Investigation of Surface Water for Water Supply and
1072 Hydropower.
- 1073 Douglas, I., 1996. The impact of land-use changes, especially logging, shifting cultivation,
1074 mining and urbanization on sediment yields in humid tropical Southeast Asia: A review
1075 with special reference to Borneo. IAHS-AISH Publ. 236, 463–471.
- 1076 ~~Dunne, T., Leopold, L.B., 1978. Water in environmental planning. W.H. Freeman and Company,~~
1077 ~~New York.~~
- 1078 ~~Duvert, C., Gratiot, N., 2010. Construction of the stage-discharge rating curve and the SSC-~~
1079 ~~turbidity calibration curve in San Antonio Coapa 2009 hydrological season.~~
- 1080 Duvert, C., Nord, G., Gratiot, N., Navratil, O., Nadal-Romero, E., Mathys, N., Némery, J.,
1081 Regués, D., García-Ruiz, J.M., Gallart, F., Esteves, M., 2012. Towards prediction of
1082 suspended sediment yield from peak discharge in small erodible mountainous catchments
1083 (0.45–22 km²) of France, Mexico and Spain. J. Hydrol. 454-455, 42–55.
1084 doi:10.1016/j.jhydrol.2012.05.048

- 1085 | ~~Eyre, P.R., 1989. Ground water quality reconnaissance, Tutuila, American Samoa, U.S.~~
- 1086 | ~~Geological Survey Water Resources Investigations Report 94-4142. Honolulu, HI.~~
- 1087 | Fabricius, K.E., 2005. Effects of terrestrial runoff on the ecology of corals and coral reefs:
1088 | review and synthesis. Mar. Pollut. Bull. 50, 125–46. doi:10.1016/j.marpolbul.2004.11.028
- 1089 | Fahey, B.D., Marden, M., 2000. Sediment yields from a forested and a pasture catchment,
1090 | coastal Hawke's Bay, North Island, New Zealand. J. Hydrol. 39, 49–63.
- 1091 | Fahey, B.D., Marden, M., Phillips, C.J., 2003. Sediment yields from plantation forestry and
1092 | pastoral farming, coastal Hawke's Bay, North Island, New Zealand. J. Hydrol. 42, 27–38.
- 1093 | Fenner, D., Speicher, M., Gulick, S., Aeby, G., Aletto, S.C., Anderson, P., Carroll, B.P.,
1094 | DiDonato, E.M., DiDonato, G.T., Farmer, V., Fenner, D., Gove, J., Gulick, S., Houk, P.,
1095 | Lundblad, E., Nadon, M., Riolo, F., Sabater, M.G., Schroeder, R., Smith, E., Speicher, M.,
1096 | Tuitele, C., Tagarino, A., Vaitautolu, S., Vaoli, E., Vargas-angel, B., Vroom, P., 2008. The
1097 | State of Coral Reef Ecosystems of American Samoa, in: The State of Coral Reef
1098 | Ecosystems of the United States and Pacific Freely Associated States. pp. 307–351.
- 1099 | Ferrier, K.L., Taylor Perron, J., Mukhopadhyay, S., Rosener, M., Stock, J.D., Huppert, K.L.,
1100 | Slosberg, M., 2013. Covariation of climate and long-term erosion rates across a steep
1101 | rainfall gradient on the Hawaiian island of Kaua'i. Bull. Geol. Soc. Am. 125, 1146–1163.
1102 | doi:10.1130/B30726.1
- 1103 | Fuka, D., Walter, M., Archibald, J., Steenhuis, T., Easton, Z., 2014. EcoHydRology.

- 1104 Gellis, A.C., 2013. Factors influencing storm-generated suspended-sediment concentrations and
1105 loads in four basins of contrasting land use, humid-tropical Puerto Rico. *Catena* 104, 39–57.
1106 doi:10.1016/j.catena.2012.10.018
- 1107 Gippel, C.J., 1995. Potential of turbidity monitoring for measuring the transport of suspended
1108 solids in streams. *Hydrol. Process.* 9, 83–97.
- 1109 Gomi, T., Moore, R.D., Hassan, M.A., 2005. Suspended sediment dynamics in small forest
1110 streams of the Pacific Northwest. *J. Am. Water Resour. Assoc.*
- 1111 Gray, J.R., 2014. Measuring Suspended Sediment, in: Ahuja, S. (Ed.), *Comprehensive Water*
1112 *Quality and Purification*. Elsevier, pp. 157–204. doi:10.1016/B978-0-12-382182-9.00012-8
- 1113 Gray, J.R., Glysson, G.D., Turcios, L.M., Schwarz, G.E., 2000. Comparability of Suspended-
1114 Sediment Concentration and Total Suspended Solids Data U.S. Geological Survey Water-
1115 Resources Investigations Report 00-4191. Reston, Va.
- 1116 Harmel, R.D., Cooper, R.J., Slade, R.M., Haney, R.L., Arnold, J.G., 2006. Cumulative
1117 uncertainty in measured streamflow and water quality data for small watersheds. *Trans.*
1118 *Am. Soc. Agric. Biol. Eng.* 49, 689–701.
- 1119 Harmel, R.D., Smith, D.R., King, K.W., Slade, R.M., 2009. Estimating storm discharge and
1120 water quality data uncertainty: A software tool for monitoring and modeling applications.
1121 *Environ. Model. Softw.* 24, 832–842.

- 1122 Harrelson, C.C., Rawlins, C.L., Potyondy, J.P., 1994. Stream channel reference sites: an
1123 illustrated guide to field technique. USDA Forest Service General Technical Report RM-
1124 245. US Department of Agriculture, Fort Collins, CO.
- 1125 Henderson, G.W., Toews, D.A.A., 2001. Using Sediment Budgets to Test the Watershed
1126 Assessment Procedure in Southeastern British Columbia, in: Toews, D.A.A., Chatwin, S.
1127 (Eds.), Watershed Assessment in the Southern Interior of British Columbia. B.C. Ministry
1128 of Forests, Research Branch, Victoria, British Columbia, pp. 189–208.
- 1129 Hettler, J., Irion, G., Lehmann, B., 1997. Environmental impact of mining waste disposal on a
1130 tropical lowland river system: a case study on the Ok Tedi Mine, Papua New Guinea.
1131 Miner. Depos. 32, 280–291. doi:10.1007/s001260050093
- 1132 Hicks, D.M., 1990. Suspended sediment yields from pasture and exotic forest basins, in:
1133 Proceedings of the New-Zealand Hydrological Society Symposium. Auckland, New
1134 Zealand.
- 1135 Hicks, D.M., Hoyle, J., Roulston, H., 2009. Analysis of sediment yields within Auckland region.
1136 ARC Technical Report 2009/064. Prepared by NIWA for Auckland Regional Council.
- 1137 Holst-Rice, S., Messina, A., Biggs, T.W., Vargas-Angel, B., Whitall, D., 2015. Baseline
1138 Assessment of Faga‘alu Watershed: A Ridge to Reef Assessment in Support of Sediment
1139 Reduction Activities. NOAA Coral Reef Conservation Program, Silver Spring, MD.
- 1140 Horsley-Witten, 2011. American Samoa Erosion and Sediment Control Field Guide.

- 1141 Horsley-Witten, 2012. Post-Construction Stormwater Training Memorandum.
- 1142 ~~Izuka, S.K., Giambelluca, T.W., Nullet, M.A., 2005. Potential Evapotranspiration on Tutuila,~~
- 1143 ~~American Samoa. U.S. Geological Survey Scientific Investigations Report 2005-5200.~~
- 1144 ~~Kearns, R., 2013. Personal Communication.~~
- 1145 Kinnell, P.I.A., 2013. Modelling event soil losses using the Q R EI 30 index within RUSLE2.
- 1146 Hydrol. Process. doi:10.1002/hyp
- 1147 Kroon, F.J., Kuhnert, P.M., Henderson, B.L., Wilkinson, S.N., Kinsey-Henderson, A., Abbott,
- 1148 B., Brodie, J.E., Turner, R.D.R., 2012. River loads of suspended solids, nitrogen,
- 1149 phosphorus and herbicides delivered to the Great Barrier Reef lagoon. Mar. Pollut. Bull. 65,
- 1150 167–81. doi:10.1016/j.marpolbul.2011.10.018
- 1151 Latinis, D.K., Moore, J., Kennedy, J., 1996. Archaeological Survey and Investigations
- 1152 Conducted at the Faga'alu Quarry, Ma'oputasi County, Tutuila, American Samoa, February
- 1153 1996: Prepared for George Poysky, Sr., Samoa Maritime, PO Box 418, Pago Pago,
- 1154 American Samoa, 96799. Archaeological Consultants of the Pacific Inc., 59-624 Pupukea
- 1155 Rd., Haleiwa, HI 96712.
- 1156 Lewis, J., 1996. Turbidity-controlled suspended sediment sampling for runoff-event load
- 1157 estimation. Water Resour. Res. 32, 2299–2310.
- 1158 Lewis, J., Mori, S.R., Keppeler, E.T., Ziemer, R.R., 2001. Impacts of Logging on Storm Peak
- 1159 Flows , Flow Volumes and Suspended Sediment Loads in Caspar Creek, CA, in: Land Use

- 1160 and Watersheds: Human Influence on Hydrology and Geomorphology in Urban and Forest
1161 Areas. pp. 1–76.
- 1162 McDougall, I., 1985. Age and Evolution of the Volcanoes of Tutuila American Samoa. Pacific
1163 Sci. 39, 311–320.
- 1164 Megahan, W.F., 1980. Erosion from roadcuts in granitic slopes of the Idaho Batholith, in:
1165 Proceedings Cordilleran Sections of the Geological Society of America, 76th Annual
1166 Meeting. Oregon State University, Corvallis, OR, p. 120.
- 1167 Megahan, W.F., Wilson, M., Monsen, S.B., 2001. Sediment production from granitic cutslopes
1168 on forest roads in Idaho, USA. Earth Surf. Process. Landforms 26, 153–163.
- 1169 Menking, J. a., Han, J., Gasparini, N.M., Johnson, J.P.L., 2013. The effects of precipitation
1170 gradients on river profile evolution on the Big Island of Hawai'i. Bull. Geol. Soc. Am. 125,
1171 594–608. doi:10.1130/B30625.1
- 1172 Milliman, J.D., Syvitski, J.P.M., 1992. Geomorphic/tectonic control of sediment discharge to the
1173 ocean: the importance of small mountainous rivers. J. Geol. 100, 525–544.
- 1174 Nakamura, S., 1984. Soil Survey of American Samoa. US Department of Agriculture Soil
1175 Conservation Service, Pago Pago, American Samoa.
- 1176 Nathan, R.J., McMahon, T. a, 1990. Evaluation of Automated Techniques for Base Flow and
1177 Recession Analyses. Water Resour. Res. 26, 1465–1473. doi:10.1029/WR026i007p01465

1178 Nearing, M. a, Nichols, M.H., Stone, J.J., Renard, K.G., Simanton, J.R., 2007. Sediment yields
1179 from unit-source semiarid watersheds at Walnut Gulch. Water Resour. Res. 43, 1–10.
1180 doi:10.1029/2006WR005692

1181 ~~NOAA's Ocean Service, Coastal Services Center, 2010. 2010 C-CAP Land Cover, Territory of~~
1182 ~~American Samoa, Tutuila.~~

1183 Perreault, J., 2010. Development of a Water Budget in a Tropical Setting Accounting for
1184 Mountain Front Recharge: Tutuila, American Samoa. University of Hawai'i.

1185 Perroy, R.L., Bookhagen, B., Chadwick, O. a., Howarth, J.T., 2012. Holocene and Anthropocene
1186 Landscape Change: Arroyo Formation on Santa Cruz Island, California. Ann. Assoc. Am.
1187 Geogr. 102, 1229–1250. doi:10.1080/00045608.2012.715054

1188 Ramos-Scharrón, C.E., Macdonald, L.H., 2005. Measurement and prediction of sediment
1189 production from unpaved roads, St John, US Virgin Islands. Earth Surf. Process. Landforms
1190 30, 1283–1304.

1191 Ramos-Scharrón, C.E., Macdonald, L.H., 2007. Measurement and prediction of natural and
1192 anthropogenic sediment sources, St. John, US Virgin Islands. Catena 71, 250–266.

1193 Rankl, J.G., 2004. Relations Between Total-Sediment Load and Peak Discharge for Rainstorm
1194 Runoff on Five Ephemeral Streams in Wyoming. U.S. Geological Survey Water-Resources
1195 Investigations Report 02-4150. Denver, CO.

- 1196 Rapp, A., 1960. Recent development of mountain slopes in Karkevagge and surroundings,
1197 northern Scandinavia. *Geogr. Ann.* 42, 65–200.
- 1198 Reid, L.M., Dunne, T., 1984. Sediment production from forest road surfaces. *Water Resour. Res.*
1199 20, 1753–1761.
- 1200 Reid, L.M., Dunne, T., 1996. Rapid evaluation of sediment budgets. *Catena Verlag*, Reiskirchen,
1201 Germany.
- 1202 Risk, M.J., 2014. Assessing the effects of sediments and nutrients on coral reefs. *Curr. Opin.*
1203 *Environ. Sustain.* 7, 108–117. doi:10.1016/j.cosust.2014.01.003
- 1204 Rodrigues, J.O., Andrade, E.M., Ribeiro, L.A., 2013. Sediment loss in semiarid small watershed
1205 due to the land use. *Rev. Ciênc. Agronômica* 44, 488–498.
- 1206 Sadeghi, S.H.R., Mizuyama, T., Miyata, S., Gomi, T., Kosugi, K., Mizugaki, S., Onda, Y., 2007.
1207 Is MUSLE apt to small steeply reforested watershed? *J. For. Res.* 12, 270–277.
1208 doi:10.1007/s10310-007-0017-9
- 1209 Slaymaker, O., 2003. The sediment budget as conceptual framework and management tool.
1210 *Hydrobiologia* 494, 71–82.
- 1211 Stock, J.D., Rosener, M., Schmidt, K.M., Hanshaw, M.N., Brooks, B.A., Tribble, G., Jacobi, J.,
1212 2010. Sediment budget for a polluted Hawaiian reef using hillslope monitoring and process
1213 mapping, in: American Geophysical Union Fall Meeting. p. #EP22A–01.

- 1214 Stock, J.D., Tribble, G., 2010. Erosion and sediment loads from two Hawaiian watersheds, in:
1215 2nd Joint Federal Interagency Conference. Las Vegas, NV.
- 1216 Storlazzi, C.D., Norris, B.K., Rosenberger, K.J., 2015. The influence of grain size, grain color,
1217 and suspended-sediment concentration on light attenuation: Why fine-grained terrestrial
1218 sediment is bad for coral reef ecosystems. *Coral Reefs* 34, 967–975. doi:10.1007/s00338-
1219 015-1268-0
- 1220 Syvitski, J.P.M., Vörösmarty, C.J., Kettner, A.J., Green, P., 2005. Impact of humans on the flux
1221 of terrestrial sediment to the global coastal ocean. *Science* (80-.). 308, 376–380.
1222 doi:10.1126/science.1109454
- 1223 Thomas, S., Ridd, P. V, Day, G., 2003. Turbidity regimes over fringing coral reefs near a mining
1224 site at Lihir Island, Papua New Guinea. *Mar. Pollut. Bull.* 46, 1006–14. doi:10.1016/S0025-
1225 326X(03)00122-X
- 1226 Tonkin & Taylor International Ltd., 1989. Hydropower feasibility studies interim report - Phase
1227 1. Ref: 97/10163.
- 1228 Topping, J., 1972. Errors of Observation and their Treatment, 4th ed. Chapman and Hall,
1229 London, UK.
- 1230 Tropeano, D., 1991. High flow events, sediment transport in a small streams in the “Tertiary
1231 Basin” area in Piedmont (northwest Italy). *Earth Surf. Process. Landforms* 16, 323–339.

- 1232 Turnipseed, D.P., Sauer, V.B., 2010. Discharge Measurements at Gaging Stations, in: U.S.
1233 Geological Survey Techniques and Methods Book 3, Chap. A8. Reston, Va., p. 87.
- 1234 ~~URS Company, 1978. American Samoa Water Resources Study: Assessment of Water Systems~~
1235 ~~American Samoa Coastal Zone Information Center, Honolulu, HI.~~
- 1236 Walling, D.E., 1977. Assessing the accuracy of suspended sediment rating curves for a small
1237 basin. *Water Resour. Res.* 13, 531–538.
- 1238 Walling, D.E., 1999. Linking land use, erosion and sediment yields in river basins.
1239 *Hydrobiologia* 410, 223–240.
- 1240 Walling, D.E., Collins, a. L., 2008. The catchment sediment budget as a management tool.
1241 *Environ. Sci. Policy* 11, 136–143. doi:10.1016/j.envsci.2007.10.004
- 1242 Wemple, B.C., Jones, J.A., Grant, G.E., 1996. Channel Network Extension by Logging Roads in
1243 Two Basins, Western Cascades, Oregon. *Water Resour. Bull.* 32, 1195–1207.
- 1244 ~~West, K., van Woesik, R., 2001. Spatial and temporal variance of river discharge on Okinawa~~
1245 ~~(Japan): inferring the temporal impact on adjacent coral reefs. Mar. Pollut. Bull.~~ 42, 864–
1246 ~~72.~~
- 1247 Wolman, M.G., Schick, A.P., 1967. Effects of construction on fluvial sediment, urban and
1248 suburban areas of Maryland. *Water Resour. Res.* 3, 451–464.
- 1249 Wong, M., 1996. Analysis of Streamflow Characteristics for Streams on the Island of Tutuila,
1250 American Samoa. U.S. Geological Survey Water-Resources Investigations Report 95-4185.

- 1251 Wulf, H., Bookhagen, B., Scherler, D., 2012. Climatic and geologic controls on suspended
1252 sediment flux in the Sutlej River Valley, western Himalaya. *Hydrol. Earth Syst. Sci.* 16,
1253 2193–2217. doi:10.5194/hess-16-2193-2012
- 1254 Zimmermann, A., Francke, T., Elsenbeer, H., 2012. Forests and erosion: Insights from a study of
1255 suspended-sediment dynamics in an overland flow-prone rainforest catchment. *J. Hydrol.*
1256 170–181.

1257 |

1258 | APPENDIX 1. Dams in Faga'alu watershed

1259 | Faga'alu stream was dammed at 4 locations above the village: 1) Matafao Dam (elevation
1260 | 244 m) near the base of Mt. Matafao, draining 0.20 km², 2) Vaitanoa Dam at Virgin Falls
1261 | (elevation 140 m), draining an additional 0.44 km², 3) a small unnamed dam below Vaitanoa
1262 | Dam at elevation 100m, and 4) Lower Faga'alu Dam (elevation 48 m), immediately upstream of
1263 | a large waterfall 30 m upstream of the quarry, draining an additional 0.26 km² (Tonkin & Taylor
1264 | International Ltd., 1989). A 2012 aerial LiDAR survey (Photo Science, Inc.) indicates the
1265 | drainage area at the Lower Faga'alu Dam is 0.90 km². A small stream capture/reservoir (~35 m³)
1266 | is also present on a side tributary that joins Faga'alu stream on the south bank, opposite the
1267 | quarry. It is connected to a ~6 cm diameter pipe but it is unknown when or by whom it was built,
1268 | its initial capacity, or if it is still conveying water. During all site visits water was overtopping
1269 | this small structure through the spillway crest, suggesting it is fed by a perennial stream.

1270 | Matafao Dam was constructed in 1917 for water supply to the Pago Pago Navy base,
1271 | impounding a reservoir with initial capacity of 1.7 million gallons (6,400 m³) and piping the flow
1272 | out of the watershed to a hydropower and water filtration plant in Fagatogo. In the early 1940's
1273 | the Navy replaced the original cement tube pipeline and hydropower house with cast iron pipe
1274 | but it is unknown when the scheme fell out of use (Tonkin & Taylor International Ltd., 1989;
1275 | URS Company, 1978). Remote sensing and a site visit on 6/21/13 confirmed the reservoir is still
1276 | filling to the spillway crest with water and routing some flow to the Fagatogo site, though the
1277 | amount is much less than the 10 in. diameter pipes conveyance capacity and the flow rate
1278 | variability is unknown. A previous site visit on 2/21/13 by American Samoa Power Authority
1279 | (ASPA) found the reservoir empty of water but filled with an estimated 3-5 meters of fine
1280 | sediment (Kearns, 2013). Interviews with local maintenance staff and historical photos

1281 confirmed the Matafao Reservoir was actively maintained and cleaned of sediment until the early
1282 70's.

1283 The Vaitanoa (Virgin Falls) Dam, was built in 1964 to provide drinking water but the
1284 pipe was not completed as of 10/19/89, and a stockpile of some 40 (8 ft. length) 8 in. diameter
1285 asbestos cement pipes was found on the streambanks. Local quarry staff recall the pipes were
1286 removed from the site sometime in the 1990's. The Vaitanoa Reservoir had a design volume of
1287 4.5 million gallons ($17,000\text{m}^3$), but is assumed to be full of sediment since the drainage valves
1288 were never opened and the reservoir was overtopping the spillway as of 10/18/89 (Tonkin &
1289 Taylor International Ltd., 1989). A low masonry weir was also constructed downstream of the
1290 Vaitanoa Dam, but not connected to any piping.

1291 The Lower Faga'alu Dam was constructed in 1966/67 just above the Samoa Maritime,
1292 Ltd. Quarry, as a source of water for the LBJ Medical Centre. It is unknown when this dam went
1293 out of use but in 1989 the 8 in. conveyance pipe was badly leaking and presumed out of service.
1294 The 8 in. pipe disappears below the floor of the Samoa Maritime quarry and it is unknown if it is
1295 still conveying water or has plugged with sediment. The derelict filtration plant at the entrance to
1296 the quarry was disconnected prior to 1989 (Tonkin & Taylor International Ltd., 1989). The
1297 original capacity was 0.03 million gallons (114 m^3) but is now full of coarse sediment up to the
1298 spillway crest. No reports were found indicating this structure was ever emptied of sediment.

1299 APPENDIX 2. Stream gaging in Faga'alu Watershed

1300 Stream gaging sites were chosen to take advantage of an existing control structure at FG1
1301 (Figure A2.1) and a stabilized stream cross section at FG3 (Figure A2.2)(Duvert and Gratiot,
1302 2010). At FG1 and FG3, Q was calculated from 15 minute interval stream stage measurements,
1303 using a stage-Q rating curve calibrated to manual Q measurements made under baseflow and

1304 stormflow conditions (Figures A2.3 and A2.4). Stream stage was measured with non-vented
1305 pressure transducers (PT) (Solinst Levelogger or Onset HOBO Water Level Logger) installed in
1306 stilling wells at FG1 and FG3. Barometric pressure data collected at Wx were used to calculate
1307 stage from the pressure data recorded by the PT. Data gaps in barometric pressure from Wx were
1308 filled by data from stations at Pago Pago Harbor (NSTP6) and NOAA Climate Observatory at
1309 Tula (TULA) (Figure 1). Priority was given to the station closest to the watershed with valid
1310 barometric pressure data. Barometric data were highly correlated and the data source made little
1311 (\leq 1cm) difference in the resulting water level. Q was measured in the field by the area velocity
1312 method (AV) using a Marsh-McBirney flowmeter to measure flow velocity and channel surveys
1313 measure cross-sectional area (Harrelson et al., 1994; Turnipseed and Sauer, 2010).

1314 AV-Q measurements could not be made at high stages at FG1 and FG3 for safety
1315 reasons, so stage-Q relationships were constructed to estimate a continuous record of Q. At FG3,
1316 the channel is rectangular with stabilized rip rap on the banks and bed (Figure A2.2). Recorded
1317 stage varied from 4 to 147 cm. AV-Q measurements ($n=14$) were made from 30 to 1,558.0
1318 L/sec, covering a range of stages from 6 to 39 cm. The highest recorded stage was much higher
1319 than the highest stage with measured Q so the rating could not be extrapolated by a power law.
1320 Stream conditions at FG3 fit the assumption for Manning's equation, so the stage-Q rating at
1321 FG3 was created using Manning's equation, calibrating Manning's n (0.067) to the Q
1322 measurements (Figure A2.3).

1323 At FG1, the flow control structure is a masonry ogee spillway crest of a defunct stream
1324 capture. The structure is a rectangular channel 43 cm deep that transitions abruptly to gently
1325 sloping banks, causing an abrupt change in the stage-Q relationship (Figure A2.1). At FG1,
1326 recorded stage height ranged from 4 to 120 cm, while area velocity Q measurements ($n=22$)

1327 covered stages from 6 to 17 cm. Since the highest recorded stage (120 cm) was higher than the
1328 highest stage with measured Q (17 cm), and there was a distinct change in channel geometry
1329 above 43 cm the rating could not be extrapolated by a power law. The flow structure did not
1330 meet the assumptions for using Manning's equation to predict flow so the HEC-RAS model was
1331 used (Brunner, 2010). The surveyed geometry of the upstream channel and flow structure at FG1
1332 were input to HEC-RAS, and the HEC-RAS model was calibrated to the Q measurements
1333 (Figure A2.4). While a power function fit Q measurements better than HEC-RAS for low flow,
1334 HEC-RAS fit better for Q above the storm threshold used in analyses of SSY (Figure A2.4).

1335 APPENDIX 3. Water discharge during storm events

1336 Insert Table A3.1 here

1337 APPENDIX 4. Turbidity-Suspended Sediment Concentration rating curves for turbidimeters 1338 in Faga'alu

1339 Turbidity (T) was measured at FG1 and FG3 using three types of turbidimeters: 1)
1340 Greenspan TS3000 (TS), 2) YSI 6000 OMS with 6136 turbidity probe (YSI), and 3) Campbell
1341 Scientific OBS500 (OBS). All turbidimeters were permanently installed in protective PVC
1342 housings near the streambed where the turbidity probe would be submerged at all flow
1343 conditions, with the turbidity probe oriented downstream. Despite regular maintenance, debris
1344 fouling during storm and baseflows was common and caused data loss during several storm
1345 events. Storm events with incomplete or invalid T data were not used in the analysis. A three-
1346 point calibration was performed on the YSI turbidimeter with YSI turbidity standards (0, 126,
1347 and 1000 NTU) at the beginning of each field season and approximately every 3–6 months
1348 during data collection. Turbidity measured with 0, 126, and 1000 NTU standards differed by less

1349 than 10% (4.8%) during each recalibration. The OBS requires calibration every two years, so
1350 recalibration was not needed during the study period. All turbidimeters were cleaned following
1351 storms to ensure proper operation.

1352 At FG3, a YSI turbidimeter recorded T (NTU) at 5 min intervals from January 30, 2012,
1353 to February 20, 2012, and at 15 min intervals from February 27, 2012 to May 23, 2012, when it
1354 was damaged during a large storm. The YSI turbidimeter was replaced with an OBS, which
1355 recorded Backscatter (BS) and Sidescatter (SS) at 5 min intervals from March 7, 2013, to July
1356 15, 2014 (OBSa), and was resampled to 15 min intervals. No data was recorded from August
1357 2013–January 2014 when the wiper clogged with sediment. A new OBS was installed at FG3
1358 from January, 2014, to August, 2014 (OBSb). To correct for some periods of high noise
1359 observed in the BS and SS data recorded by the OBSa in 2013, the OBSb installed in 2014 was
1360 programmed to make a burst of 100 BS and SS measurements at 15 min intervals, and record
1361 Median, Mean, STD, Min, and Max. All BS and SS parameters were analyzed to determine
1362 which showed the best relationship with SSC. Mean SS showed the highest r^2 and is a physically
1363 comparable measurement to NTU measured by the YSI and TS (Anderson, 2005).

1364 At FG1, the TS turbidimeter recorded T (NTU) at 5 min intervals from January 2012
1365 until it was vandalized and destroyed in July 2012. The YSI turbidimeter, previously deployed at
1366 FG3 in 2012, was repaired and redeployed at FG1 and recorded T (NTU) at 5 min intervals from
1367 June 2013 to October 2013, and January 2014 to August 2014. T data was resampled to 15 min
1368 intervals to compare with SSC samples for the T–SSC relationship, and to correspond to Q for
1369 calculating SSY.

1370 The T–SSC relationship can be unique to each region, stream, instrument or even each
1371 storm event (Lewis et al., 2001), and can be influenced by water color, dissolved solids and

1372 organic matter, temperature, and the shape, size, and composition of sediment. However, T has
1373 proved to be a robust surrogate measure of SSC in streams (Gippel, 1995), and is most accurate
1374 when a unique T-SSC relationship is developed for each instrument separately, using in-situ grab
1375 samples under storm conditions (Lewis, 1996). A unique T-SSC relationship was developed for
1376 each turbidimeter, at each location, using 15 min interval T data and SSC samples from storm
1377 periods only (Figure A4.1). A "synthetic" T-SSC relationship was also developed by placing the
1378 turbidimeter in a black tub with water, and sampling T and SSC as sediment was added (Figure
1379 4.2), but results were not comparable to T-SSC relationships developed under actual storm
1380 conditions and were not used in further analyses.

1381 The T-SSC relationships varied among sampling sites and sensors but all showed acceptable r^2
1382 values (0.79–0.99). Lower scatter was achieved by using grab samples collected during
1383 stormflows only. For the TS (not shown) and YSI deployed at FG1, the r^2 values were high
1384 (0.58, 0.99) but the ranges of T and SSC values used to develop the relationships were
1385 considered too small (0–16 NTU) compared to the maximum observed during the deployment
1386 period (1,077 NTU) to develop a robust relationship for higher T values. Instead, the T-SSC
1387 relationship developed for the YSI turbidimeter installed at FG3 (Figure A4.1a) was used to
1388 calculate SSC from T data collected by the TS and the YSI at FG1. For the YSI turbidimeter,
1389 more scatter was observed in the T-SSC relationship at FG3 than at FG1 (Figure A4.1a), which
1390 could be attributed to the higher number and wider range of values sampled, and to temporal
1391 variability in sediment characteristics. The OBSa and OBSb turbidimeters had high r^2 values
1392 (0.82, 0.93) and compared well between the two periods of deployment (Figure A4.1b).

1 TITLE:

2 Contributions of human activities to suspended sediment yield during storm events

3 from a small, steep, tropical watershed

4 Authors:

5 Messina, A.M.^{a*}, Biggs, T.W.^a

⁶ ^a San Diego State University, Department of Geography, San Diego, CA 92182,

7 amessina@rohan.sdsu.edu, +1-619-594-5437, tbiggs@mail.sdsu.edu, +1-619-594-0902

ABSTRACT

Suspended sediment concentrations (SSC) and yields (SSY) were measured during storm and non-storm periods from undisturbed and human-disturbed portions of a small (1.8 km^2), mountainous watershed that drains to a sediment-stressed coral reef. Event-wise SSY (SSY_{EV}) was calculated for 142 storms from measurements of water discharge (Q), turbidity (T), and SSC measured downstream of three key sediment sources: undisturbed forest, an aggregate quarry, and a village. SSC and SSY_{EV} were significantly higher downstream of the quarry during both storm- and non-storm periods. The human-disturbed subwatershed accounted for an average of 71-87% of SSY_{EV} from the total watershed, and has increased loads to the coast by 3.9x over natural background. Specific SSY (tons/area) from the disturbed quarry area was 49x higher than from natural forest compared with 8x higher from the village. The quarry, which covers 1.1% of the total watershed area, contributed 36% of total SSY_{EV} at the outlet. Similar to mountainous watersheds in semi-arid and temperate climates, SSY_{EV} from both the undisturbed and disturbed watersheds correlated closely with maximum event discharge (Q_{max}), event total precipitation and event total Q, but not with a precipitation erosivity index. Best estimates of annual SSY_{EV}

23 varied from 41-61 tons/yr (45-68 tons/km²/yr) from the undisturbed subwatershed, 310-388
24 tons/yr (350-441 tons/km²/yr) from the human-disturbed subwatershed, and 360-439 tons/yr
25 (200-247 tons/km²/yr) from the total watershed. Sediment yield was very sensitive to
26 disturbance; only 5.2% of the watershed is disturbed by humans but sediment yield increased
27 significantly (3.9x). While unpaved roads are often identified as a source of sediment in humid
28 forested regions, field observations suggested that most roads in the urban area were paved or
29 stabilized with aggregate. Repeated surface disturbance at the quarry is a key process
30 maintaining high rates of sediment generation. Given the large distance to other sources of
31 building material, aggregate mining and associated sediment disturbance may be a critical
32 sediment source on remote islands in the Pacific and elsewhere. Identification of sediment
33 hotspots like the quarry using rapid, event-wise measures of suspended sediment yield will help
34 efforts to mitigate sediment loads and restore coral reefs.

35 **Keywords:**

36 Sediment yield, volcanic islands, land use, storm events, coastal sediment load, American Samoa

37 **1. Introduction**

38 Human activities including deforestation, agriculture, road construction, mining, and
39 urbanization alter the timing, composition, and amount of sediment loads to downstream
40 ecosystems (Syvitski et al., 2005). Increased sediment loads can stress aquatic ecosystems,
41 including coral reefs that occur near the outlets of impacted watersheds. Sediment impacts coral
42 by decreasing light for photosynthesis and increasing sediment accumulation rates (Fabricius,
43 2005; Storlazzi et al., 2015). Anthropogenic sediment disturbance can be particularly high on
44 volcanic islands in the humid tropics, which have a high potential for erosion due to high rainfall,

45 extreme weather events, steep slopes, and erodible soils. Sediment yield in densely vegetated
46 watersheds can be particularly sensitive to land clearing, which alters the fraction of exposed soil
47 more than in sparsely-vegetated regions. The steep topography and small floodplains on small
48 volcanic islands further limits sediment storage and the capacity of the watershed to buffer
49 increased hillslope sediment supply. Such environments characterize many volcanic islands in
50 the south Pacific where coral reefs are impacted by sediment.

51 A large proportion of a watershed's sediment yield can originate from disturbed areas that
52 cover a relatively small fraction of the watershed area. Unpaved roads covering 0.3-0.9% of the
53 watershed area were the dominant sediment source in disturbed watersheds on St. John in the
54 Caribbean, and increased sediment yield to the coast by 5-9 times relative to undisturbed
55 watersheds (Ramos-Scharrón and Macdonald, 2007). In the Pacific Northwest of the United
56 States, several studies found most road-generated sediment can originate from just a small
57 fraction of unpaved roads (Gomi et al., 2005; Henderson and Toews, 2001; Megahan et al., 2001;
58 Wemple et al., 1996), and heavily used roads could generate 130 times as much sediment as
59 abandoned roads (Reid and Dunne, 1984). In a watershed disturbed by grazing on Molokai,
60 Hawaii, less than 5% of the land produces most of the sediment, and only 1% produces
61 approximately 50% of the sediment (Risk, 2014; Stock et al., 2010), suggesting that management
62 should focus on identifying, quantifying, and mediating erosion hotspots.

63 Sediment management requires linking land use changes and mitigation strategies to
64 changes in sediment yields at the watershed outlet (Walling and Collins, 2008). A sediment
65 budget quantifies sediment as it moves from key sources like hillslope erosion, channel-bank
66 erosion, and mass movements, to its eventual exit from a watershed (Rapp, 1960). Walling
67 (1999) used a sediment budget to show that sediment yield from watersheds can be insensitive to

68 both land use change and erosion management due to high sediment storage capacity on
69 hillslopes and in the channel. Sediment yield from disturbed areas can be large but may not be
70 important compared to naturally high yields from undisturbed areas. While a full description of
71 all sediment production and transport processes are of scientific interest, the sediment budget
72 needs to be simplified to be used as a management tool (Slaymaker, 2003). Most management
73 applications require only that the order of magnitude or the relative importance of process rates
74 be known, so Reid and Dunne (1996) argue a management-focused sediment budget can be
75 developed quickly in situations where the management problem is clearly defined and the
76 management area can be divided into homogenous sub-units.

77 Knowledge of suspended sediment yield (SSY) under both natural and disturbed
78 conditions on most tropical, volcanic islands remains limited, due to the challenges of in situ
79 monitoring in these remote, challenging environments. The limited data has also made it difficult
80 to develop reliable sediment yield models for ungauged watersheds. Existing sediment yield
81 models are often designed for agricultural landscapes and are not well-calibrated to the climatic,
82 topographic, and geologic conditions found on steep, tropical islands. Most readily available
83 models also do not incorporate many of the important processes that generate sediment in steep
84 watersheds, including mass movements (Calhoun and Fletcher, 1999; Ramos-Scharrón and
85 Macdonald, 2005; Sadeghi et al., 2007). Developing models that predict SSY_{EV} from small,
86 mountainous catchments is a significant contribution for establishing baselines for change-
87 detection for sediment mitigation projects, and can also further improve models applied at the
88 regional scale (Duvert et al., 2012).

89 Traditional approaches to quantifying human impact on sediment budgets, including
90 comparison of total annual yields (Fahey et al., 2003) and sediment rating curves (Asselman,

91 2000; Walling, 1977), are complicated by interannual climatic variability and hysteresis in the
92 discharge-concentration relationship. Sediment yield can be highly variable over various time
93 scales, even under natural conditions. At geologic time scales, if an undisturbed watershed is not
94 in a steady-state condition, sediment yields may decrease over time as it reaches equilibrium, or
95 the sediment contributions from different subwatersheds may change with time (Ferrier et al.,
96 2013; Perroy et al., 2012). At decadal scales, cyclical climatic variability like El Nino-Southern
97 Oscillation (ENSO) events or Pacific Decadal Oscillation (PDO) patterns can significantly alter
98 sediment yield from undisturbed watersheds (Wulf et al., 2012).

99 As an alternative to comparing annual sediment loads, SSY generated by storm events of
100 the same magnitude can be compared to assess the contribution of individual subwatersheds to
101 total SSY (Zimmermann et al., 2012), determine changes in SSY from the same watershed over
102 time (Bonta, 2000), and compare the responses of different watersheds to various precipitation or
103 discharge variables ("storm metrics") (Basher et al., 2011; Duvert et al., 2012; Fahey et al., 2003;
104 Hicks, 1990). Event-wise SSY (SSY_{EV}) may correlate with storm metrics such as total
105 precipitation, the Erosivity Index (Kinnell, 2013), or total discharge, but the best correlation has
106 consistently been found with maximum event discharge (Qmax). Several researchers have
107 hypothesized that Qmax integrates the hydrological response of a watershed, making it a good
108 predictor of SSY_{EV} in diverse environments (Duvert et al., 2012; Rankl, 2004). High correlation
109 between SSY_{EV} and Qmax has been found in semi-arid, temperate, and sub-humid watersheds in
110 Wyoming (Rankl, 2004), Mexico, Italy, France (Duvert et al., 2012), and New Zealand (Basher
111 et al., 2011; Hicks, 1990), but this approach has not been attempted for steep, tropical watersheds
112 on volcanic islands.

113 The anthropogenic impact on SSY_{EV} may vary by storm magnitude, as documented in
114 Pacific Northwest forests (Lewis et al., 2001). As storm magnitude increases, water yield and/or
115 SSY_{EV} from natural areas may increase relative to human-disturbed areas, diminishing
116 anthropogenic impact relative to the natural baseline. While large storms account for most SSY
117 under undisturbed conditions, human-disturbed areas may show the largest disturbance,
118 expressed as a percentage increase above the natural background, for smaller storms (Lewis et
119 al., 2001). The disturbance ratio (DR) may be highest for small storms, when background SSY_{EV}
120 from the undisturbed forest is low and erodible sediment from disturbed surfaces is the dominant
121 source. For large storms, mass movements and bank erosion may contribute to naturally high
122 SSY_{EV} from undisturbed watersheds, increasing the background and reducing the DR for large
123 events.

124 This study uses in situ measurements of precipitation (P), stream discharge (Q), turbidity
125 (T) and suspended sediment concentration (SSC) to accomplish three objectives: Objective 1)
126 Quantify suspended sediment concentrations (SSC) and yields (SSY) from undisturbed and
127 human-disturbed portions of a small watershed in the south Pacific during storm and non-storm
128 periods. The research questions addressed under this objective include: How much has human
129 disturbance increased suspended sediment yield to the coast during storm events? What human
130 activities dominate the anthropogenic contribution to suspended sediment yield? How do
131 concentrations vary between storm and non-storm periods? Objective 2) Develop an empirical
132 model of SSY during storm events (SSY_{EV}). This objective will answer the questions: Which
133 storm metric is the best predictor of SSY_{EV}: total event precipitation, Erosivity Index, total event
134 discharge, or maximum event discharge? How do sediment contributions from undisturbed areas
135 and human-disturbed areas vary with storm size? Objective 3) Estimate annual sediment yields

136 and compare with other volcanic tropical islands. This objective will use the results from
137 Objective 2 to model annual sediment load from the study watersheds, for comparison with other
138 literature on volcanic tropical islands and disturbed watersheds.

139 **2. Study Area**

140 The study watershed, Faga'alu, is located on Tutuila (14S, 170W), American Samoa.
141 Tutuila has steep, heavily forested mountains with villages and roads mostly confined to the flat
142 areas near the coast. The main stream in Faga'alu (~3 km) drains an area of 1.78 km² into
143 Faga'alu Bay (area draining to FG3 in Figure 1). The mean slope of the main Faga'alu watershed
144 is 0.53 m/m and total relief is 653 m. The administrative boundary of Faga'alu includes the
145 watersheds of the main stream and several small ephemeral streams that drain directly to the bay
146 (0.63 km²) (grey dotted boundary in Figure 1). The coral reef in Faga'alu Bay is highly degraded
147 by sediment (Fenner et al., 2008), and Faga'alu watershed was selected by the US Coral Reef
148 Task Force (USCRTF) as a Priority Watershed for conservation and remediation efforts (Holst-
149 Rice et al., 2015).

150 <Figure 1 here please>

151 Faga'alu occurs on intracaldera Pago Volcanics formed about 1.20 Mya (McDougall,
152 1985). Soil types in the steep uplands are rock outcrops (15%) with well-drained Lithic
153 Hapludolls ranging from silty clay to clay loams 20-150 cm deep (Nakamura, 1984). Soils in the
154 lowlands include a mix of deep (>150 cm), well drained very stony silty clay loams, and poorly
155 drained silty clay to fine sandy loam along streams and valley bottoms.

156 **2.1 Climate**

157 Annual precipitation in Faga'alu watershed is 6,350 mm at Matafao Mtn. (653 m m.a.s.l),
158 5,280 mm at Matafao Reservoir (249 m m.a.s.l.) and about 3,800 mm on the coastal plain (Craig,
159 2009; Dames & Moore, 1981; Perreault, 2010; Tonkin & Taylor International Ltd., 1989; Wong,
160 1996). There are two subtle rainfall seasons: a drier winter season from June through September
161 that accounts for 25% of annual precipitation and a wetter summer season, from October through
162 May (Perreault, 2010; data from USGS rain gauges and Parameter-elevation Relationships on
163 Independent Slopes Model (PRISM) Climate Group (Daly et al., 2008)). While total rainfall is
164 lower in the drier season, large storm events are still observed. At 11 sites around the island, 35%
165 of annual peak flows occurred during the drier season over 1959-1990 (Wong, 1996).

166 **2.2 Land Cover and Land Use**

167 *2.2.1. Vegetation, agriculture, and urban areas*

168 The predominant land cover in Faga'alu watershed is undisturbed vegetation (94.8%),
169 including forest (85.7%) and scrub/shrub (9.0%) on the steep hillsides (Table 1). The upper
170 watershed, draining to FG1 in Figure 1, is dominated by undisturbed rainforest on steep
171 hillslopes. The lower subwatershed, draining areas between FG1 and FG3 in Figure 1, has steep
172 vegetated hillslopes and a relatively small flat area in the valley bottom that is urbanized (3.2%
173 of the watershed area "High Intensity Developed" in Table 1). A small portion of the watershed
174 (0.9%) is developed open space, which includes landscaped lawns and parks. In addition to some
175 small household gardens there are several small agricultural areas of banana and taro on the steep
176 hillsides. These agricultural plots were classified as grassland (0.2% GA, Table 1) due to the
177 high fractional grass cover in the plots. There are several small footpaths and unpaved driveways

178 in the village, but most unpaved roads are stabilized with compacted gravel and do not appear to
179 be a major contributor of sediment (Horsley-Witten, 2012).

180 <Table 1 here please>

181 *2.2.2 Aggregate quarry and reservoirs*

182 An open-pit aggregate quarry covers 1.6 ha and accounts for nearly all of the bare land
183 (1.1% of the watershed) (Table 1). The quarry has been in continuous operation since the 1960's
184 (Latinis et al., 1996). With few sediment runoff controls in place, sediment has been discharged
185 directly to Faga'alu stream. In 2011, the quarry operators installed some sediment runoff
186 management practices such as silt fences and small settling ponds (Horsley-Witten, 2011) but
187 they were unmaintained and inadequate to control the large amount of sediment mobilized
188 during storm events (Horsley-Witten, 2012). During the study period (2012-2014), additional
189 sediment control measures were installed and some large piles of overburden were overgrown by
190 vegetation (Figure 2), altering the sediment availability. In late 2014, large sediment retention
191 ponds were installed to mitigate sediment runoff, but these mitigation activities happened after
192 the sample collection reported here. See Holst-Rice et al. (2015) for a full description of
193 sediment mitigation efforts at the quarry.

194 <Figure 2 here please>

195 Three water impoundment structures were built in the early 20th century in the upper part
196 of the watershed for drinking water supply and hydropower, but none are in use and the one at
197 FG1 is filled with sediment. We assume the other reservoirs are similarly filled with coarse
198 sediment and are not currently retaining fine suspended sediment. A full description of stream
199 impoundments is in Appendix A.

200 **3. Methods**

201 The equations used to accomplish Objectives 1-3 are described in sections 3.1-3.3, and
202 the field methods to measure precipitation, discharge, SSC and SSY are described in section 3.4.

203 **3.1 Objective 1: Compare SSC and SSY_{EV} for disturbed and undisturbed subwatersheds**

204 Stream discharge (Q) and suspended sediment concentrations (SSC) and yields (SSY)
205 were measured during both storm and interstorm periods at three sampling points that define
206 three subwatersheds with different land covers. The UPPER subwatershed drains undisturbed
207 forest and is sampled at point FG1; the LOWER_QUARRY subwatershed is sampled at FG2 and
208 includes the forest and quarry between FG1 and FG2; the LOWER_VILLAGE subwatershed is
209 sampled at FG3 and drains undisturbed forest and the village between FG2 and FG3 (Figure 1;
210 Table 1). FG3 is also the watershed outlet for the TOTAL watershed.

211 ***3.1.1. Calculation of SSY_{EV}***

212 SSY during individual storm events (SSY_{EV}) were calculated for each sample location by
213 integrating continuous estimates of SSY, calculated from measured or modeled water discharge
214 (Q) and measured or modeled suspended sediment concentration (SSC) (Duvert et al., 2012):

$$SSY_{EV} = k \int_{t=0}^T Q(t) * SSC(t) * dt \quad \text{Equation 1}$$

where SSY_{EV} is suspended sediment yield (tons) for an event from $t=0$ at storm start to $T=$ storm end, SSC is suspended sediment concentration (mg/L), and Q is water discharge (L/sec), and k converts from mg to tons (10^{-6}).

215 Storm events can be defined by precipitation (Hicks, 1990) or discharge parameters
216 (Duvert et al., 2012), and the method used to identify storm events on the hydrograph can
217 significantly influence the analysis of SSY_{EV} (Gellis, 2013). Due to the large number of storm

218 events and the prevalence of complex storm events recorded at the study site, we used a digital
219 filter signal processing technique (Nathan and McMahon, 1990) in the R-statistical package
220 EcoHydRology (Fuka et al., 2014). Spurious events were sometimes identified due to instrument
221 noise, so only events with quickflow for at least one hour and peak flow greater than 10% of
222 baseflow were included (See Appendix C for example).

223 *3.1.2. SSY from disturbed and undisturbed portions of subwatersheds*

224 Land cover in the LOWER subwatersheds includes both undisturbed and human-
225 disturbed surfaces. SSY_{EV} from disturbed areas only was estimated as:

$$SSY_{EV_distrb} = SSY_{EV_subws} - (sSSY_{EV_UPPER} * Area_{undist}) \quad \text{Equation 3}$$

where SSY_{EV_distrb} is SSY_{EV} from disturbed areas only (tons), SSY_{EV_subws} is SSY_{EV} (tons) measured from the LOWER subwatershed (e.g. SSY_{EV_FG3}- SSY_{EV_FG2}), $sSSY_{EV_UPPER}$ is specific SSY_{EV} (tons/km²) from the UPPER subwatershed (SSY_{EV_FG1}), and $Area_{undist}$ is the area of undisturbed forest in the LOWER subwatershed (km²). Similar calculations were made for the LOWER_QUARRY and LOWER_VILLAGE subwatersheds to isolate the contributions from the disturbed quarry and village.

226 The disturbance ratio (DR) is the ratio of SSY_{EV} under current conditions to SSY_{EV} under
227 pre-disturbance conditions:

$$DR = \frac{SSY_{EV_subw}}{A_{subw} * sSSY_{EV_UPPER}} \quad \text{Equation 4}$$

where A_{subw} is the area of the subwatershed.

228 Both Equations 3 and 4 assume that sSSY_{EV} from forested areas in the LOWER subwatershed
229 equals sSSY_{EV} from the undisturbed UPPER watershed.

230 *3.1.3. Relationship of sediment load to sediment budget*

231 We use the measured sediment yield at three locations to quantify the in-stream
232 suspended sediment budget. Other components of sediment budgets include channel erosion and
233 or channel and floodplain deposition (Walling and Collins, 2008). Sediment storage and
234 remobilization can significantly complicate the interpretation of in-stream loads, and complicate
235 the identification of a land use signal. In Faga'alu, the channel bed is predominantly large
236 volcanic cobbles and coarse gravel, with no significant deposits of fine sediment. Upstream of
237 the village, the valley is very narrow with no floodplain. In the downstream reaches of the lower
238 watershed, where fines might deposit in the floodplain, the channel has been stabilized with
239 cobble reinforced by fencing, so overbank flows and sediment deposition on the floodplain are
240 not observed. We therefore assume that channel erosion and channel and floodplain deposition
241 are insignificant components of the sediment budget, so the measured sediment yields at the
242 three locations reflect differences in hillslope sediment supply. Minimal sediment storage also
243 reduces the lag time between landscape disturbance and observation of sediment at the watershed
244 outlet.

245 **3.2 Objective 2: Modeling SSY_{EV} with storm metrics**

246 The relationship between SSY_{EV} and storm metrics can be modelled by a power law
247 function:

$$SSY_{EV} = \alpha X^{\beta} \quad \text{Equation 5}$$

where X is a storm metric, and the regression coefficients α and β are obtained by ordinary least squares regression on the logarithms of SSY_{EV} and X (Basher et al., 2011; Duvert et al., 2012; Hicks, 1990). Model fits for each storm metric were compared using coefficients of determination (r^2) and

Root Mean Square Error (RMSE). The correlation between storm metrics (X) and SSY_{EV} was also quantified using both parametric (Pearson) and non-parametric (Spearman) correlation coefficients.

Four storm metrics were tested as predictors of SSY_{EV}: total event precipitation (Psum), event Erosivity Index (EI30) (Hicks, 1990; Kinnell, 2013), total event water discharge (Qsum), and maximum event water discharge (Qmax) (Duvert et al., 2012; Rodrigues et al., 2013). SSY_{EV} and the discharge metrics (Qsum and Qmax) were normalized by watershed area to compare different sized subwatersheds.

248 The regression coefficients (α and β) for the UPPER and TOTAL watersheds were tested
249 for statistically significant differences using Analysis of Covariance (ANCOVA) (Lewis et al.,
250 2001). A higher intercept (α) for the human-disturbed watershed indicates higher sediment yield
251 for the same size storm event, compared to sediment yield from the undisturbed watershed. A
252 difference in slope (β) would indicate the relative sediment contributions from the subwatersheds
253 change with increasing storm size.

254 **3.3. Objective 3: Estimation of annual SSY**

255 Annual estimates of SSY and sSSY were estimated to compare Faga'alu with other
256 watersheds reported in the literature. A continuous annual time-series of SSY was not possible at
257 the study site due to the discontinuous field campaigns and failure of or damage to the
258 instruments during some months. Continuous records of P and Q were available for 2014, so the
259 Psum-SSY_{EV} and Qmax-SSY_{EV} models (Equation 5) were used to predict SSY_{EV} for all storms
260 in 2014 (Basher et al., 1997). Construction of sediment mitigation structures at the quarry began
261 in October 2014, greatly reducing SSY_{EV} from the LOWER_QUARRY subwatershed
262 (unpublished data), so the Qmax-SSY_{EV} relationship developed prior to the mitigation was used
263 to calculate the annual pre-mitigation sediment yield. For storms missing Qmax data at FG3,

264 Qmax was predicted from a linear regression between Qmax at FG1 and Qmax at FG3 for the
265 study period ($R^2 = 0.88$).

266 Annual SSY and sSSY were also estimated by multiplying SSY_{EV} from measured storms
267 by the ratio of annual storm precipitation (P_{EVann}) to the precipitation measured during storms
268 where SSY_{EV} was measured (P_{EVmeas}):

$$SSY_{ann} = SSY_{EV_meas} * \frac{P_{EVann}}{P_{EVmeas}} \quad \text{Equation 6}$$

where SSY_{ann} is estimated annual SSY from storms, SSY_{EVmeas} is SSY_{EV} from sampled storms (all, Tables 2 and 4), P_{EVmeas} is precipitation measured during the sampled storms, and P_{EVann} is the precipitation during all storm events defined by the hydrograph separation.

269 Equation 6 assumes that the sediment yield per mm of storm precipitation is constant
270 over the year, and that the size distribution of storms has no effect on SSY_{EV}, though there is
271 some evidence that SSY_{EV} increases exponentially with storm size (Lewis et al., 2001; Rankl,
272 2004). Equation 6 also ignores sediment yield during non-storm periods, which is justified by the
273 low SSC and Q observed between storms.

274 **3.4. Field Data Collection**

275 Data on precipitation (P), water discharge (Q), suspended sediment concentration (SSC)
276 and turbidity (T) were collected during four field campaigns: January-March 2012, February-
277 July 2013, January-March 2014, and October-December 2014, and several intervening periods of
278 unattended monitoring by instruments with data loggers. Field sampling campaigns were
279 scheduled to coincide with the period of most frequent storms in the November-May wet season,
280 though large storms were sampled throughout the year.

281 *3.4.1. Precipitation (P)*

282 P was measured at three locations in Faga'alu watershed using Rainwise RAINEW
283 tipping-bucket rain gages (RG1 and RG2) and a Vantage Pro Weather Station (Wx) (Figure 1).
284 Data at RG2 was only recorded January-March, 2012 to determine a relationship between
285 elevation and precipitation in the LOWER subwatershed. The total event precipitation (Psum)
286 and event Erosivity Index (EI30) were calculated using data from RG1, with data gaps filled by
287 15 minute interval precipitation data from Wx.

288 *3.4.2. Water Discharge (Q)*

289 Stream gaging sites were chosen to take advantage of an existing control structure (FG1)
290 and a stabilized stream cross section (FG3) (Duvert et al, 2010). At FG1 and FG3, Q was
291 calculated from stream stage measurements taken at 15 minute intervals using HOBO pressure
292 transducers (PT) and a stage-Q rating curve calibrated to manual Q measurements. Q was
293 measured manually in the field under both baseflow and stormflow conditions by the area-
294 velocity method (AV) using a Marsh-McBirney flowmeter (Harrelson et al., 1994; Turnipseed
295 and Sauer, 2010). The PTs recorded stages that exceeded the highest stage with manually-
296 measured Q, so the stage-Q rating at FG3 was extrapolated using Manning's equation, calibrating
297 Manning's n (0.067) to the Q measurements. At FG1, the flow control structure is a masonry
298 spillway crest of a defunct stream capture. The highest stage recorded by the PT (120 cm)
299 exceeded the highest stage with manually-measured Q (17 cm), and the flow structure did not
300 meet the assumptions for using Manning's equation to predict flow, so the HEC-RAS model was
301 used to create the stage-Q relationship (Brunner, 2010). See Appendix B for details of the cross
302 sections and rating curves.

303 A suitable site for stream gaging was not present at the outlet of the LOWER_QUARRY
304 subwatershed (FG2), so water discharge at FG2 was calculated as the product of the specific
305 water discharge from FG1 ($\text{m}^3/\text{0.9 km}^2$) and the watershed area draining to FG2 (1.17 km^2). This
306 assumes that specific water discharge from the subwatershed above FG2 is similar to above FG1.
307 Discharge may be higher from the quarry surface, which represents 5.7% of the
308 LOWER_QUARRY subwatershed, so Q and SSY at FG2 are conservative, lower bound
309 estimates, particularly during small events when specific discharge from the UPPER watershed
310 was small relative to specific discharge from the quarry. The quarry surface is continually being
311 disturbed, sometimes with large pits excavated and refilled in the course of weeks, as well as
312 intentional water control structures implemented over time. Given the changes in the
313 contributing area of the quarry, estimates of water yield from the quarry were uncertain, so we
314 assumed a uniform specific discharge for the whole LOWER_QUARRY subwatershed.

315 *3.4.3. Suspended Sediment Concentration (SSC)*

316 SSC was estimated at 15 minute intervals from either 1) linear interpolation of SSC
317 measured from water samples, or 2) turbidity data (T) recorded at 15 minute intervals and a T-
318 SSC relationship calibrated to stream water samples collected over a range of Q and SSC. Stream
319 water samples were collected by grab sampling with 500 mL HDPE bottles at FG1, FG2, and
320 FG3. At FG2, water samples were also collected at 30 min intervals during storm events by an
321 ISCO 3700 Autosampler triggered by a stage height sensor. Samples were analyzed for SSC on-
322 island using gravimetric methods (Gray, 2014; Gray et al., 2000). Water samples were vacuum
323 filtered on pre-weighed 47mm diameter, 0.7 um Millipore AP40 glass fiber filters, oven dried at
324 100 C for one hour, cooled and weighed to determine SSC (mg/L).

325 Interpolation of SSC values from grab samples was performed if at least three stream
326 water samples were collected during a storm event (Nearing et al., 2007), and if an SSC sample
327 was collected within 30 minutes of peak Q. SSC was assumed to be zero at the beginning and
328 end of each storm if no grab sample data was available for those times (Lewis et al., 2001).

329 Turbidity (T) was measured at FG1 and FG3 using three types of turbidimeters: 1)
330 Greenspan TS3000 (TS), 2) YSI 600OMS with 6136 turbidity probe (YSI), and 3) Campbell
331 Scientific OBS500 (OBS). All turbidimeters were permanently installed in protective PVC
332 housings near the streambed where the turbidity probe would be submerged at all flow
333 conditions, with the turbidity probe oriented downstream. Despite regular maintenance, debris
334 fouling during storm and baseflows was common and caused data loss during several storm
335 events (Lewis et al., 2001).

336 The T-SSC relationship can be unique to each region, stream, instrument or even each
337 storm event (Lewis et al., 2001), and can be influenced by water color, dissolved solids and
338 organic matter, temperature, and the shape, size, and composition of sediment. However, T has
339 proved to be a robust surrogate measure of SSC in streams (Gippel, 1995), and is most accurate
340 when a unique T-SSC relationship is developed for each instrument separately, using in situ grab
341 samples under storm conditions (Lewis, 1996). A unique T-SSC relationship was developed for
342 each turbidimeter, at each location, using T data and SSC samples from storm periods only (r^2
343 values 0.79-0.99). See Appendix D for details on the T-SSC relationships.

344 3.4.4. *Cumulative Probable Error (PE)*

345 Uncertainty in SSY_{EV} estimates arises from both measurement and model errors,
346 including stage-Q and T-SSC (Harmel et al., 2006). The Root Mean Square Error (RMSE)
347 method estimates the "most probable value" of the cumulative or combined error by propagating

348 the error from each measurement and modeling procedure to the final SSY_{EV} calculation
349 (Topping, 1972). The resulting cumulative probable error (PE) is the square root of the sum of
350 the squares of the maximum values of the separate errors:

$$PE = \sqrt{\sum (E_{Qmeas}^2 + E_{SSCmeas}^2) + (E_{Qmod}^2 + E_{SSCmod}^2)} \quad \text{Equation 2}$$

where PE is the cumulative probable error for individual measured values ($\pm\%$), E_{Qmeas} is uncertainty in Q measurements ($\pm\%$), $E_{SSCmeas}$ is uncertainty in SSC measurements ($\pm\%$), E_{Qmod} is uncertainty in Q modeled by the Stage-Q relationship (RMSE, as $\pm\%$ of the mean observed Q), E_{SSCmod} is uncertainty in SSC modeled by the T-SSC relationship (RMSE, as $\pm\%$ of the mean observed SSC) (Harmel et al., 2009).

351 E_{Qmeas} and $E_{SSCmeas}$ were estimated using lookup tables from the DUET-H/WQ software
352 tool (Harmel et al., 2009). The effect of uncertain SSY_{EV} estimates may complicate conclusions
353 about contributions from subwatersheds, anthropogenic impacts, and SSY_{EV}-Storm Metric
354 relationships. This is common in sediment yield studies where successful models estimate SSY
355 with ± 50 -100% accuracy (Duvert et al., 2012) but the difference in SSY from undisturbed and
356 disturbed areas was expected to be much larger than the cumulative uncertainty. PE was
357 calculated for SSY_{EV} from the UPPER and TOTAL watersheds, but not calculated for SSY_{EV}
358 from the LOWER subwatershed since it was calculated as the difference of SSY_{EV_UPPER} and
359 SSY_{EV_TOTAL}.

360 **4. Results**

361 **4.1 Precipitation and discharge**

362 Annual precipitation (P) measured at RG1 was 3,502 mm, 3,529 mm, and 3,709 mm in
363 2012, 2013, and 2014, respectively, which averages 94% of long-term precipitation (=3,800 mm)

364 from PRISM data (Craig, 2009). No difference in measured P was found between RG1 and Wx,
365 or between RG1 and RG2, so P was assumed to be homogenous over the watershed for all
366 analyses. Rain gauges could only be placed as high as ~300 m (RG2), though the highest point in
367 the watershed is ~600 m. Long-term rain gage records show a strong precipitation gradient with
368 increasing elevation, with average annual P of 3,000-4,000 mm on the lowlands, increasing to
369 more than 6,350 mm at high elevations (>400 m.a.s.l.) (Craig, 2009; Dames & Moore, 1981;
370 Wong, 1996). P data measured at higher elevations would be useful to determine the orographic
371 effect. For this analysis, however, the absolute values of P in each subwatershed are not
372 important since P and the erosivity index are only used as predictive storm metrics for Objective
373 2.

374 Discharge (Q) at both FG1 and FG3 was characterized by periods of low but perennial
375 baseflow, punctuated by short, flashy hydrograph peaks (Figure 3). Though Q data was
376 unavailable for some periods, storm events were generally smaller but more frequent in the
377 October-April wet season compared to the May-September dry season. The largest event in the
378 three year monitoring period was observed in the dry season (August 2014).

379 <Figure 3 here please>

380 **4.2 Objective 1: Compare SSC and SSY_{EV} for disturbed and undisturbed subwatersheds**

381 *4.2.1 Suspended sediment concentrations (SSC) during storm and non-storm periods*

382 <Figure 4 here please>

383 SSC was consistently lowest downstream of the forested watershed (FG1), highest
384 downstream of the quarry (FG2), and intermediate downstream of the village (FG3), during both
385 storm and non-storm periods (Figure 5a, 5b). A single storm event from 2/14/2014 (Figure 4)
386 shows that SSC was highest at FG2 on the rising limb of the hydrograph, and that turbidity and

387 SSC at FG3 were always higher than at FG1 throughout the storm event. Mean (μ) and
388 maximum SSC of all water samples, including those collected during both storm and non-storm
389 periods, were lowest at FG1 ($\mu=28$ mg/L, max=500 mg/L, n=59), highest at FG2 ($\mu=337$ mg/L,
390 max=12,600 mg/L, n=90 grab samples, n=198 from the Autosampler), and intermediate at FG3
391 ($\mu=148$ mg/L, max=3,500 mg/L, n=159). SSC collected during non-storm periods were lowest at
392 FG1, highest at FG2 (n=21), and in between at FG3 (n=45) (Figure 5a). Similarly, SSC during
393 storms was highest at FG1 (n=45), highest at FG 2, (n=69) and intermediate at FG3 (n=120).
394 SSC data collected at FG1, FG2 and FG3 were highly non-normal, so non-parametric tests for
395 statistical significance were applied. SSC was statistically significantly different among the three
396 sampled site during non-storms ($p<10^{-4}$) and storms ($p<10^{-4}$). Pair-wise Mann-Whitney tests
397 between FG1 and FG2 were significant ($p<10^{-4}$ for both storms and non-storms), but between
398 FG2 and FG3 were significant for non-storm periods ($p<0.05$) but not for storms ($p>0.10$).
399 <Figure 5 here please>

400 SSC varied by several orders of magnitude for a given Q at FG1, FG2, and FG3 due to
401 significant hysteresis observed during storm periods (Figure 4, 6). At FG1, variability of SSC
402 during stormflow was assumed to be caused by randomly occurring landslides or mobilization of
403 sediment stored in the watershed during large storm events. The maximum SSC at FG1 (500
404 mg/L), was sampled on 04/23/2013 at high discharge ($Q_{FG1}=3,724$ L/sec) (Figure 6a). Anecdotal
405 and field observations reported higher than normal SSC upstream of the quarry during the 2013
406 field season, possibly due to landsliding from previous large storms (G. Poinsky, pers. comm.).

407 <Figure 6 here please>

408 At FG2 and FG3, additional variability in the Q-SSC relationship was due to the
409 changing sediment availability associated with quarrying operations and construction in the

410 village. The high SSC values observed downstream of the quarry (FG2) during low Q were
411 caused by two mechanisms: 1) precipitation events that did not result in stormflow as defined by
412 the hydrograph separation algorithm, but generated runoff from the quarry with high SSC and 2)
413 washing fine sediment into the stream during rock crushing operations at the quarry.

414 The maximum SSC sampled at FG2 (12,600 mg/L) and FG3 (3,500 mg/L) were sampled
415 during the same rainfall event (03/05/2012), but during low Q (Figure 6b-c). During this event,
416 brief but intense precipitation caused high sediment runoff from the quarry. SSC was diluted
417 further downstream of the quarry at FG3 by the addition of runoff with lower SSC from the
418 village.

419 Given the close proximity of the quarry to the stream, SSC downstream of the quarry can
420 be highly influenced by mining activity like rock extraction, crushing, and/or hauling operations.
421 During 2012, a common practice for removing fine sediment from crushed aggregate was to
422 rinse it with water pumped from the stream. In the absence of retention structures the fine
423 sediment was discharged directly to Faga'alu stream, causing high SSC during non-storm
424 periods with no P in the preceding 24 hours (solid symbols, Figure 6b-c). Riverine discharge of
425 fine sediment rinsed from aggregate was discontinued in 2013. In 2013 and 2014, waste
426 sediment was piled on-site and severe erosion of these changing stockpiles caused high SSC only
427 during storm events.

428 *4.2.2. Suspended sediment yield during storm events (SSYEV)*

429 A total of 210 storm events were identified using hydrograph separation on the Q data at
430 FG1 and FG3 between January, 2012, and December 2014. A total of 169 events had
431 simultaneous Q data at FG1 and FG3 (Appendix C, Table 1). SSC data from T or interpolated
432 grab samples were recorded during 112 (FG1) and 74 events (FG3). Of those storms, 42 events

433 had data for P, Q, and SSC at both FG1 and FG3. SSY data from interpolated grab samples were
434 collected at FG2 for 8 storms to calculate SSY_{EV} from the LOWER_QUARRY and
435 LOWER_VILLAGE subwatersheds separately. Storm event durations ranged from 1 hour to 2
436 days, with mean duration of 13 hours.

437 For the 42 storms with complete data at both FG1 and FG3 (Table 2), SSY_{EV_TOTAL} was
438 129±121 tons, with 17±7 tons from the UPPER subwatershed and 112 tons from the LOWER
439 subwatershed. The UPPER and LOWER subwatersheds are similar in size (0.90 km² and 0.88
440 km²) but SSY_{EV_LOWER} accounted for 87% of SSY_{EV} at the watershed outlet (Table 2). The DR
441 estimated using Equation 4, with sSSY_{EV_UPPER} = 18.8 tons/km², suggests sSSY_{EV} has increased
442 by 6.8x in the LOWER subwatershed, and 3.9x for the TOTAL watershed compared with
443 undisturbed forest.

444 <Table 2 here please>

445 Disturbed areas accounted for 10% of the LOWER subwatershed area but approximately
446 87% of the SSY_{EV} from the LOWER subwatershed. Only 5.2% of the TOTAL watershed area
447 was disturbed, but SSY from disturbed areas accounted for 75% of SSY_{EV_TOTAL}. sSSY from
448 disturbed areas in the LOWER subwatershed was 1,095 tons/km², or 58x the sSSY of
449 undisturbed forest (Table 3).

450 <Table 3 here please>

451 The separate contributions to SSY from the quarry and village were determined for eight
452 storm events (Table 4), where 29% of SSY_{EV} came from the UPPER subwatershed, 36% from
453 the LOWER_QUARRY subwatershed, and 35% from the LOWER_VILLAGE subwatershed.
454 sSSY from the UPPER, LOWER_QUARRY, and LOWER_VILLAGE subwatersheds, and the
455 TOTAL watershed was 15, 61, 27, and 26 tons/km², respectively. The storms in Table 4 show a

456 smaller increase in SSY from the TOTAL watershed ($1.7 \times \text{SSY}_{\text{UPPER}}$) compared with the 42
457 storms with data at FG1 and FG3 ($3.9 \times \text{SSY}_{\text{UPPER}}$ Table 2), so these storms may underrepresent
458 the contributions of the quarry and village to SSY. sSSY increased by 4.1x in the
459 LOWER_QUARRY subwatershed and 1.8x in the LOWER_VILLAGE subwatershed compared
460 with the undisturbed UPPER watershed.

461 <Table 4 here please>

462 Very small fractions of the subwatershed areas are disturbed, yet roughly 77% of SSY
463 $\text{EV}_{\text{LOWER_QUARRY}}$ (6.5% disturbed) and 51% of SSY $\text{EV}_{\text{LOWER_VILLAGE}}$ (11.7% disturbed)
464 subwatersheds was from disturbed areas. Similarly, 5.2% of the TOTAL watershed was
465 disturbed but 75-45% of SSY EV_{TOTAL} was from disturbed areas (Tables 3 and 5). The quarry
466 significantly increased SSY and contributed the majority of SSY from disturbed areas in Faga'alu
467 watershed. sSSY from disturbed areas in the UPPER (37 tons/km²), LOWER_QUARRY (722
468 tons/km²), and LOWER_VILLAGE subwatersheds (116 tons/km²) suggested that disturbed areas
469 increase sSSY over forested conditions by 49x and 8x in the LOWER_QUARRY and
470 LOWER_VILLAGE subwatersheds, respectively. Human disturbance in the
471 LOWER_VILLAGE subwatershed also increased SSY above natural levels but the magnitude of
472 disturbance was much lower than the quarry.

473 <Table 5 here please>

474 [4.2.3 Cumulative Probable Error \(PE\)](#)

475 Cumulative Probable Error (RMSE %) for SSY_{EV} estimates were calculated from the
476 measurement errors for Q (8.5%) and SSC grab samples (16.3%), and the model errors of the
477 respective stage-Q and T-SSC relationships for that location. Cumulative Probable Errors (PE) in
478 SSY_{EV} were 28-49% ($\mu=43\%$) at FG1 and 36-118% ($\mu=94\%$) at FG3.

479 The measurement error (RMSE) for Q at FG1 and FG3 was 8.5 %, which included error
480 in the area-velocity measurements (6%), continuous Q measurement in a natural channel (6%),
481 pressure transducer error (0.1%), and streambed condition (firm, stable bed=0%) (DUET-H/WQ
482 look-up table (Harmel et al., 2006)). The model errors (RMSE) were 32% for the stage-Q rating
483 curve using Manning's equation at FG3, and 22% using HEC-RAS at FG1.

484 The measurement error (RMSE) for SSC was 16.3%, which included errors for sample
485 collection and analysis. Sample collection error consisted of interpolating over a 30 min interval
486 (5%) and sampling during stormflows (3%). Sample analysis error was from measuring SSC by
487 filtration (3.9%). The model errors (RMSE) of the T-SSC relationships were 16% (4 mg/L) for
488 the YSI and TS turbidimeters at FG1, 113% (348 mg/L) for the YSI turbidimeter at FG3, and
489 46% (48 mg/L) for the OBS turbidimeter at FG3.

490 **4.3 Objective 2: Modeling SSY_{EV} with storm metrics**

491 *4.3.1. Selecting the best predictor of SSY_{EV}*

492 Qsum and Qmax were the best predictors of SSY_{EV} for the forested UPPER watershed,
493 and Psum and Qmax were the best predictors for the TOTAL watershed. SSY_{EV} is calculated
494 from Q so it is expected that Qsum should correlate closely with SSY_{EV} (Duvert et al., 2012;
495 Rankl, 2004). Discharge metrics were also highly correlated with SSY_{EV} in the TOTAL
496 watershed, suggesting discharge metrics are good predictors in both disturbed and undisturbed
497 watersheds. Most of the scatter in the Qmax-SSY_{EV} relationship is observed for small events, and
498 Qmax correlated strongly with the largest SSY_{EV} values, when most of the annual sediment load
499 is generated (Table 6).

500 <Table 6 here please>

501 Precipitation was measured at the quarry, which may reflect precipitation characteristics
502 more accurately in the LOWER than the UPPER watershed, and account for the lower
503 correlation coefficients between precipitation and SSY_{EV_UPPER}. SSY from the LOWER
504 subwatershed is hypothesized to be mostly generated by hillslope erosion by sheetwash and rill
505 formation at the quarry and on dirt roads, and agricultural plots, whereas SSY from the UPPER
506 subwatershed is hypothesized to be mainly from channel processes and mass wasting. Mass
507 wasting can contribute large pulses of sediment which can be deposited near or in the streams
508 and entrained at high discharges during later storm events. Given the high correlation
509 coefficients between SSY_{EV} and Qmax in both watersheds, Qmax may be a promising predictor
510 that integrates both precipitation and discharge processes.

511 *4.3.2. Effect of event size and watershed disturbance*

512 SSY_{EV} from the TOTAL watershed was higher than from the UPPER watershed for the
513 full range of measured storms with the exception of a few events that are considered outliers.
514 The outlier events could be attributed to measurement error or to landslides or other mass
515 movements in the UPPER subwatershed. The separation of multi-peak storm events, storm
516 sequence, and antecedent conditions may also play a role. While the climate on Tutuila is
517 tropical, without strong seasonality, periods of low rainfall can persist for several weeks, perhaps
518 altering the water and sediment dynamics in the subsequent storm events.

519 All model intercepts (α) were significantly different ($p < 0.01$), but only the Qsum-SSY_{EV}
520 model showed significantly different slopes (β , $p < 0.01$). The Qsum-SSY_{EV} models indicate that
521 SSY_{EV} from the UPPER and TOTAL watersheds converge at higher Qsum values. Conversely,
522 the Psum- and Qmax-SSY_{EV} models show no change in relative contributions of SSY over the
523 range of storm sizes (Figure 7).

524 <Figure 7 here please>

525 The relative contribution of SSY from the human-disturbed watershed was hypothesized
526 to diminish with increasing storm size. The results from precipitation metrics and discharge
527 metrics were contradictory. The relative contribution of SSY_{EV} from the human-disturbed
528 watershed decreases with storm size in the Qsum- SSY_{EV} model, but the Psum- and Qmax- SSY_{EV}
529 models show no change in relative contributions over increasing storm size (Figure 7). It was
530 hypothesized that SSY_{EV} from undisturbed forest areas would become the dominant source for
531 larger storm events, but the DR remains high for large storm events due to the naturally low
532 SSY_{EV} from natural forest areas in Faga'alu watershed. This suggests that disturbed areas were
533 not supply limited for the range of sampled storms.

534 **4.4 Objective 3: Estimation of annual SSY**

535 Estimates of annual sSSY depended on which predictor was used to estimate SSY_{EV} . The
536 Psum model resulted in a much lower estimate of sSSY than the Qmax model (Table 7). The
537 large difference in sSSY between the two methods was due to higher scatter about the Psum-
538 SSY_{EV} relationship for large events compared with the Qmax- SSY_{EV} , and the Qmax model is
539 likely more robust. Annual SSY was also calculated for 2014 using Equation 6 for three sets of
540 storm events: a) all events with SSY_{EV} data, including those where SSY_{EV} data were only
541 available for a single site; b) only events where data was available for both UPPER (FG1) and
542 TOTAL (FG3) and c) only events where data was available for UPPER (FG1),
543 LOWER_QUARRY (FG2), and TOTAL (FG3). Including all storms (method a) will provide the
544 best estimate at a given location, while b) and c) allow more direct comparison of different
545 subwatersheds.

546 <Table 7 here please>

547 Annual storm precipitation (P_{EVann}) in 2014 was 2,770 mm, representing 69% of total
548 annual precipitation (3,709 mm). The remaining 31% of precipitation did not result in a rise in
549 stream level sufficient to be classified as an event with the hydrograph separation method used
550 here. All storms with measured SSY_{EV} at FG1 from 2012-2014 included 3,457 mm of
551 precipitation (P_{EVmeas}), or 125% of P_{EVann} , so estimated annual SSY from the UPPER
552 subwatershed from Equation 6 was 41 tons/yr (45 tons/km²/yr). All storms with measured SSY_{EV}
553 at FG3 from 2012-2014 included 2,628 mm of precipitation, or 95% of expected annual storm
554 precipitation so estimated annual SSY from the TOTAL watershed was 428 tons/yr (241
555 tons/km²/yr).

556 Overall, the Qmax model and Equation 6 using all events gave similar estimates of
557 annual SSY at both the UPPER watershed (41-61 tons/yr) and the TOTAL watershed (428-439
558 tons/yr). The accuracy of the Psum model was compromised by significant scatter for large
559 events, while the Qsum model had significantly less scatter for large events. The eight storms
560 sampled at all three locations (Table 4) had unusually high loads from the UPPER watershed but
561 similar SSY from the LOWER watershed, likely resulting in a low estimate of sediment loading
562 and DR from the quarry.

563 **5. Discussion**

564 **5.1 Objective 1: Compare SSC and SSYEV for disturbed and undisturbed subwatersheds**

565 Event wise analysis of SSY_{EV} was useful because hysteresis and interstorm variability
566 caused significant scatter in the instantaneous Q-SSC relationship. While the instantaneous Q-
567 SSC relationship illustrated large increases in SSC downstream of the quarry, the hysteresis and
568 interstorm variability meant that a single Q-SSC relationship could not be used to estimate

569 sediment loading, which complicated detection of human impact on sediment concentrations and
570 yields.

571 Measurement of SSY_{EV} allows comparison of similar size storms to determine change
572 over space and time without problems of interannual variability in precipitation totals. The
573 simple regression models that predict annual sediment load from either precipitation or
574 stormflow measurements eliminate the need for long-term field work to estimate annual total
575 yields. From a management perspective, the event-wise approach to estimating human impacts
576 on sediment is less expensive than efforts to measure annual yields since it does not require a
577 complete year of monitoring, and can be rapidly conducted if mitigation or disturbance activities
578 are already planned. With predictive models of SSY_{EV} that are based on an easily-monitored
579 storm metric like maximum event discharge, SSY_{EV} can be modeled to compare with either post-
580 mitigation or post-disturbance SSY_{EV}.

581 **5.2 Objective 2: Modeling SSYEV with storm metrics**

582 Several researchers have attempted to explain values of the intercept (α) and slope (β)
583 coefficients of the sediment rating curve as a function of watershed characteristics. A traditional
584 sediment rating curve (Q-SSC) is considered a 'black box' model, and though the slope and
585 intercept have no physical meaning, some physical interpretation has been ascribed to them
586 (Asselman, 2000). Rankl (2004) hypothesized that the intercept in the Qmax-SSY_{EV} relationship
587 varied with sediment availability and erodibility in watersheds. While slopes in log-log space can
588 be compared directly (Duvert et al., 2012), intercepts must be plotted in similar units, and
589 normalized by watershed area. In five semi-arid to arid watersheds (2.1-1,538 km²) in Wyoming,
590 United States (Rankl, 2004), intercepts of the SSY_{EV}-Qmax relationship ranged from 111-4,320
591 (Qmax in m³/s/km², SSY_{EV} in Mg/km²). In eight sub-humid to semi-arid watersheds (0.45-22

592 km²) (Duvert et al., 2012), the intercepts ranged from 25-5,039. In Faga'alu, the intercept in the
593 undisturbed, UPPER subwatershed was 0.35, and in the disturbed, TOTAL watershed the
594 intercept was 1.38, which are an order of magnitude or two lower than the lowest intercepts in
595 Rankl (2004) and Duvert et al. (2012). This suggests that sediment availability is relatively low
596 in Faga'alu, under natural and human-disturbed conditions, likely due to the dense forest cover.

597 High slope values in the log-log plots (β coefficient) suggest that small changes in stream
598 discharge lead to large increases in sediment load due to the erosive power of the river or the
599 availability of new sediment sources at high Q (Asselman, 2000). Rankl (2004) assumed that the
600 slope was a function of rainfall intensity on hillslopes, and found that the slopes ranged from
601 1.07-1.29 in five semi-arid to arid watersheds in Wyoming, and were not statistically different
602 among watersheds. In the watersheds in Duvert et al. (2012), slopes ranged from 0.95-1.82, and
603 from 1.06-2.45 in eighteen other watersheds (0.60-1,538 km²) in diverse geographical settings
604 (Basher et al., 1997; Fahey and Marden, 2000; Hicks et al., 2009; Rankl, 2004; Tropeano, 1991)
605 compiled by Duvert et al. (2012). In Faga'alu, slopes were 1.51 and 1.40 in the UPPER and
606 TOTAL watersheds, respectively. These slopes are very consistent with the slopes presented in
607 Rankl (2004) and Duvert et al. (2012), despite large differences in climate and land cover.

608 In Faga'alu, SSY_{EV} was least correlated with the Erosivity Index (EI30). Duvert et al.
609 (2012) also found low correlation coefficients with 5 min rainfall intensity for 8 watersheds in
610 France and Mexico. Rodrigues et al. (2013) hypothesized that EI30 is poorly correlated with
611 SSY_{EV} due to the effect of previous events on antecedent moisture conditions and in-channel
612 sediment storage. Cox et al. (2006) found EI30 was more correlated with soil loss in an
613 agricultural watershed than a forested watershed, and Faga'alu is mainly covered in dense forest.
614 Similar to other studies, the highest correlations with SSY_{EV} at Faga'alu were observed for

615 discharge metrics Qsum and Qmax (Basher et al., 2011; Duvert et al., 2012; Fahey et al., 2003;
616 Hicks, 1990; Rankl, 2004; Rodrigues et al., 2013). While Qsum and Psum had higher
617 correlations in individual watersheds, Qmax was a good predictor of SSY_{EV} in both the disturbed
618 and undisturbed watershed.

619 **5.3 Objective 3: Estimation of annual SSY and comparison with other tropical islands**

620 Sediment yield is highly variable among individual watersheds, but is generally
621 controlled by climate, vegetation cover, and geology, with human disturbance playing an
622 increasing role in the 20th century (Syvitski et al., 2005). Sediment yields in tropical Southeast
623 Asia and high-standing islands between Asia and Australia range from ~10 tons/km²/yr in the
624 granitic Malaysian Peninsula to ~10,000 tons/km²/yr in the tectonically active, steeply sloped
625 island of Papua New Guinea (Douglas, 1996). Sediment yields from Faga'alu are on the lower
626 end of the range, with sSSY of 45-68 tons/km²/yr from the undisturbed UPPER watershed, and
627 241-247 tons/km²/yr from the disturbed TOTAL watershed.

628 Milliman and Syvitski (1992) report high average sSSY (1,000-3,000 tons/km²/yr) from
629 watersheds (10-100,000 km²) in tropical Asia and Oceania, though their regional models of sSSY
630 as a function of basin size and maximum elevation predict only 13 tons/km²/yr from watersheds
631 with peak elevation 500-1,000 m (highest point of UPPER Faga'alu subwatershed is 653 m), and
632 68 tons/km²/yr for max elevations of 1,000-3,000. Given the high vegetation cover and lack of
633 human activity in the UPPER Faga'alu subwatershed, its sSSY should be lower than sSSY from
634 watersheds presented in Milliman and Syvitski (1992), which included watersheds with human
635 disturbance. sSSY from the forested UPPER Faga'alu subwatershed (45-68 tons/km²/yr) was
636 approximately three to five times higher than the prediction from the Milliman and Syvitski
637 (1992) model (13 tons/km²/yr), though the scatter around their model is large for smaller

638 watersheds, and the Faga'alu data fall within the range of scatter (Figures 5e and 6e in Milliman
639 and Syvitski (1992)).

640 Sediment yield has been measured using modern fluvial measurements similar to ours for
641 two Hawaiian watersheds: Hanalei watershed on Kauai ("Hanalei"), and Kawela watershed on
642 Molokai ("Kawela") (Table 8) (Ferrier et al., 2013; Stock and Tribble, 2010). Hanalei (54 km²)
643 has steep relief and mean areal precipitation of 3,866 mm/yr (Ferrier et al., 2013), which is
644 slightly higher than rainfall at Faga'alu during the monitoring period (3,247 mm/yr). Over a four
645 year period, SSC at Hanalei averaged 63 mg/L and reached a maximum of 2,750 mg/L (Stock
646 and Tribble, 2010), which is slightly lower than observations at the outlet of Faga'alu (mean 148
647 mg/L, maximum 3,500 mg/L). Calhoun and Fletcher (1999) estimated sSSY from Hanalei as
648 140±55 tons/km²/yr, but had fewer data than Stock and Tribble (2010), who estimated sSSY as
649 525 tons/km²/yr. Ferrier et al., (2013) reported annual suspended sediment yield at Hanalei as
650 369 ± 114 tons/km²/yr. These values are higher than observed from the undisturbed
651 subwatershed in Faga'alu (45-68 tons/km²/yr) but similar to the disturbed (430-441 tons/km²/yr)
652 subwatersheds. Rocks at Hanalei are of similar age (1.5 Mya) or older (3.95-4.43 Mya) (Ferrier
653 et al., 2013) compared with Faga'alu (1.2 Mya) (McDougall, 1985), so landscape age does not
654 explain the difference in observed SSY between Hanalei and Faga'alu. Kawela (14 km²) is
655 disturbed by grazing and is in a sub-humid climate, where precipitation varies with elevation
656 from 500-3,000 mm. Stock and Tribble (2010) estimated sSSY from Kawela was 459
657 tons/km²/yr, which is similar to the disturbed subwatershed in Faga'alu, but nearly twice as high
658 as the TOTAL Faga'alu watershed. In Kawela, SSC (mean 3,490 mg/L, maximum 54,000 mg/L)
659 was much higher than measured in Faga'alu TOTAL watershed, so the difference in SSY is due
660 in part to higher SSC rather than to higher observed runoff. Overall, both Hawaiian watersheds

661 have higher SSY than Faga’alu, which is consistent with the low intercepts of Faga’alu in the
662 Q_{max}-SSY_{EV} relationships, and suggests that Faga’alu may have uniquely low erosion rates for a
663 steep volcanic watershed. Precipitation variability may contribute to the difference in SSY, so a
664 more thorough comparison between Hanalei and Faga’alu would require a storm-wise analysis of
665 the type performed here.

666 <Table 8 here please>

667 Annual sSSY from the quarry was estimated from Equation 6 to be approximately 2,800
668 tons/km²/yr. The quarry surfaces are comprised of haul roads, piles of overburden, and steep rock
669 faces which can be described as a mix of unpaved roads and cut-slopes. sSSY from cutslopes
670 varies from 0.01 tons/km²/yr in Idaho (Megahan, 1980) to 105,000 tons/km²/yr in Papua New
671 Guinea (Blong and Humphreys, 1982), so the sSSY ranges measured in this study are well
672 within the ranges found in the literature.

673 **5.4 Comparison with other kinds of sediment disturbance**

674 SSY at Faga’alu was increased by 3.9x compared with the natural background. Other
675 studies in small, mountainous watersheds have documented one to several orders of magnitude
676 increases in SSY from land use that disturbs a small fraction of the watershed area. Urbanization
677 and mining can increase sediment yield by two to three orders of magnitudes in catchments of
678 several km². Yields from construction sites can exceed those from the most unstable, tectonically
679 active natural environments of Southeast Asia (Douglas, 1996). In Kawela watershed on
680 Molokai, less than 5% of the land produces most of the sediment, and only 1% produces ~50%
681 of the sediment (Risk, 2014; Stock et al., 2010). In three basins on St. John, US Virgin Islands
682 unpaved roads increased sediment delivery rates by 3-9 times (Ramos-Scharrón and Macdonald,
683 2005).

684 Disturbances at larger scales have resulted in increases in total SSY to coral
685 environments, similar to Faga'alu. The development of the Great Barrier Reef (GBR) catchment
686 ($423,000 \text{ km}^2$) since European settlement (ca.1830) led to increases in SSY by an estimated
687 factor of 5.5x (Kroon et al., 2012). Mining has been a major contributor of sediment in other
688 watersheds on volcanic islands with steep topography and high precipitation, increasing sediment
689 yields by 5-10 times in a watershed in Papua New Guinea (Hettler et al., 1997; Thomas et al.,
690 2003). In contrast to other land disturbances like fire, logging, or urbanization where sediment
691 disturbance decreases over time, the disturbance from mining is persistently high. Disturbance
692 magnitudes are similar to the construction phase of urbanization (Wolman and Schick, 1967), or
693 high-traffic unpaved roads (Reid and Dunne, 1984), but persist or even increase over time.

694 While unpaved roads are often identified as a source of sediment in humid forested
695 regions (Lewis et al., 2001; Ramos-Scharrón and Macdonald, 2005; Reid and Dunne, 1984),
696 field observations at Faga'alu suggested that most roads in the urban area were stabilized with
697 aggregate and not generating significant amounts of sediment. Other disturbances in Faga'alu
698 included a few small agricultural plots, small construction sites and bare dirt on roadsides.
699 Repeated surface disturbance at the quarry is a key process maintaining high rates of sediment
700 generation. Given the large distance to other sources of building material, aggregate mining and
701 associated sediment disturbance may be a critical sediment source on remote islands in the
702 Pacific and elsewhere.

703 **6. Conclusion**

704 Human disturbance has increased sediment yield to Faga'alu Bay by 3.9x over pre-
705 disturbance levels. The human-disturbed subwatershed accounted for the majority (87%) of total
706 sediment yield, and the quarry (1.1% of watershed area) contributed about a third of total SSY to

707 the Bay. Qmax was a good predictor of SSY_{EV} in both the disturbed and undisturbed watersheds,
708 making it a promising predictor in diverse environments. The slopes of the Qmax-SSY_{EV}
709 relationships were comparable with other studies, but the model intercepts were an order of
710 magnitude lower than intercepts from watersheds in semi-arid to semi-humid climates. This
711 suggests that sediment availability is relatively low in the Faga'alu watershed, either because of
712 the heavy forest cover or volcanic rock type. The event-wise approach did not require continuous
713 in situ monitoring for a single or multiple years, which would not have been logistically possible
714 in this remote study area. This study presents an innovative method to combine sampling and
715 analysis strategies to measure sediment contributions from key sources, estimate baseline annual
716 sediment yields prior to management, and rapidly develop an empirical sediment yield model for
717 a remote, data-poor watershed.

718 **Acknowledgements**

719 Funding for this project was provided by NOAA Coral Reef Conservation Program
720 (CRCP) through the American Samoa Coral Reef Advisory Group (CRAG). Kristine
721 Buccianeri at CRAG and Susie Holst at NOAA CRCP provided necessary and significant
722 support. Christianera Tuitele, Phil Wiles, and Tim Bodell at American Samoa Environmental
723 Protection Agency (ASEPA), and Fatima Sauafea-Leau and Hideyo Hattori at NOAA, provided
724 on-island coordination with traditional local authorities. Dr. Mike Favazza provided critical
725 logistical assistance in American Samoa. Robert Koch at the American Samoa Coastal Zone
726 Management Program (ASCMP) and Travis Bock at ASEPA assisted in accessing historical
727 geospatial and water quality data. Many others helped and supported the field and laboratory
728 work including Professor Jameson Newtonson, Rocco Tinali, and Valentine Vaeoso at American
729 Samoa Community College (ASCC), Meagan Curtis and Domingo Ochavillo at American

730 Samoa Department of Marine and Wildlife Resources (DMWR), Don and Agnes Vargo at
731 American Samoa Land Grant, Christina Hammock at NOAA American Samoa Climate
732 Observatory, and Greg McCormick at San Diego State University. George Poysky, Jr., George
733 Poysky III, and Mitch Shimisaki at Samoa Maritime Ltd. provided unrestricted access to the
734 Faga'alu quarry site, and historical operation information. Faafetai tele lava.

735 [References](#)

736 Asselman, N.E.M., 2000. Fitting and interpretation of sediment rating curves. *J. Hydrol.* 234,
737 228–248. doi:10.1016/S0022-1694(00)00253-5

738 Basher, L., Hicks, D., Clapp, B., Hewitt, T., 2011. Sediment yield response to large storm events
739 and forest harvesting, Motueka River, New Zealand. *New Zeal. J. Mar. Freshw. Res.* 45,
740 333–356. doi:10.1080/00288330.2011.570350

741 Basher, L.R., Hicks, D.M., Handyside, B., Ross, C.W., 1997. Erosion and sediment transport
742 from the market gardening lands at Pukekohe, Auckland, New Zealand. *J. Hydrol.* 36, 73–
743 95.

744 Blong, R.J., Humphreys, G.S., 1982. Erosion of road batters in Chim Shale, Papua New Guinea.
745 Civ. Eng. Trans. Inst. Eng. Aust. CE24 1, 62–68.

746 Bonta, J. V, 2000. Impact of Coal Surface Mining and Reclamation on Suspended Sediment in
747 Three Ohio Watersheds. *JAWRA J. Am. Water Resour. Assoc.* 36, 869–887.

748 Brunner, G., 2010. HEC-RAS River Analysis System.

- 749 Calhoun, R.S., Fletcher, C.H., 1999. Measured and predicted sediment yield from a subtropical,
750 heavy rainfall, steep-sided river basin: Hanalei, Kauai, Hawaiian Islands. *Geomorphology*
751 30, 213–226.
- 752 Cox, C.A., Sarangi, A., Madramootoo, C.A., 2006. Effect of land management on runoff and soil
753 losses from two small watersheds in St Lucia. *L. Degrad. Dev.* 17, 55–72.
754 doi:10.1002/ldr.694
- 755 Craig, P., 2009. Natural History Guide to American Samoa. National Park of American Samoa,
756 Pago Pago, American Samoa.
- 757 Daly, C., Halbleib, M., Smith, J.I., Gibson, W.P., Doggett, M.K., Taylor, G.H., Curtis, J.,
758 Passteris, P.P., 2008. Physiographically sensitive mapping of climatological temperature
759 and precipitation across the conterminous United States. *Int. J. Climatol.* 28, 2031.
760 doi:10.1002/joc
- 761 Dames & Moore, 1981. Hydrologic Investigation of Surface Water for Water Supply and
762 Hydropower.
- 763 Douglas, I., 1996. The impact of land-use changes, especially logging, shifting cultivation,
764 mining and urbanization on sediment yields in humid tropical Southeast Asia: A review
765 with special reference to Borneo. *IAHS-AISH Publ.* 236, 463–471.
- 766 Duvert, C., Nord, G., Gratiot, N., Navratil, O., Nadal-Romero, E., Mathys, N., Némery, J.,
767 Regués, D., García-Ruiz, J.M., Gallart, F., Esteves, M., 2012. Towards prediction of
768 suspended sediment yield from peak discharge in small erodible mountainous catchments

- 769 (0.45–22km²) of France, Mexico and Spain. *J. Hydrol.* 454-455, 42–55.
770 doi:10.1016/j.jhydrol.2012.05.048
- 771 Fabricius, K.E., 2005. Effects of terrestrial runoff on the ecology of corals and coral reefs:
772 review and synthesis. *Mar. Pollut. Bull.* 50, 125–46. doi:10.1016/j.marpolbul.2004.11.028
- 773 Fahey, B.D., Marden, M., 2000. Sediment yields from a forested and a pasture catchment,
774 coastal Hawke's Bay, North Island, New Zealand. *J. Hydrol.* 39, 49–63.
- 775 Fahey, B.D., Marden, M., Phillips, C.J., 2003. Sediment yields from plantation forestry and
776 pastoral farming, coastal Hawke's Bay, North Island, New Zealand. *J. Hydrol.* 42, 27–38.
- 777 Fenner, D., Speicher, M., Gulick, S., Aeby, G., Aletto, S.C., Anderson, P., Carroll, B.P.,
778 DiDonato, E.M., DiDonato, G.T., Farmer, V., Fenner, D., Gove, J., Gulick, S., Houk, P.,
779 Lundblad, E., Nadon, M., Riolo, F., Sabater, M.G., Schroeder, R., Smith, E., Speicher, M.,
780 Tuitele, C., Tagarino, A., Vaitautolu, S., Vaoli, E., Vargas-angel, B., Vroom, P., 2008. The
781 State of Coral Reef Ecosystems of American Samoa, in: The State of Coral Reef
782 Ecosystems of the United States and Pacific Freely Associated States. pp. 307–351.
- 783 Ferrier, K.L., Taylor Perron, J., Mukhopadhyay, S., Rosener, M., Stock, J.D., Huppert, K.L.,
784 Slosberg, M., 2013. Covariation of climate and long-term erosion rates across a steep
785 rainfall gradient on the Hawaiian island of Kaua'i. *Bull. Geol. Soc. Am.* 125, 1146–1163.
786 doi:10.1130/B30726.1
- 787 Fuka, D., Walter, M., Archibald, J., Steenhuis, T., Easton, Z., 2014. EcoHydRology.

- 788 Gellis, A.C., 2013. Factors influencing storm-generated suspended-sediment concentrations and
789 loads in four basins of contrasting land use, humid-tropical Puerto Rico. *Catena* 104, 39–57.
790 doi:10.1016/j.catena.2012.10.018
- 791 Gippel, C.J., 1995. Potential of turbidity monitoring for measuring the transport of suspended
792 solids in streams. *Hydrol. Process.* 9, 83–97.
- 793 Gomi, T., Moore, R.D., Hassan, M.A., 2005. Suspended sediment dynamics in small forest
794 streams of the Pacific Northwest. *J. Am. Water Resour. Assoc.*
- 795 Gray, J.R., 2014. Measuring Suspended Sediment, in: Ahuja, S. (Ed.), *Comprehensive Water*
796 *Quality and Purification*. Elsevier, pp. 157–204. doi:10.1016/B978-0-12-382182-9.00012-8
- 797 Gray, J.R., Glysson, G.D., Turcios, L.M., Schwarz, G.E., 2000. Comparability of Suspended-
798 Sediment Concentration and Total Suspended Solids Data U.S. Geological Survey Water-
799 Resources Investigations Report 00-4191. Reston, Va.
- 800 Harmel, R.D., Cooper, R.J., Slade, R.M., Haney, R.L., Arnold, J.G., 2006. Cumulative
801 uncertainty in measured streamflow and water quality data for small watersheds. *Trans.*
802 *Am. Soc. Agric. Biol. Eng.* 49, 689–701.
- 803 Harmel, R.D., Smith, D.R., King, K.W., Slade, R.M., 2009. Estimating storm discharge and
804 water quality data uncertainty: A software tool for monitoring and modeling applications.
805 *Environ. Model. Softw.* 24, 832–842.

- 806 Harrelson, C.C., Rawlins, C.L., Potyondy, J.P., 1994. Stream channel reference sites: an
807 illustrated guide to field technique. USDA Forest Service General Technical Report RM-
808 245. US Department of Agriculture, Fort Collins, CO.
- 809 Henderson, G.W., Toews, D.A.A., 2001. Using Sediment Budgets to Test the Watershed
810 Assessment Procedure in Southeastern British Columbia, in: Toews, D.A.A., Chatwin, S.
811 (Eds.), Watershed Assessment in the Southern Interior of British Columbia. B.C. Ministry
812 of Forests, Research Branch, Victoria, British Columbia, pp. 189–208.
- 813 Hettler, J., Irion, G., Lehmann, B., 1997. Environmental impact of mining waste disposal on a
814 tropical lowland river system: a case study on the Ok Tedi Mine, Papua New Guinea.
815 Miner. Depos. 32, 280–291. doi:10.1007/s001260050093
- 816 Hicks, D.M., 1990. Suspended sediment yields from pasture and exotic forest basins, in:
817 Proceedings of the New-Zealand Hydrological Society Symposium. Auckland, New
818 Zealand.
- 819 Hicks, D.M., Hoyle, J., Roulston, H., 2009. Analysis of sediment yields within Auckland region.
820 ARC Technical Report 2009/064. Prepared by NIWA for Auckland Regional Council.
- 821 Holst-Rice, S., Messina, A., Biggs, T.W., Vargas-Angel, B., Whitall, D., 2015. Baseline
822 Assessment of Faga‘alu Watershed: A Ridge to Reef Assessment in Support of Sediment
823 Reduction Activities. NOAA Coral Reef Conservation Program, Silver Spring, MD.
- 824 Horsley-Witten, 2011. American Samoa Erosion and Sediment Control Field Guide.

- 825 Horsley-Witten, 2012. Post-Construction Stormwater Training Memorandum.
- 826 Kinnell, P.I.A., 2013. Modelling event soil losses using the Q R EI 30 index within RUSLE2.
- 827 Hydrol. Process. doi:10.1002/hyp
- 828 Kroon, F.J., Kuhnert, P.M., Henderson, B.L., Wilkinson, S.N., Kinsey-Henderson, A., Abbott,
829 B., Brodie, J.E., Turner, R.D.R., 2012. River loads of suspended solids, nitrogen,
830 phosphorus and herbicides delivered to the Great Barrier Reef lagoon. Mar. Pollut. Bull. 65,
831 167–81. doi:10.1016/j.marpolbul.2011.10.018
- 832 Latinis, D.K., Moore, J., Kennedy, J., 1996. Archaeological Survey and Investigations
833 Conducted at the Faga'alu Quarry, Ma'oputasi County, Tutuila, American Samoa, February
834 1996: Prepared for George Potsky, Sr., Samoa Maritime, PO Box 418, Pago Pago,
835 American Samoa, 96799. Archaeological Consultants of the Pacific Inc., 59-624 Pupukea
836 Rd., Haleiwa, HI 96712.
- 837 Lewis, J., 1996. Turbidity-controlled suspended sediment sampling for runoff-event load
838 estimation. Water Resour. Res. 32, 2299–2310.
- 839 Lewis, J., Mori, S.R., Keppeler, E.T., Ziemer, R.R., 2001. Impacts of Logging on Storm Peak
840 Flows , Flow Volumes and Suspended Sediment Loads in Caspar Creek, CA, in: Land Use
841 and Watersheds: Human Influence on Hydrology and Geomorphology in Urban and Forest
842 Areas. pp. 1–76.
- 843 McDougall, I., 1985. Age and Evolution of the Volcanoes of Tutuila American Samoa. Pacific
844 Sci. 39, 311–320.

- 845 Megahan, W.F., 1980. Erosion from roadcuts in granitic slopes of the Idaho Batholith, in:
846 Proceedings Cordilleran Sections of the Geological Society of America, 76th Annual
847 Meeting. Oregon State University, Corvallis, OR, p. 120.
- 848 Megahan, W.F., Wilson, M., Monsen, S.B., 2001. Sediment production from granitic cutslopes
849 on forest roads in Idaho, USA. *Earth Surf. Process. Landforms* 26, 153–163.
- 850 Milliman, J.D., Syvitski, J.P.M., 1992. Geomorphic/tectonic control of sediment discharge to the
851 ocean: the importance of small mountainous rivers. *J. Geol.* 100, 525–544.
- 852 Nakamura, S., 1984. Soil Survey of American Samoa. US Department of Agriculture Soil
853 Conservation Service, Pago Pago, American Samoa.
- 854 Nathan, R.J., McMahon, T. a, 1990. Evaluation of Automated Techniques for Base Flow and
855 Recession Analyses. *Water Resour. Res.* 26, 1465–1473. doi:10.1029/WR026i007p01465
- 856 Nearing, M. a, Nichols, M.H., Stone, J.J., Renard, K.G., Simanton, J.R., 2007. Sediment yields
857 from unit-source semiarid watersheds at Walnut Gulch. *Water Resour. Res.* 43, 1–10.
858 doi:10.1029/2006WR005692
- 859 Perreault, J., 2010. Development of a Water Budget in a Tropical Setting Accounting for
860 Mountain Front Recharge: Tutuila, American Samoa. University of Hawai'i.
- 861 Perroy, R.L., Bookhagen, B., Chadwick, O. a., Howarth, J.T., 2012. Holocene and Anthropocene
862 Landscape Change: Arroyo Formation on Santa Cruz Island, California. *Ann. Assoc. Am.*
863 Geogr.

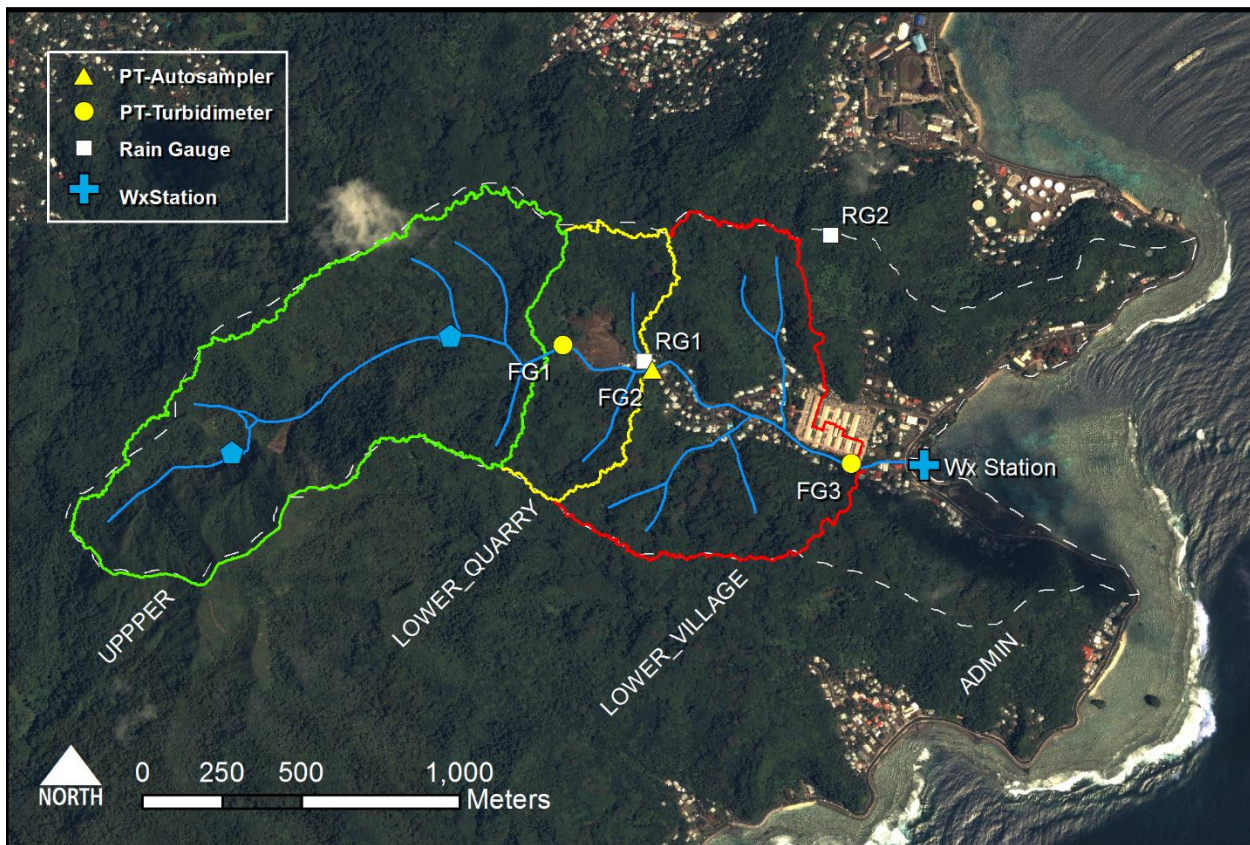
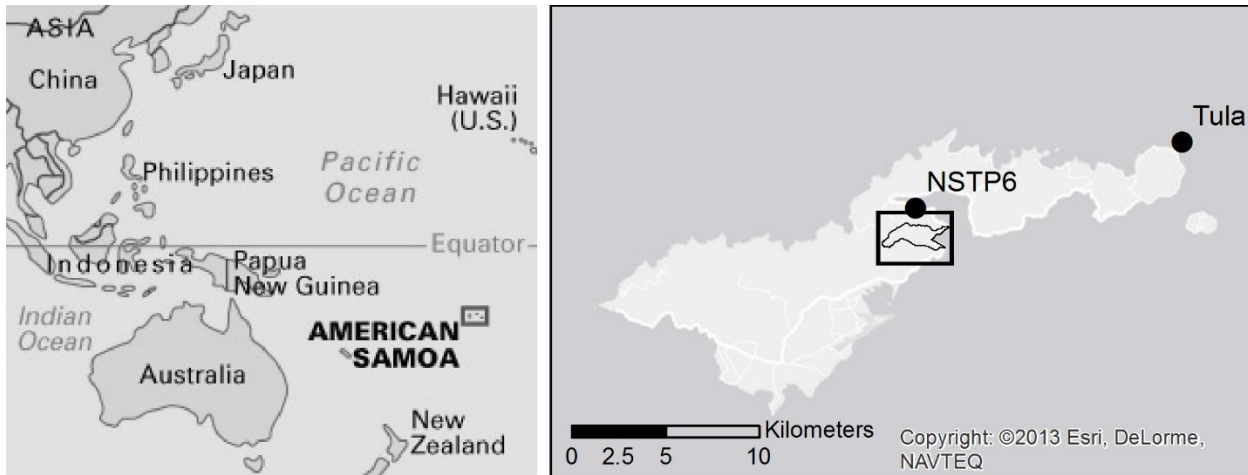
- 864 Ramos-Scharrón, C.E., Macdonald, L.H., 2005. Measurement and prediction of sediment
865 production from unpaved roads, St John, US Virgin Islands. *Earth Surf. Process. Landforms*
866 30, 1283–1304.
- 867 Ramos-Scharrón, C.E., Macdonald, L.H., 2007. Measurement and prediction of natural and
868 anthropogenic sediment sources, St. John, US Virgin Islands. *Catena* 71, 250–266.
- 869 Rankl, J.G., 2004. Relations Between Total-Sediment Load and Peak Discharge for Rainstorm
870 Runoff on Five Ephemeral Streams in Wyoming. U.S. Geological Survey Water-Resources
871 Investigations Report 02-4150. Denver, CO.
- 872 Rapp, A., 1960. Recent development of mountain slopes in Karkevagge and surroundings,
873 northern Scandinavia. *Geogr. Ann.* 42, 65–200.
- 874 Reid, L.M., Dunne, T., 1984. Sediment production from forest road surfaces. *Water Resour. Res.*
875 20, 1753–1761.
- 876 Reid, L.M., Dunne, T., 1996. Rapid evaluation of sediment budgets. *Catena Verlag*, Reiskirchen,
877 Germany.
- 878 Risk, M.J., 2014. Assessing the effects of sediments and nutrients on coral reefs. *Curr. Opin.*
879 *Environ. Sustain.* 7, 108–117. doi:10.1016/j.cosust.2014.01.003
- 880 Rodrigues, J.O., Andrade, E.M., Ribeiro, L.A., 2013. Sediment loss in semiarid small watershed
881 due to the land use. *Rev. Ciência Agronômica* 44, 488–498.

- 882 Sadeghi, S.H.R., Mizuyama, T., Miyata, S., Gomi, T., Kosugi, K., Mizugaki, S., Onda, Y., 2007.
- 883 Is MUSLE apt to small steeply reforested watershed? J. For. Res. 12, 270–277.
- 884 doi:10.1007/s10310-007-0017-9
- 885 Slaymaker, O., 2003. The sediment budget as conceptual framework and management tool.
- 886 Hydrobiologia 494, 71–82.
- 887 Stock, J.D., Rosener, M., Schmidt, K.M., Hanshaw, M.N., Brooks, B.A., Tribble, G., Jacobi, J.,
- 888 2010. Sediment budget for a polluted Hawaiian reef using hillslope monitoring and process
- 889 mapping, in: American Geophysical Union Fall Meeting. p. #EP22A–01.
- 890 Stock, J.D., Tribble, G., 2010. Erosion and sediment loads from two Hawaiian watersheds, in:
- 891 2nd Joint Federal Interagency Conference. Las Vegas, NV.
- 892 Storlazzi, C.D., Norris, B.K., Rosenberger, K.J., 2015. The influence of grain size, grain color,
- 893 and suspended-sediment concentration on light attenuation: Why fine-grained terrestrial
- 894 sediment is bad for coral reef ecosystems. Coral Reefs 34, 967–975. doi:10.1007/s00338-
- 895 015-1268-0
- 896 Syvitski, J.P.M., Vörösmarty, C.J., Kettner, A.J., Green, P., 2005. Impact of humans on the flux
- 897 of terrestrial sediment to the global coastal ocean. Science (80-.). 308, 376–380.
- 898 doi:10.1126/science.1109454
- 899 Thomas, S., Ridd, P. V, Day, G., 2003. Turbidity regimes over fringing coral reefs near a mining
- 900 site at Lihir Island, Papua New Guinea. Mar. Pollut. Bull. 46, 1006–14. doi:10.1016/S0025-
- 901 326X(03)00122-X

- 902 Tonkin & Taylor International Ltd., 1989. Hydropower feasibility studies interim report - Phase
903 1. Ref: 97/10163.
- 904 Topping, J., 1972. Errors of Observation and their Treatment, 4th ed. Chapman and Hall,
905 London, UK.
- 906 Tropeano, D., 1991. High flow events, sediment transport in a small streams in the “Tertiary
907 Basin” area in Piedmont (northwest Italy). Earth Surf. Process. Landforms 16, 323–339.
- 908 Turnipseed, D.P., Sauer, V.B., 2010. Discharge Measurements at Gaging Stations, in: U.S.
909 Geological Survey Techniques and Methods Book 3, Chap. A8. Reston, Va., p. 87.
- 910 Walling, D.E., 1977. Assessing the accuracy of suspended sediment rating curves for a small
911 basin. Water Resour. Res. 13, 531–538.
- 912 Walling, D.E., 1999. Linking land use, erosion and sediment yields in river basins.
913 Hydrobiologia 410, 223–240.
- 914 Walling, D.E., Collins, a. L., 2008. The catchment sediment budget as a management tool.
915 Environ. Sci. Policy 11, 136–143. doi:10.1016/j.envsci.2007.10.004
- 916 Wemple, B.C., Jones, J.A., Grant, G.E., 1996. Channel Network Extension by Logging Roads in
917 Two Basins, Western Cascades, Oregon. Water Resour. Bull. 32, 1195–1207.
- 918 Wolman, M.G., Schick, A.P., 1967. Effects of construction on fluvial sediment, urban and
919 suburban areas of Maryland. Water Resour. Res. 3, 451–464.

- 920 Wong, M., 1996. Analysis of Streamflow Characteristics for Streams on the Island of Tutuila,
921 American Samoa. U.S. Geological Survey Water-Resources Investigations Report 95-4185.
- 922 Wulf, H., Bookhagen, B., Scherler, D., 2012. Climatic and geologic controls on suspended
923 sediment flux in the Sutlej River Valley, western Himalaya. *Hydrol. Earth Syst. Sci.* 16,
924 2193–2217. doi:10.5194/hess-16-2193-2012
- 925 Zimmermann, A., Francke, T., Elsenbeer, H., 2012. Forests and erosion: Insights from a study of
926 suspended-sediment dynamics in an overland flow-prone rainforest catchment. *J. Hydrol.*
927 170–181.
- 928

1 Figure Captions



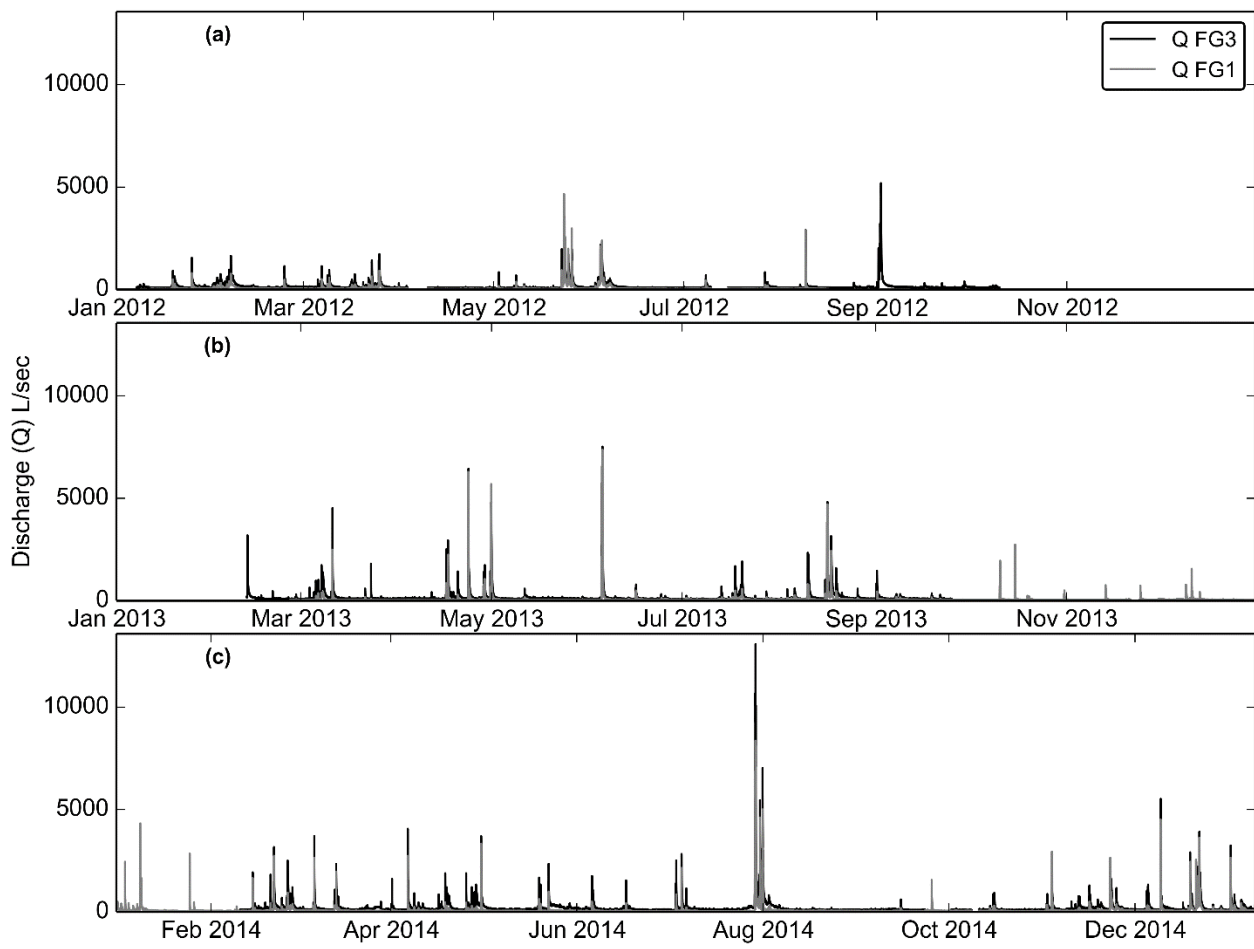
2

3 Figure 1. Faga'alau watershed showing the UPPER (undisturbed) and LOWER (human-disturbed)
4 subwatersheds. The LOWER subwatershed drains areas between FG1 and FG3, and is further
5 subdivided into the LOWER_QUARRY containing the quarry (between FG1 and FG2) and the

6 LOWER_VILLAGE containing the village areas (between FG2 and FG3). The TOTAL
7 watershed includes all subwatersheds draining to FG3. The Administrative watershed boundary
8 for government jurisdiction is outlined by the dotted grey line. Blue pentagons in the UPPER
9 watershed show the location of abandoned water supply reservoirs (see Appendix 1 for full
10 description). Barometer locations at NSTP6 and TULA are shown in top-right.
11



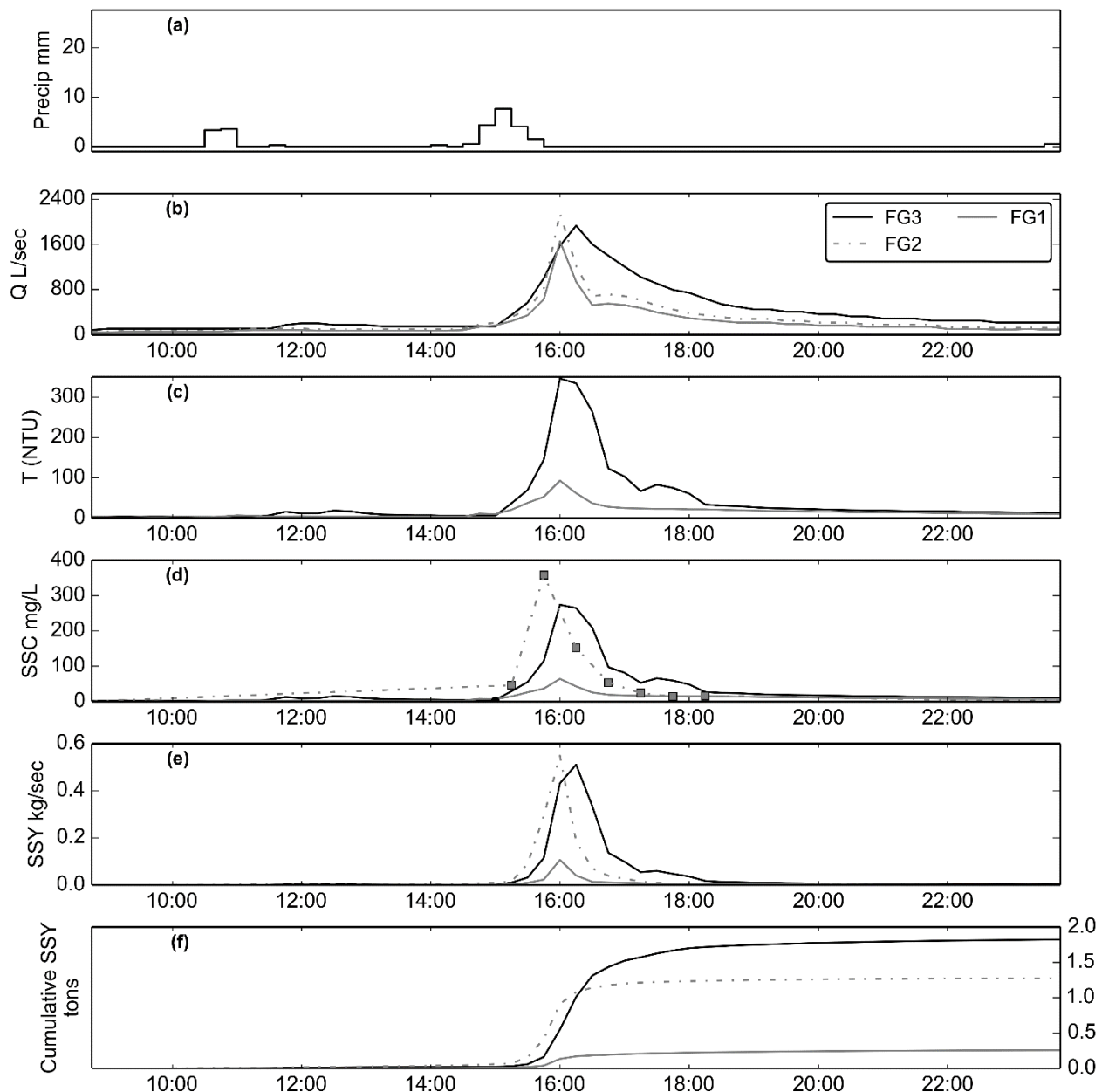
12 Figure 2. Photos of the aggregate quarry in Faga'alau in 2012, 2013, and 2014. Pictures a-b show
13 vegetation overgrowth during the period of study from 2012-2014, and the location of the
14 groundwater diversion that was installed in 2012. Pictures c-d show that haul roads were covered
15 in gravel in 2013. Photos: Messina
16
17



18

19 Figure 3. Time series of water discharge (Q), calculated from measured stage-
20 discharge rating curves in a) 2012 b) 2013 and c) 2014.

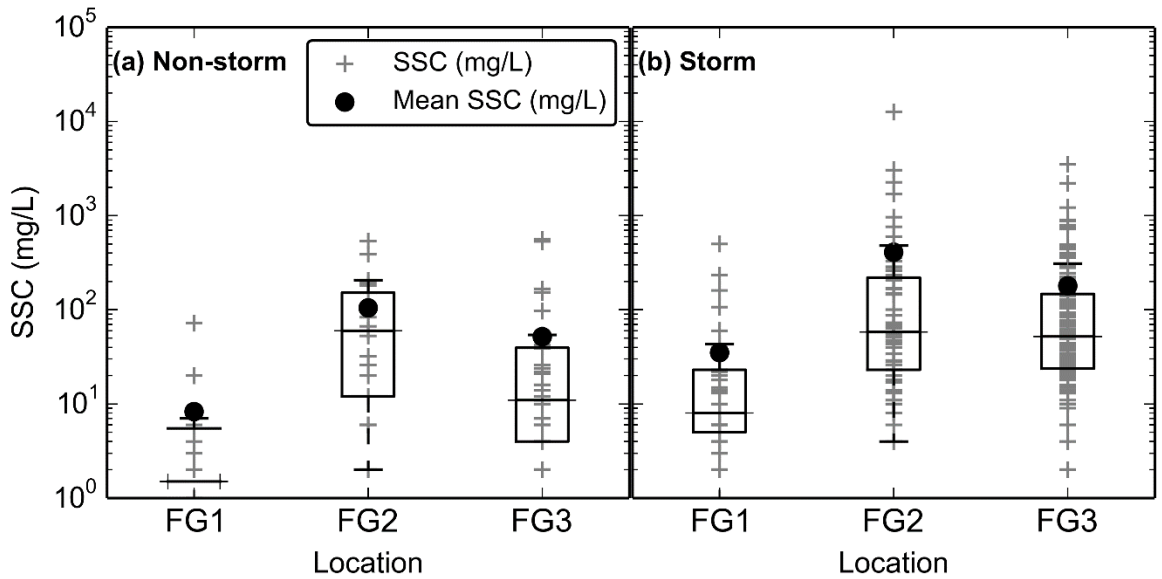
21



22

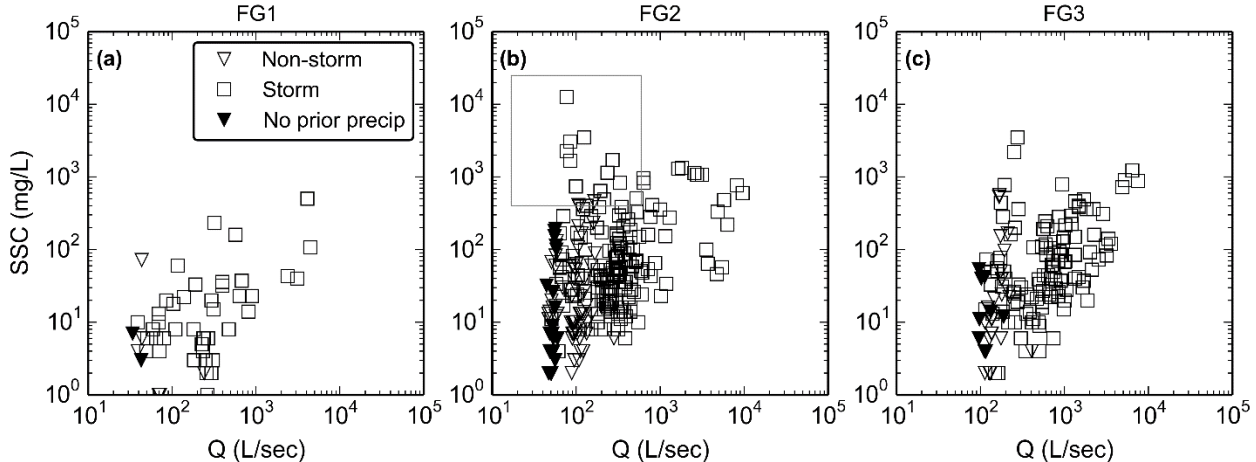
23 Figure 4. Example of a storm event (02/14/2014). SSY at FG1 and FG3 calculated from SSC
 24 modeled from T, and SSY at FG2 from SSC samples collected by the Autosampler.

25



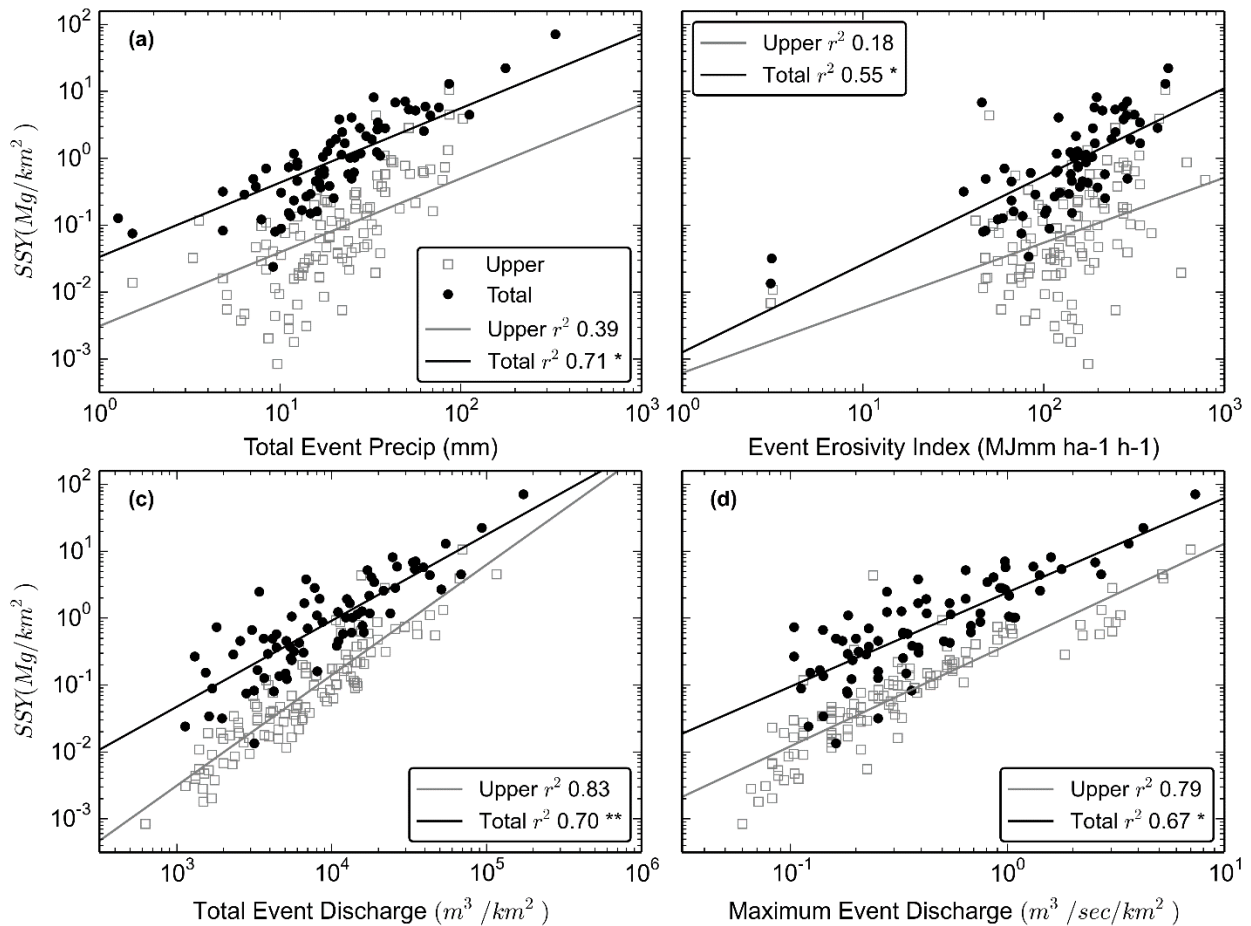
26

27 Figure 5. Boxplots of Suspended Sediment Concentration (SSC) from grab samples only (no
28 Autosampler) at FG1, FG2, and FG3 during (a) non-stormflow and (b) stormflow.
29



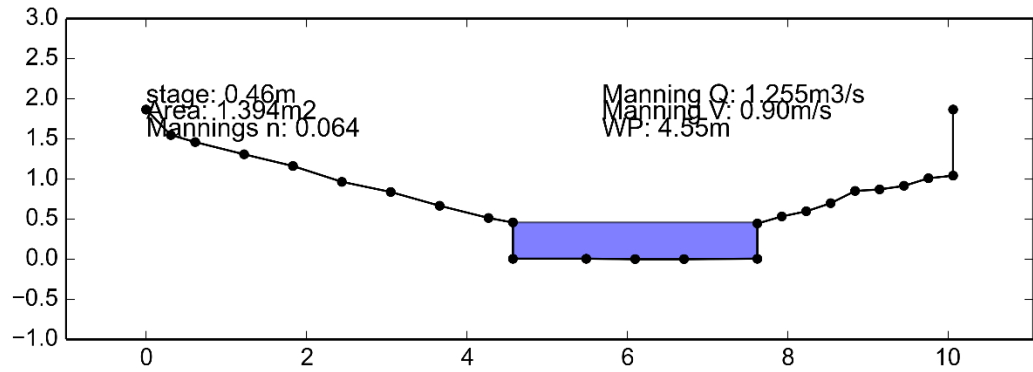
30

31 Figure 6. Water Discharge versus suspended sediment concentration measured from grab
32 samples at a) FG1, b) FG2, and c) FG3 during non-stormflow and stormflow periods. The box in
33 b) highlights the samples with high SSC during low flows. Solid symbols indicate SSC samples
34 where precipitation during the preceding 24 hours was 0 mm.
35



36

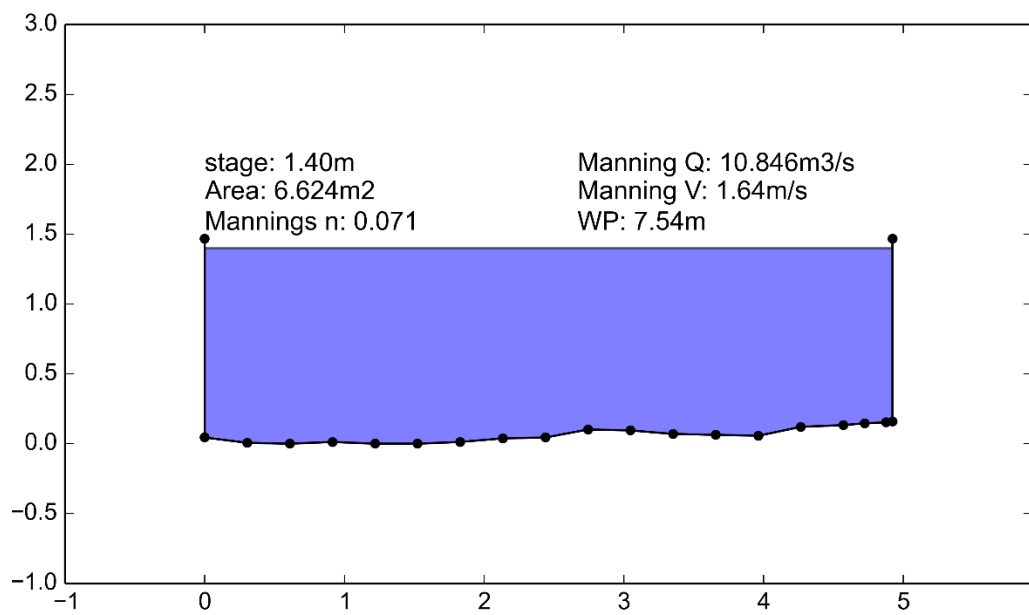
37 Figure 7. sSSY_{EV} regression models for predictive storm metrics. Each point represents a
 38 different storm event. **=slopes and intercepts were statistically different ($p<0.01$), *=intercepts
 39 were statistically different ($p<0.01$).
 40



41

42 Figure A2.1. Stream cross-section at FG1

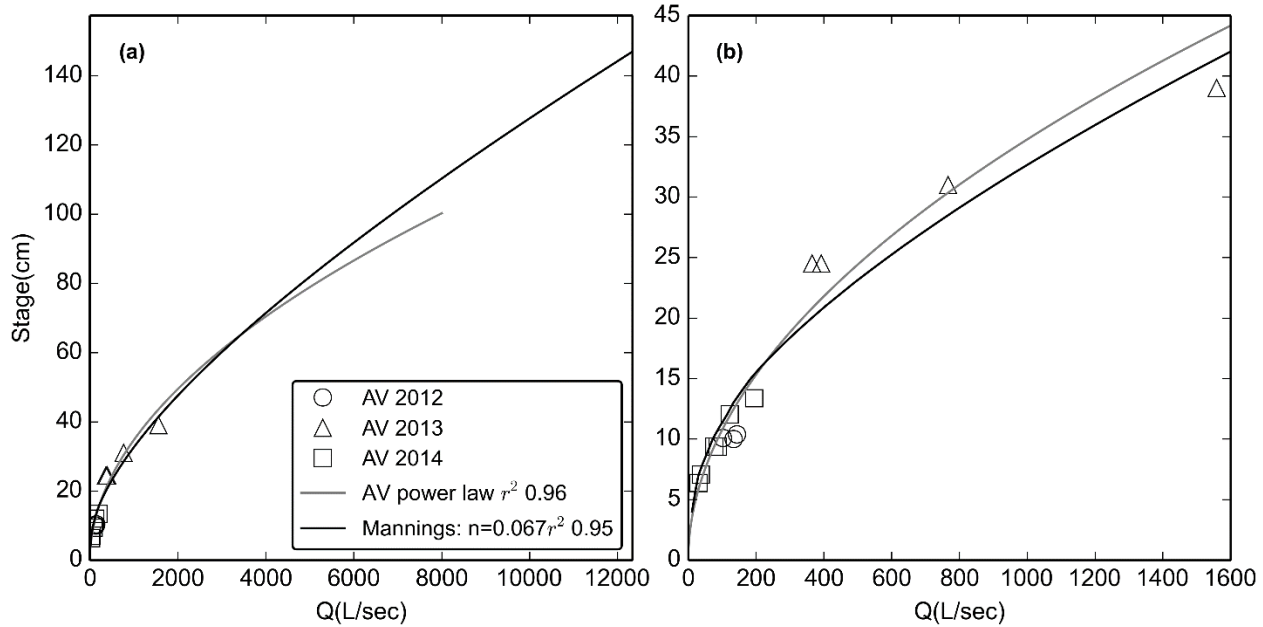
43



44

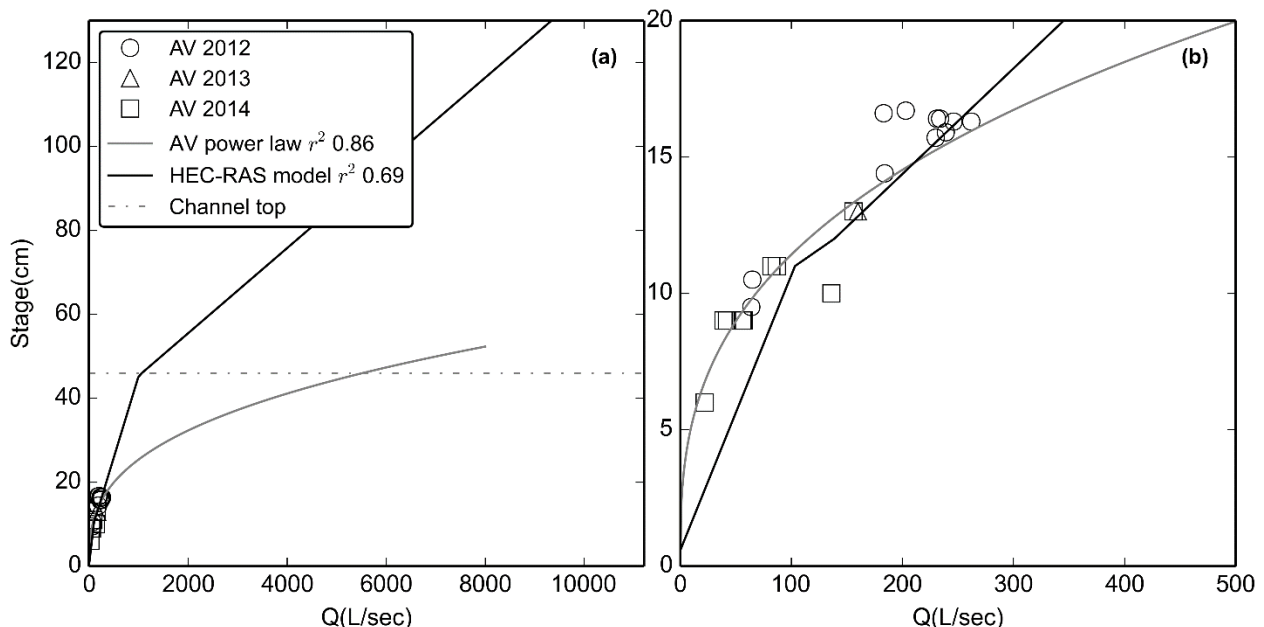
45 Figure A2.2. Stream cross-section at FG3

46



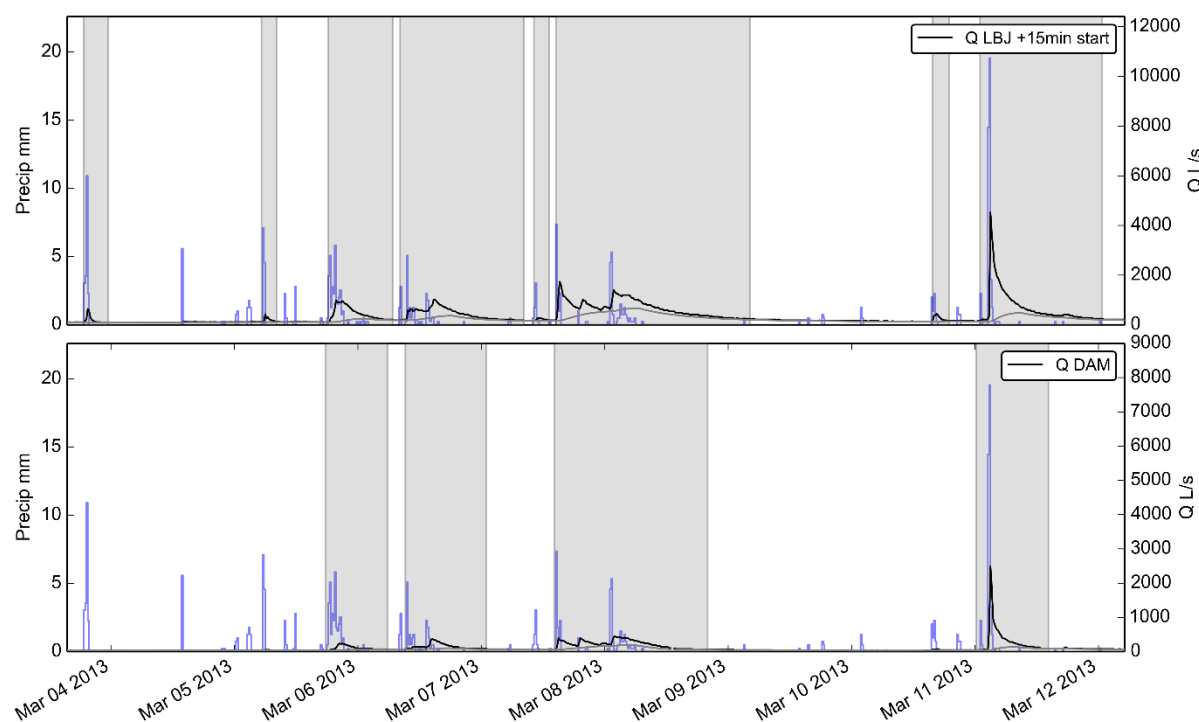
48 Figure A2.3. Stage-Discharge relationships for stream gaging site at FG3 for (a) the full range of
49 observed stage and (b) the range of stages with AV measurements of Q. RMSE was 93 L/sec, or
50 32% of observed Q.

51



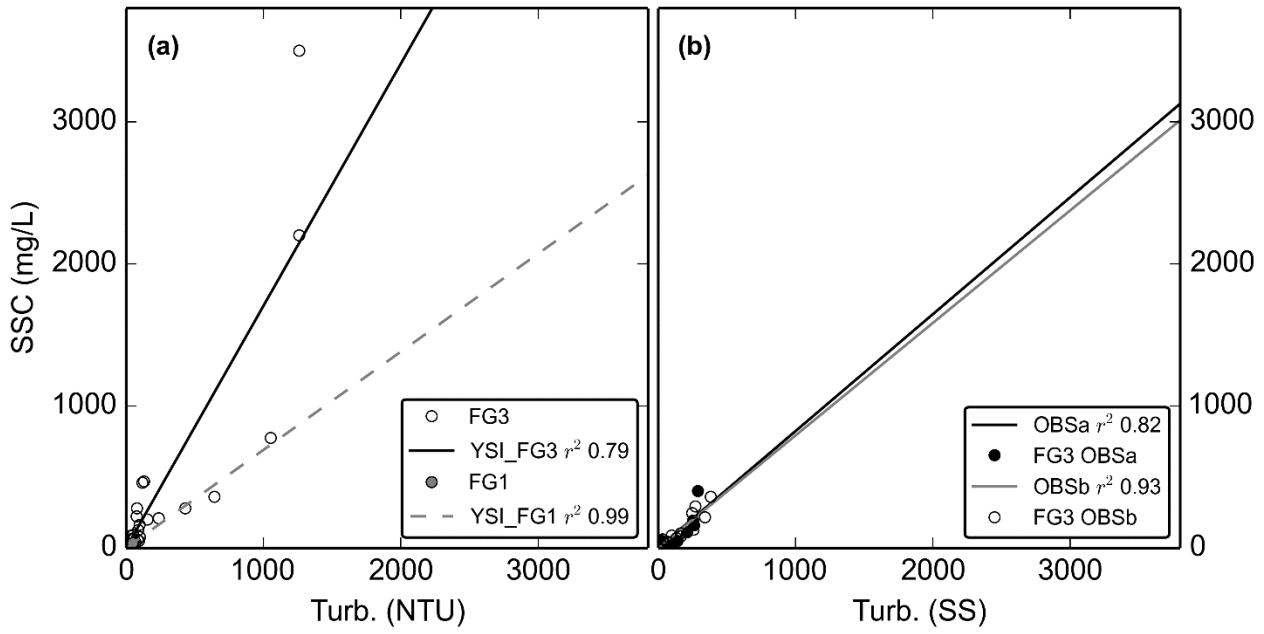
53 Figure A2.4. Stage-Discharge relationships for stream gaging site at FG1 for (a) the full range of
54 observed stage and (b) the range of stages with AV measurements of Q. RMSE was 31 L/sec, or
55 22% of observed Q. "Channel Top" refers to the point where the rectangular channel transitions
56 to a sloped bank and cross-sectional area increases much more rapidly with stage. A power-law
57 relationship is also displayed to illustrate the potential error that could result if inappropriate
58 methods are used.

59



60
61 Figure A3.1. Example of method for separating storms based on baseflow separation. Black line
62 is hydrograph, grey line is baseflow calculated by R statistical package EcoHydRology. Storm
63 periods are shaded in grey. Seven storm events are identified from March 3, 2013 to March 13,
64 2013.

65

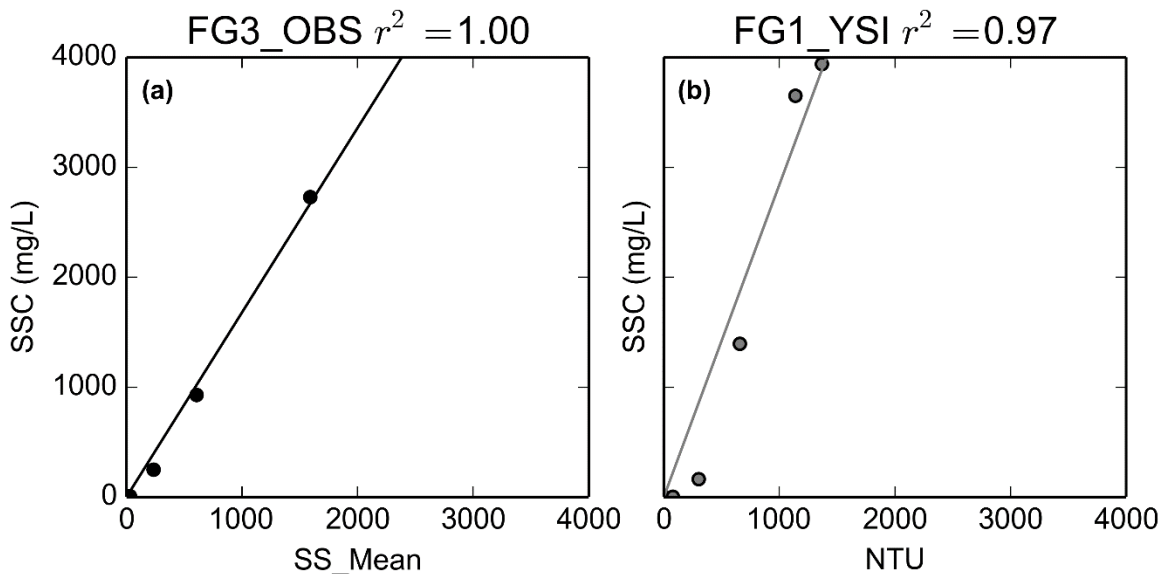


66

67 Figure A4.1. Turbidity-Suspended Sediment Concentration relationships for a) the YSI
 68 turbidimeter deployed at FG3 (02/27/2012-05/23/2012) and the same YSI turbidimeter deployed
 69 at FG1 (06/13/2013-12/31/2014). b) OBS500 turbidimeter deployed at FG3 (03/11/2013-
 70 07/11/2013) and c) OBS500 turbidimeter deployed at FG3 (01/31/2014-03/04/2014).

71

72



73

74 Figure A4.2. Synthetic Rating Curves for (a) OBS turbidimeter deployed at FG3 and (b) YSI
75 deployed at FG1.

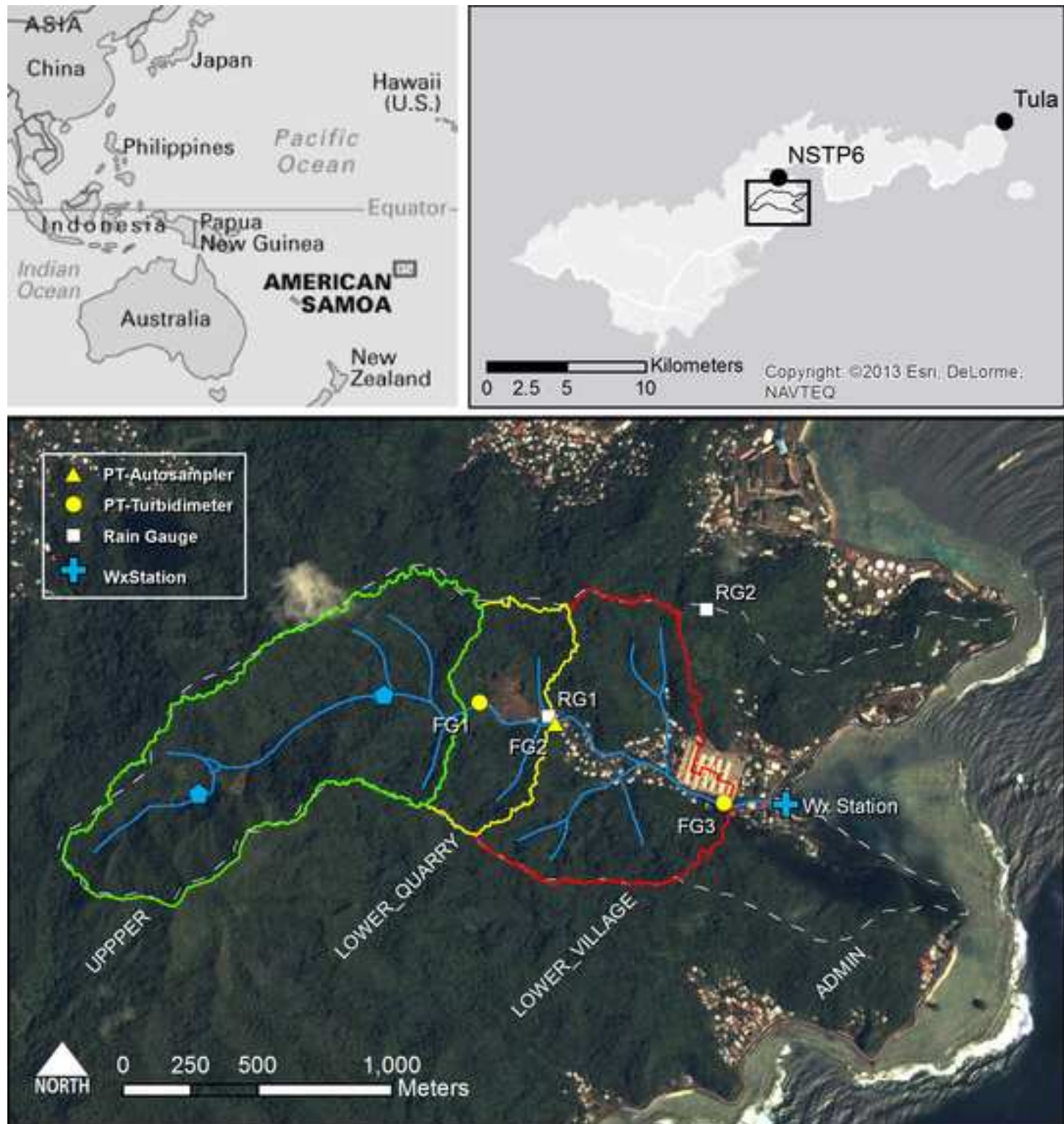
76

Supplementary material for on-line publication only

[**Click here to download Supplementary material for on-line publication only: Supplementary Material - Appendices.docx**](#)

Figure

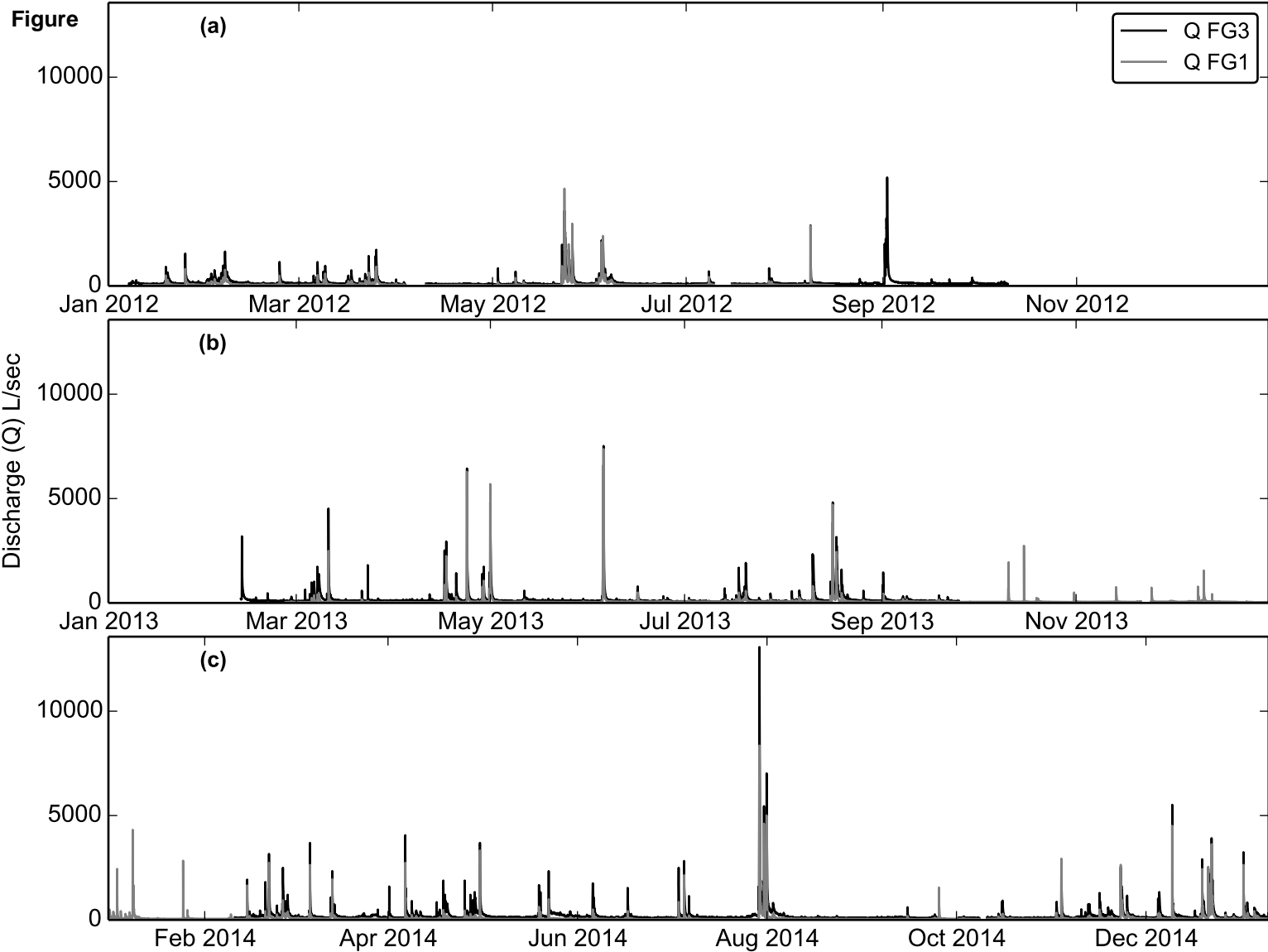
[Click here to download high resolution image](#)



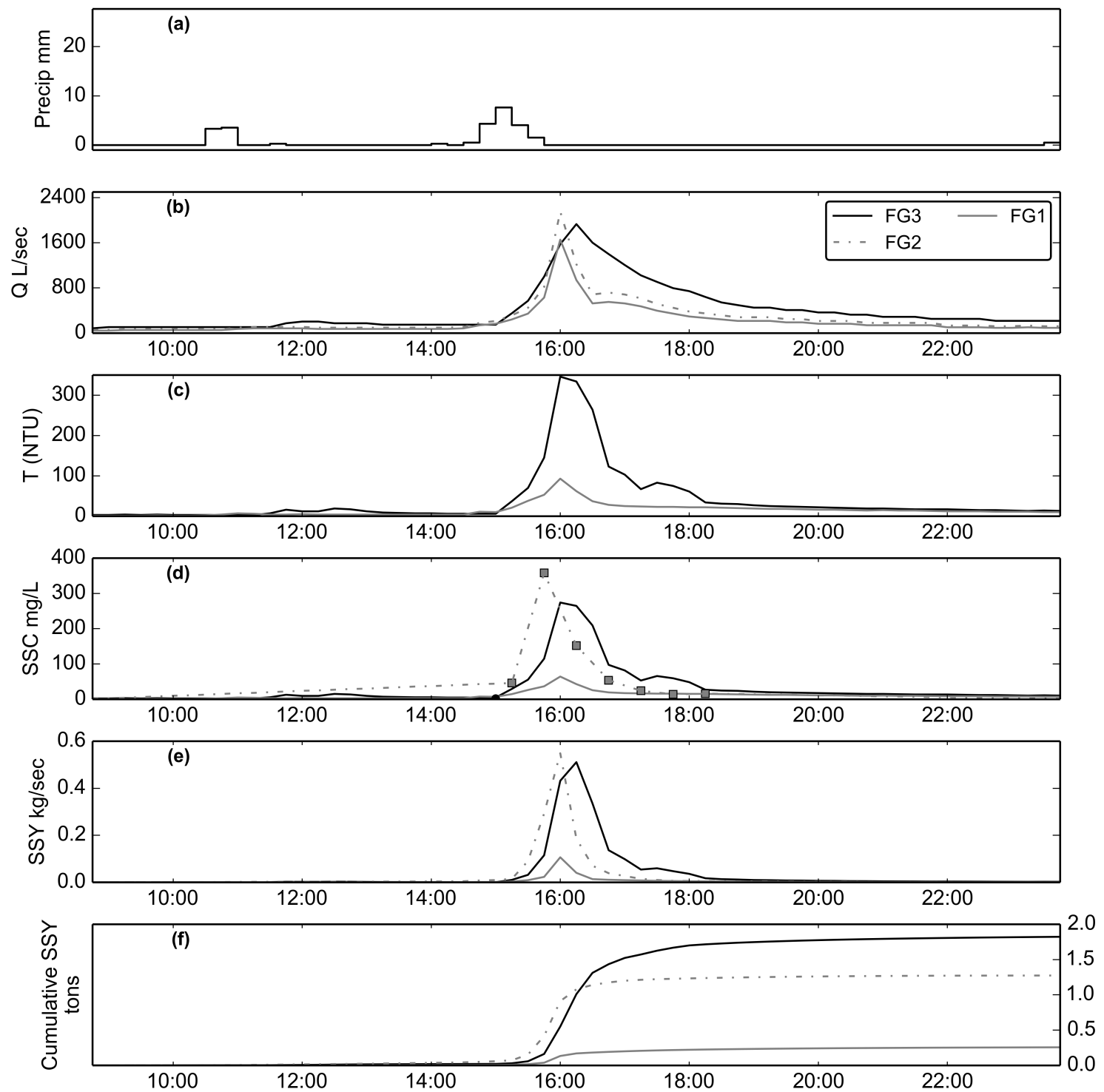
Figure

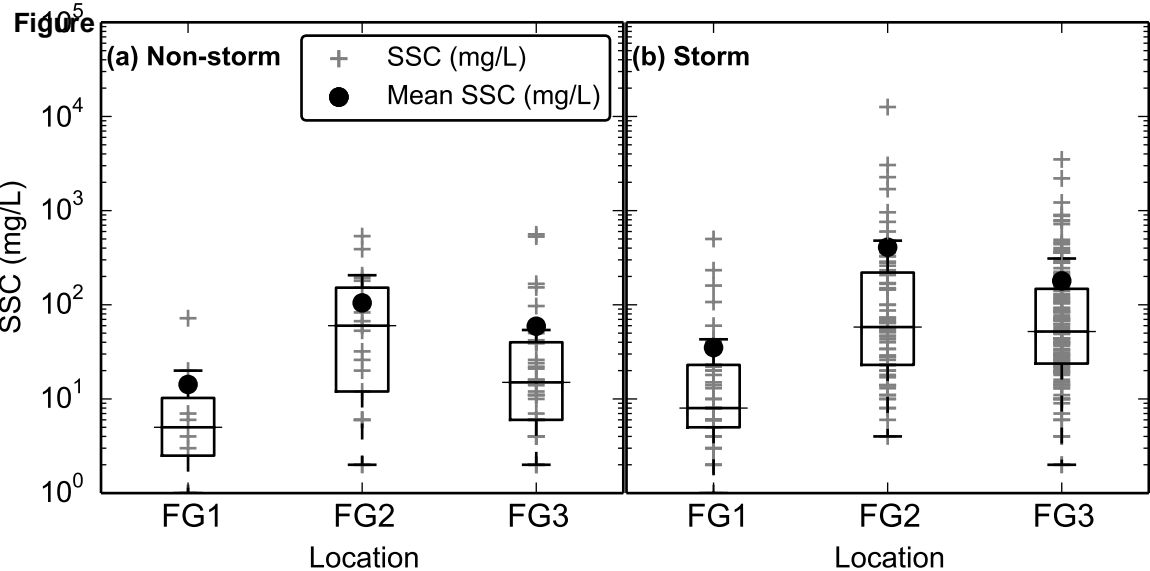
[Click here to download high resolution image](#)

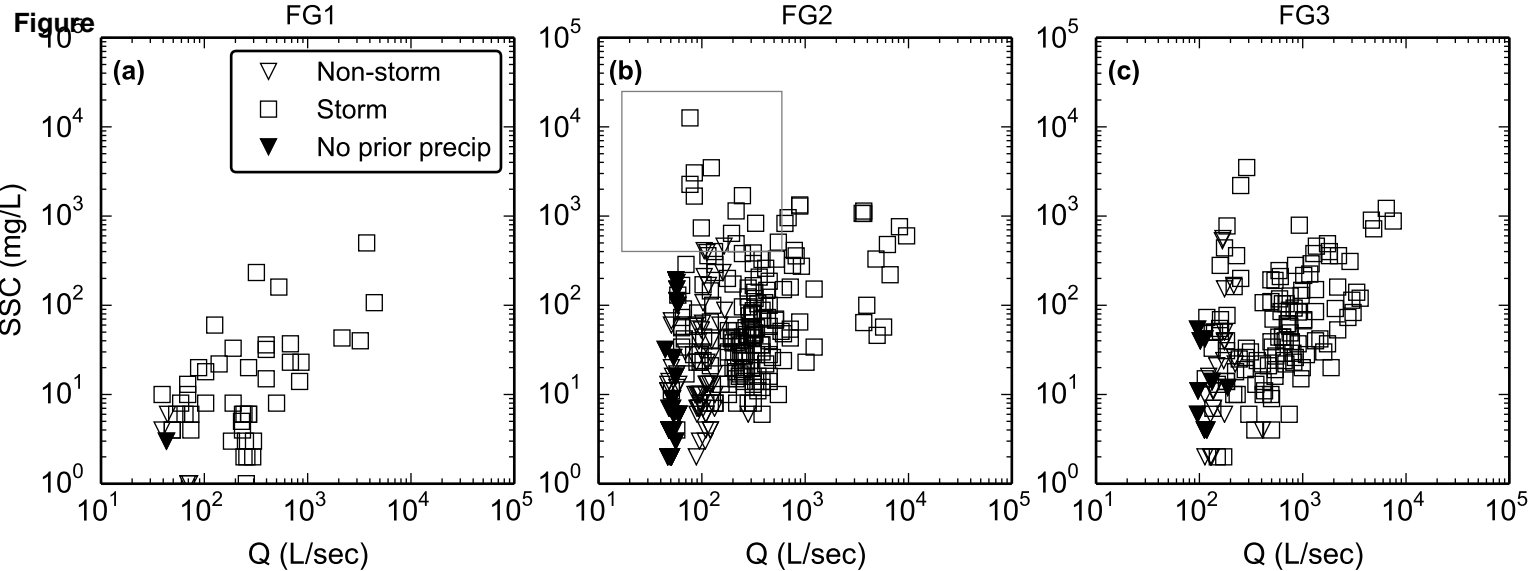


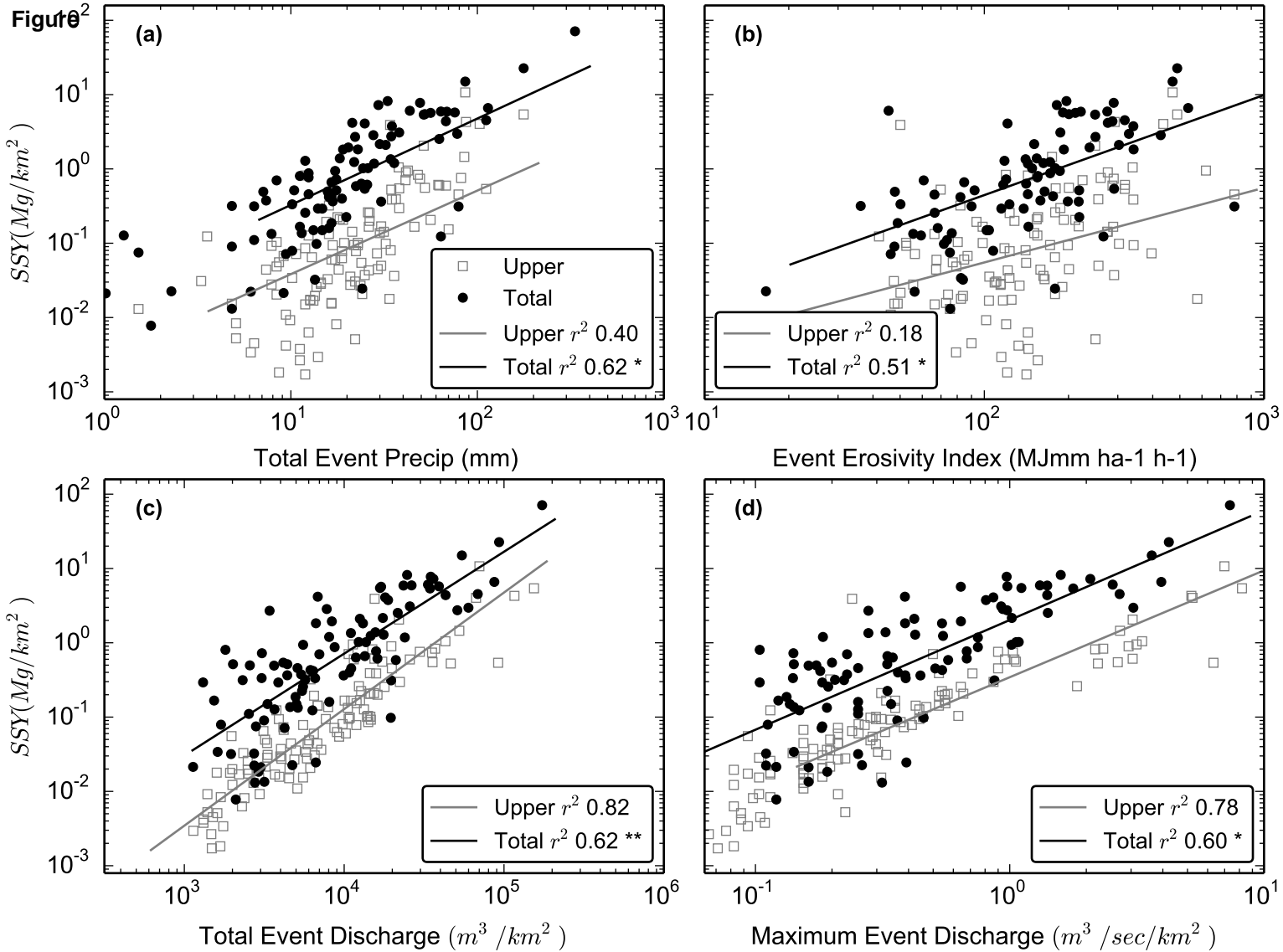


Figure

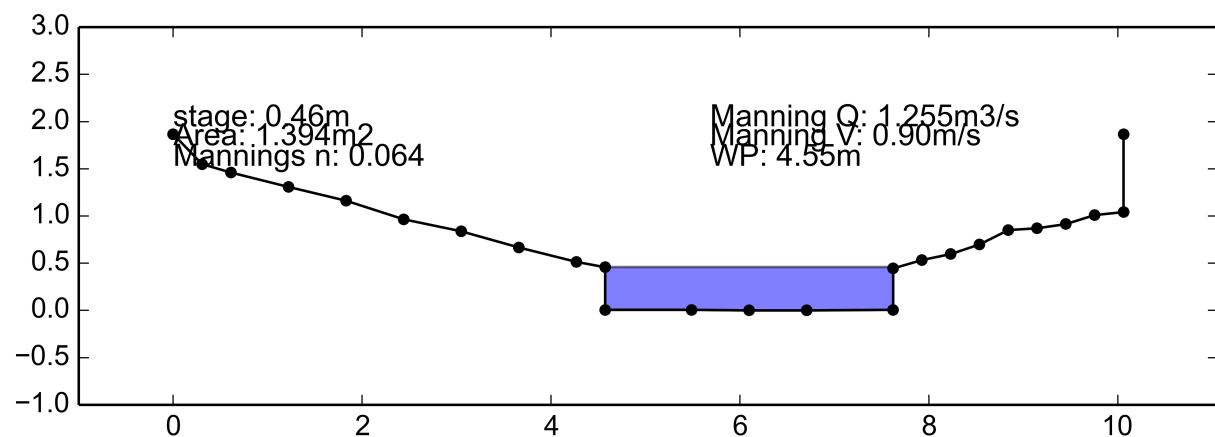




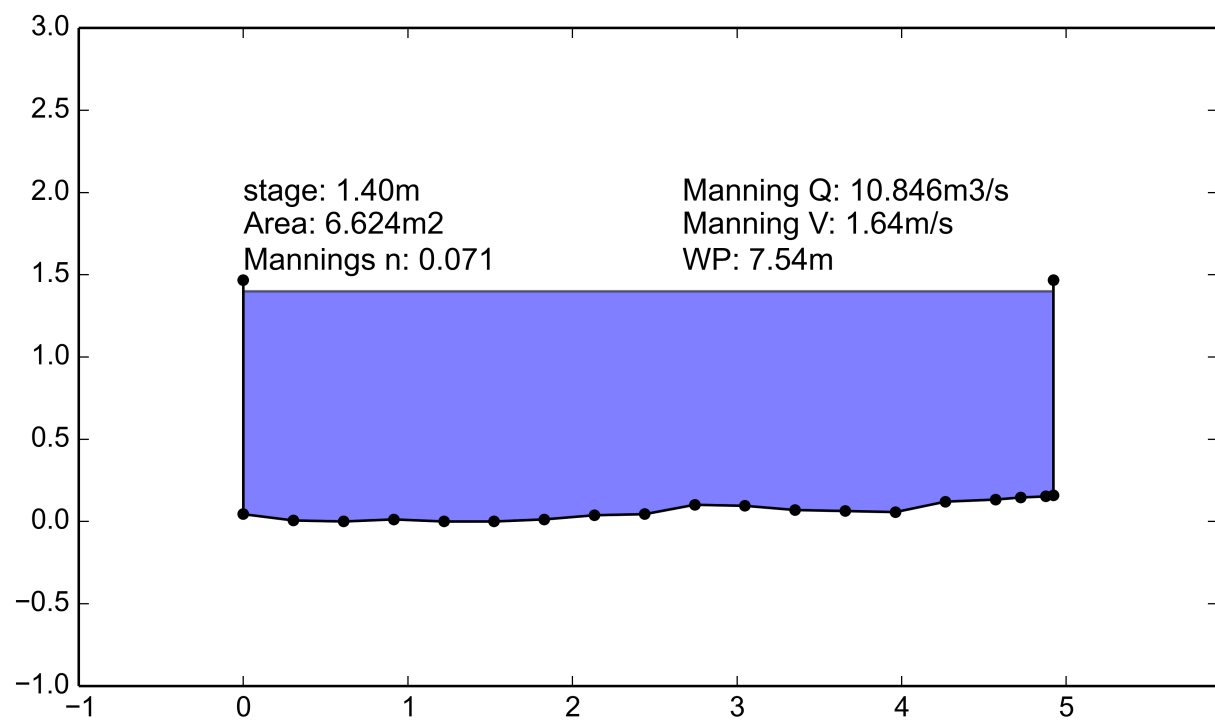


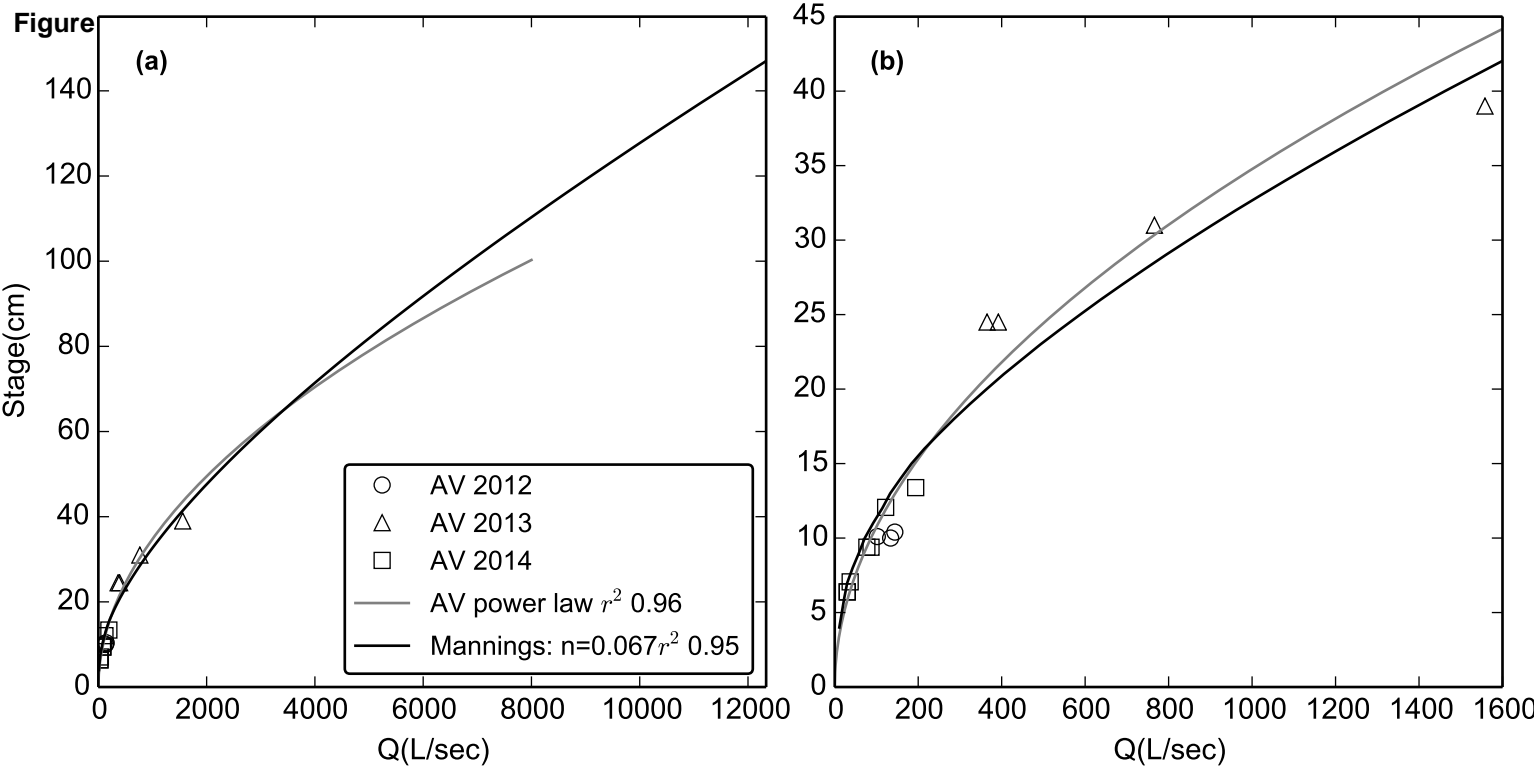


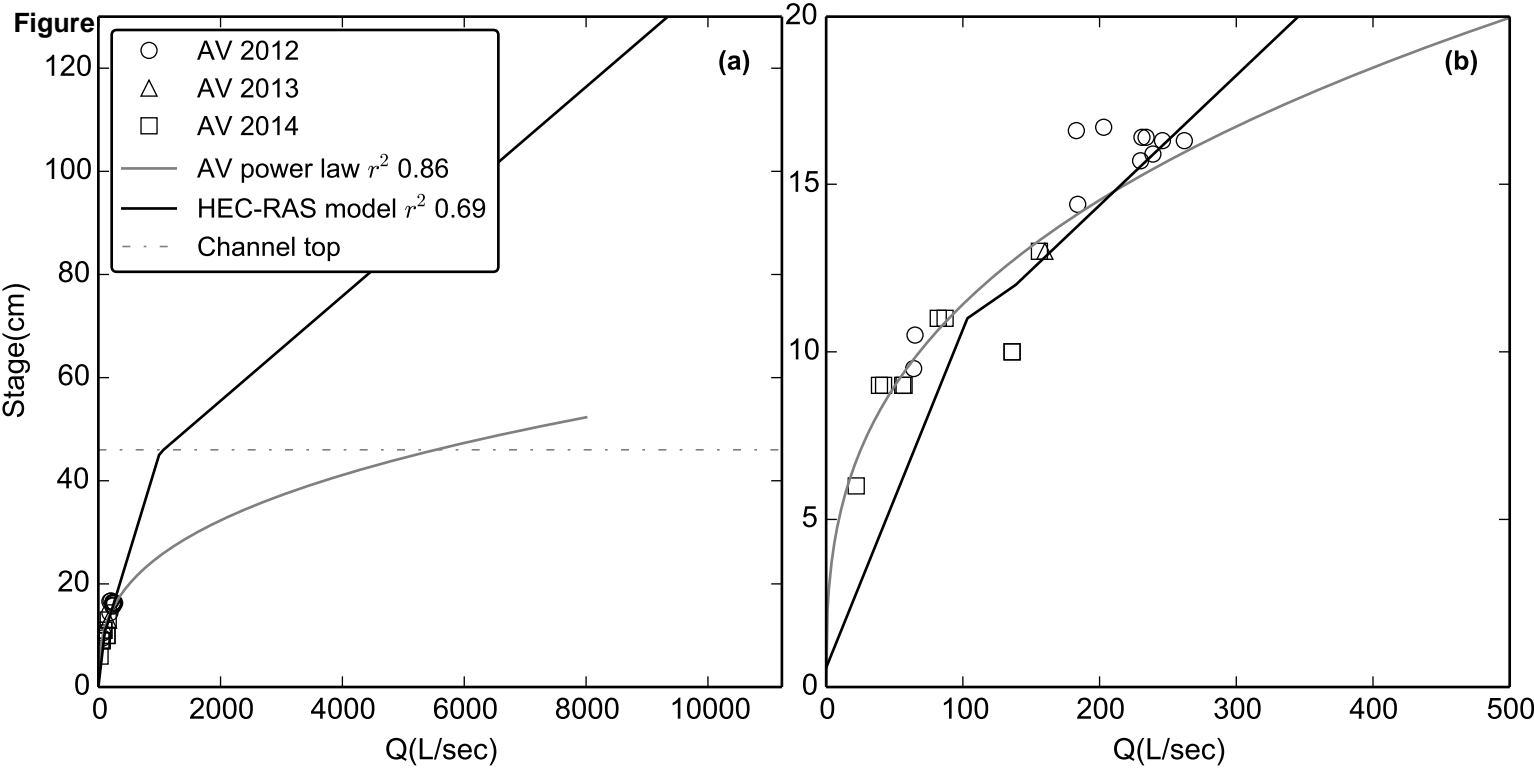
Figure

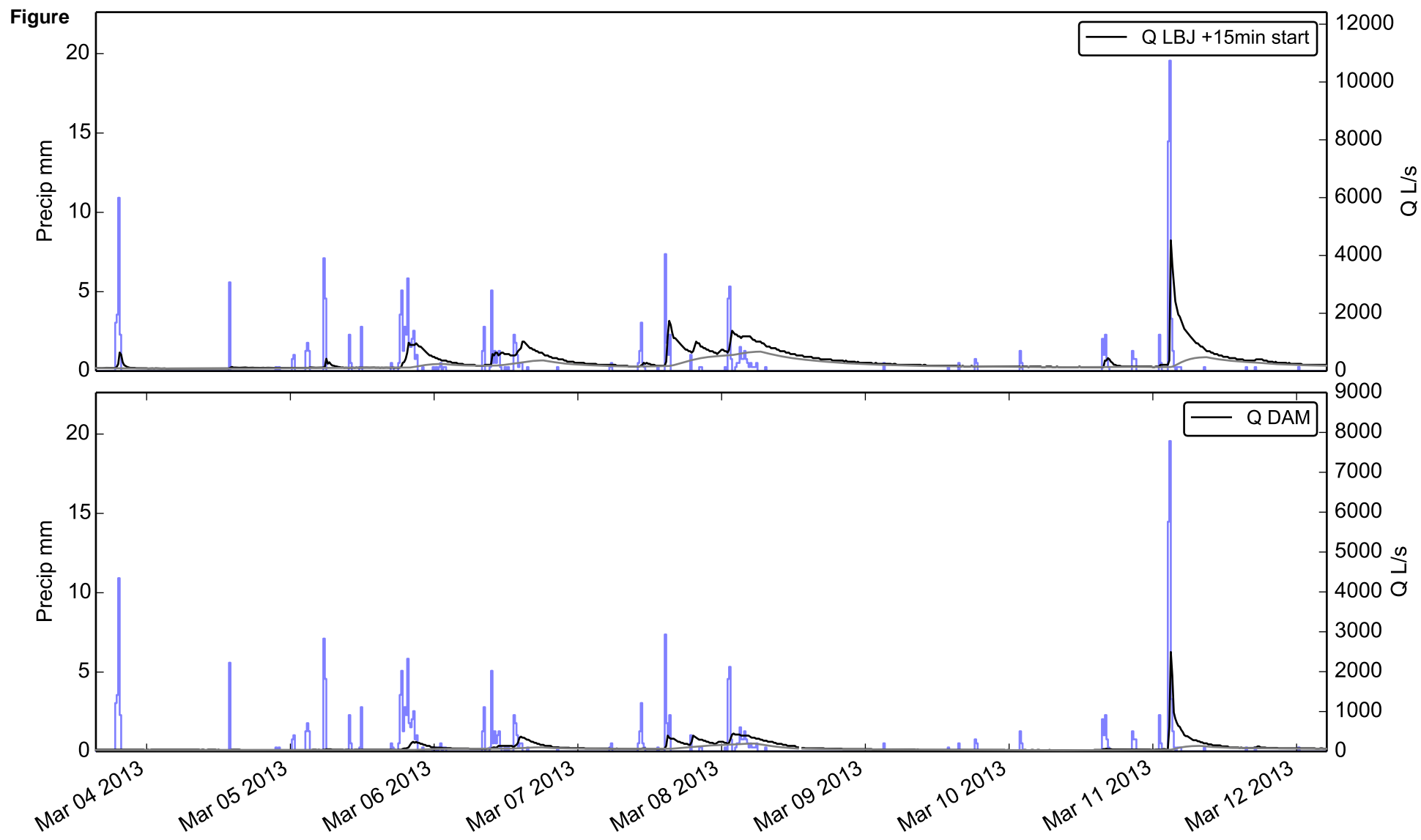


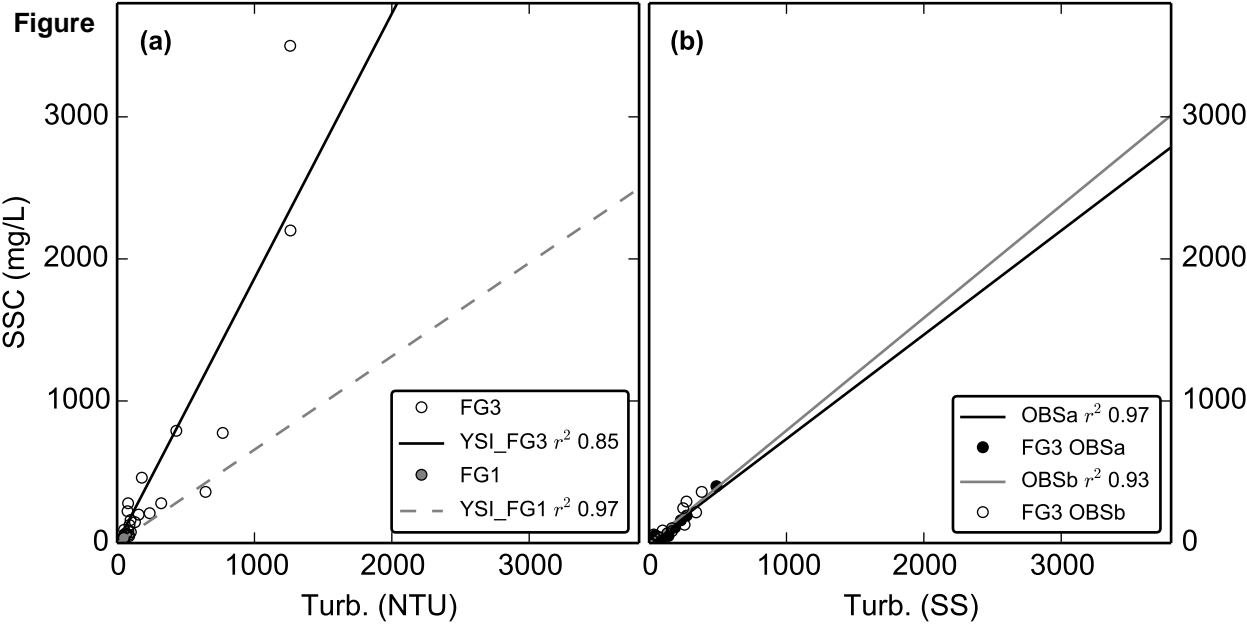
Figure

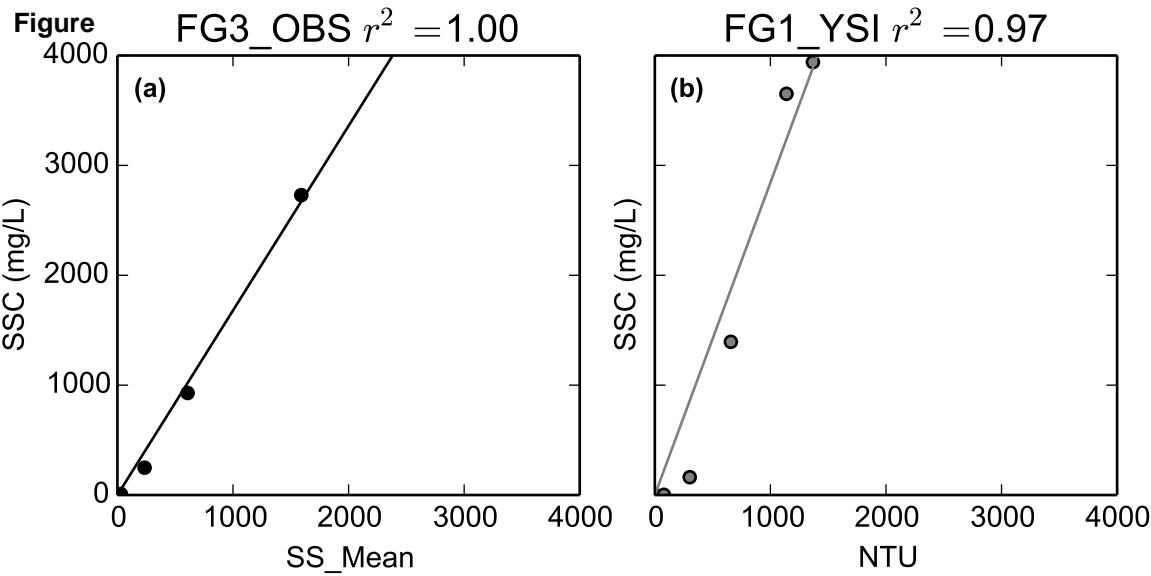


Figure









Table

[Click here to download Table: Table1_landcover.pdf](#)

Table 1. Land use categories in Faga'alu subwatersheds (NOAA Ocean Service and Coastal Services Center, 2010). Land cover percentages are of the subwatershed.

Subwatershed (pourpoint)	Cumulative Area		Subwatershed Area		Land cover as % subwatershed area ^a							
	km ²	%	km ²	%	B	HI	DOS	GA	F	S	Disturbed	Undisturbed
UPPER (FG1)	0.9	50	0.90	50	0.4	0.0	0.0	0.1	82	17.1	0.4	100
LOWER_QUARRY (FG2)	1.2	66	0.27	16	5.7	0.7	0.1	0.5	92	0.9	6.5	94
LOWER_VILLAGE (FG3)	1.8	100	0.60	34	0.0	9.0	2.6	0.2	88	0.6	11.7	88
LOWER (FG3)	1.8	100	0.88	50	1.8	6.4	1.8	0.3	89	0.7	10.1	90
TOTAL (FG3)	1.8	100	1.78	100	1.1	3.2	0.9	0.2	86	9.0	5.2	95

a. B=Bare, HI=High Intensity Developed, DOS=Developed Open Space, GA=Grassland (agriculture), F=Forest, S=Scrub/Shrub, Disturbed=B+HI+DOS+GA, Undisturbed=F+S

Table 2. Event-wise suspended sediment yield (SSY_{EV}) from subwatersheds in Faga'alu for events with simultaneous data from FG1 and FG3. Storm numbers correspond with the storms presented in Table A3.1.

Storm#	Storm	Precip	SSY _{EV} tons			% of SSY _{EV} TOTAL		PE ^a		SSC
			Start	mm	UPPER ^b	LOWER ^c	TOTAL ^d	UPPER	LOWER	
2	01/19/2012	18	0.06	0.63	0.69	8.0	91.0	49	36	int. grab
4	01/31/2012	35	0.03	1.92	1.95	1.0	98.0	49	118	T-YSI
5	02/01/2012	11	0.01	0.4	0.42	3.0	96.0	49	118	T-YSI
6	02/02/2012	16	0.06	1.02	1.08	5.0	94.0	49	118	T-YSI
7	02/03/2012	11	0.08	2.01	2.09	3.0	96.0	49	118	T-YSI
8	02/04/2012	6	0.0	0.51	0.51	0.0	99.0	49	118	T-YSI
9	02/05/2012	23	0.05	0.98	1.03	5.0	94.0	49	118	T-YSI
10	02/05/2012	21	0.09	1.93	2.02	4.0	95.0	49	118	T-YSI
11	02/06/2012	38	0.28	4.75	5.03	5.0	94.0	49	118	T-YSI
12	02/07/2012	4	0.01	0.13	0.15	9.0	90.0	49	118	T-YSI
13	02/07/2012	10	0.03	0.51	0.54	5.0	94.0	49	118	T-YSI
14	02/13/2012	11	0.0	0.27	0.27	1.0	98.0	49	118	T-YSI
16	03/05/2012	22	0.0	4.39	4.4	0.0	99.0	49	118	T-YSI
17	03/06/2012	56	0.19	9.05	9.25	2.0	97.0	49	118	T-YSI
18	03/08/2012	22	0.09	2.89	2.98	2.0	97.0	49	118	T-YSI
19	03/09/2012	19	0.2	2.78	2.97	6.0	93.0	49	118	T-YSI
20	03/15/2012	17	0.01	1.17	1.18	0.0	99.0	49	118	T-YSI
21	03/16/2012	34	0.08	2.12	2.2	3.0	96.0	49	118	T-YSI
22	03/17/2012	32	0.09	3.33	3.43	2.0	97.0	49	118	T-YSI
23	03/20/2012	24	0.04	0.84	0.88	4.0	95.0	49	118	T-YSI
24	03/21/2012	18	0.2	2.06	2.26	8.0	91.0	49	118	T-YSI
25	03/22/2012	34	0.37	5.75	6.12	5.0	94.0	49	118	T-YSI
27	03/24/2012	7	0.03	0.19	0.22	12.0	87.0	49	118	T-YSI
28	03/25/2012	49	0.7	11.92	12.62	5.0	94.0	49	118	T-YSI
29	03/31/2012	15	0.03	0.78	0.81	3.0	96.0	49	118	T-YSI
32	05/07/2012	11	0.0	1.31	1.31	0.0	99.0	49	118	T-YSI
33	05/08/2012	21	0.13	6.65	6.79	1.0	98.0	49	118	T-YSI
34	05/20/2012	13	0.0	0.47	0.48	0.0	99.0	49	118	T-YSI
64	04/16/2013	62	0.54	4.01	4.55	11.0	88.0	28	36	int. orah

											method
70	04/23/2013	86	9.57	13.51	23.08	41.0	58.0	28	36		int. grab
79	06/24/2013	9	0.01	0.13	0.14	7.0	92.0	32	77		T-OBS
80	07/02/2013	13	0.02	0.28	0.3	5.0	94.0	32	77		T-OBS
106	02/14/2014	25	0.26	1.57	1.82	14.0	85.0	32	51		T-OBS
107	02/15/2014	7	0.04	0.63	0.67	6.0	93.0	32	51		T-OBS
109	02/18/2014	12	0.01	0.81	0.81	0.0	99.0	32	51		T-OBS
110	02/20/2014	29	0.13	3.71	3.84	3.0	96.0	32	51		T-OBS
111	02/21/2014	51	2.55	7.03	9.58	26.0	73.0	32	51		T-OBS
112	02/24/2014	16	0.09	0.56	0.65	13.0	86.0	32	51		T-OBS
113	02/24/2014	1	0.01	0.12	0.13	9.0	90.0	32	51		T-OBS
114	02/25/2014	67	0.62	7.17	7.79	7.0	92.0	32	51		T-OBS
115	02/27/2014	16	0.13	0.68	0.8	15.0	84.0	32	51		T-OBS
116	02/27/2014	12	0.12	1.25	1.37	8.0	91.0	32	51		T-OBS
Total/Avg	42	1004	17.0	112.2	129.2	13	87	43	94		-
Tons/km ²	-	-	18.8	127.5	72.6	-	-	-	-		-
DR	-	-	1	6.8	3.9	-	-	-	-		-

a. PE is cumulative probable error (Eq 6) as a percentage of the mean observed SSY.

b. Measured SSY_{EV} at FG1.

c. SSY_{EV} at FG3 - SSY_{EV} at FG1.

d. SSY_{EV} at FG3.

Table
[Click here to download Table: Table3_S_budget_analysis_pre.pdf](#)

Table 3. Total Suspended sediment yield (SSY), specific suspended sediment yield (sSSY), and disturbance ratio (DR) from disturbed portions of UPPER and LOWER subwatersheds for the storm events in Table 2.

	UPPER^a	LOWER	TOTAL
Fraction of subwatershed area disturbed (%)	0.4	10.1	5.2
SSY (tons)	17.0	112.2	129.2
Forested areas	16.9	14.9	31.7
Disturbed areas	0.1	97.3	97.5
% from disturbed areas	0.9	87	75
sSSY, disturbed areas (tons/km ²)	41.0	1095.0	1053.1
DR for sSSY from disturbed areas ^b	2	58	56

a. Disturbed areas in UPPER are bare areas from landslides.

b. Calculated as (sSSY from disturbed areas)/sSSY from UPPER (17.0 tons/km²)

Table

[Click here to download Table: Table4_S_budget_2_pre.pdf](#)

Table 4. Event-wise suspended sediment yield (SSY_{EV}) from subwatersheds in Faga'alu for events with simultaneous data from FG1, FG2, and FG3. Storm numbers correspond with the storms presented in Table 2 and Appendix Table A3.1.

Storm#	Storm	Precip	SSY _{EV} tons						% of SSY _{EV} TOTAL					
			Start	mm	UPPER ^a	LOWER	QUARRY ^b	LOWER_VILLAGE ^c	LOWER ^d	TOTAL ^e	UPPER	LOWER	QUARRY	LOWER_VILLAGE
2	01/19/2012	18	0.06	0.3	0.33	0.63	0.69	8.0	43.0	47.0	47.0	91.0		
64	04/16/2013	62	0.54	2.77	1.24	4.01	4.55	11.0	60.0	27.0	27.0	88.0		
70	04/23/2013	86	9.57	8.21	5.3	13.51	23.08	41.0	35.0	22.0	22.0	58.0		
106	02/14/2014	25	0.26	1.01	0.55	1.57	1.82	14.0	55.0	30.0	30.0	86.0		
110	02/20/2014	29	0.13	1.6	2.11	3.71	3.84	3.0	41.0	54.0	54.0	96.0		
111	02/21/2014	51	2.55	2.07	4.96	7.03	9.58	26.0	21.0	51.0	51.0	73.0		
115	02/27/2014	16	0.13	0.08	0.59	0.68	0.8	16.0	9.0	73.0	73.0	85.0		
116	02/27/2014	12	0.12	0.32	0.93	1.25	1.37	8.0	23.0	67.0	67.0	91.0		
Total/Avg	8	299	13.4	16.4	16.0	32.4	45.7	29	36	35	35	71		
Tons/km ²				14.8	60.6	26.7	36.8	25.7	-	-	-	-		
DR				1.0	4.08	1.8	2.5	1.7	-	-	-	-		

a. Measured SSY_{EV} at FG1.

b. SSY_{EV} at FG2 - SSY_{EV} at FG1.

c. SSY_{EV} at FG3 - SSY_{EV} at FG2.

d. SSY_{EV} at FG3 - SSY_{EV} at FG1.

e. Measured SSY_{EV} at FG3.

Table

[Click here to download Table: Table5_S_budget_2_analysis_pre.pdf](#)

Table 5. Total Suspended sediment yield (SSY), specific suspended sediment yield (sSSY), and disturbance ratio (DR) from disturbed portions of UPPER and LOWER subwatersheds for the storm events in Table 4.

	UPPER	LOWER	QUARRY	LOWER_VILLAGE	LOWER	TOTAL		
Fraction of subwatershed area disturbed (%)	0.4		6.5		11.7	10.1	5.2	
SSY (tons)		13.4		16.4		16.0	32.4	45.7
Forested areas		13.3		3.7		7.8	11.7	25.0
Disturbed areas		0.1		12.7		8.2	20.7	20.7
% from disturbed areas		1.0		77		51	64	45
sSSY, disturbed areas (tons/km ²)		37.0		721.6		116.2	232.8	223.9
DR for sSSY from disturbed areas		3		49		8	16	15

Table

[Click here to download Table: Table6_All_Models_stats_pre.pdf](#)

Table 6. Goodness-of-fit statistics for SSY_{EV} - storm metric relationships. Pearson and Spearman correlation coefficients significant at p<0.01.

Model	Pearson	Spearman	r ²	RMSE(tons)	Intercept(α)	Slope(β)
Psum_upper	-	0.70	0.39	4.31	0.003	1.10
Psum_total	0.84	0.88	0.71	2.43	0.033	1.11
EI_upper	0.42	0.48	0.18	5.48	0.001	0.97
EI_total	0.74	0.73	0.55	2.98	0.001	1.32
Qsum_upper	0.91	0.91	0.83	2.15	0.000	1.65
Qsum_total	0.84	0.83	0.70	2.46	0.000	1.29
Qmax_upper	0.89	0.90	0.79	2.36	0.398	1.51
Qmax_total	0.82	0.80	0.67	2.59	2.429	1.41

Table 7. Estimates of Annual SSY and sSSY calculated using four different methods

	Psum model, Events in 2014	Qmax model, Events in 2014	Events in Table 2	Events in Table 4	Equation 5 All Measured Events
Precipitation					
mm (% of Ps _{ann})	2770	2770	1004 (36%)	299 (11%)	3457 (125%)
Annual SSY (tons/year)					
UPPER	13	61	50	120	41
LOWER	121	378	310	300	388
LOWER_QUARRY	-	-	-	150	-
LOWER_VILLAGE	-	-	-	150	-
TOTAL	134	439	360	420	428
Annual sSSY (tons/km²/year)					
UPPER	14	68	50	140	45
LOWER	488	430	350	340	441
LOWER_QUARRY	-	-	-	560	-
LOWER_VILLAGE	-	-	-	250	-
TOTAL	75	247	200	240	241

Table

[Click here to download Table: Table8_Lit_values_for_SSY.pdf](#)

Table 8. Annual Specific Suspended Sediment Yield (sSSY) from steep, volcanic islands in the tropical Pacific.

Location	Watershed drainage area (km ²)	Mean annual precipitation (mm)	sSSY range tons/km ² /yr	Reference
Faga'alu UPPER	0.88		45-68	This study
Faga'alu TOTAL	1.78	2,380-6,350 (varies with elevation)	241-247	This study
Kawela, Molokai	13.5	500-3,000 (varies with elevation)	394	(Stock and Tribble, 2010)
Hanalei, Kauai	60.04	500 - 9,500 (varies with elevation)	545 ± 128	(Ferrier et al., 2013)
Hanalei, Kauai	48.4	2,000-11,000 (varies with elevation)	525	(Stock and Tribble, 2010)
Hanalei, Kauai	54.4	2,000-11,000 (varies with elevation)	140±55	(Calhoun and Fletcher, 1999)
St. John, USVI ^a	3.5	1,300-1,400	18	(Ramos-Scharrón and Macdonald, 2007)
St. John, USVI	2.3	1,300-1,400	24	(Nemeth and Nowlis, 2001)
St. John, USVI	6	1,300-1,400	36	(Nemeth and Nowlis, 2001)
Oahu	10.4	1,000-3,800 (varies with elevation)	330±130; 200±100 (varies with method)	(Hill et al., 1997)
Barro Colorado, Panama	0.033	2,623±458	100-200	(Zimmermann et al., 2012)
Fly River, PNG ^b	76,000	up to 10,000	1,000-1,500	(Milliman, 1995)
Purari River, PNG	35,000		3,000	"

Milliman and Syvitski (1992) Model:

$$sSSY = cA^f$$

(Milliman and Syvitski, 1992)

<i>c,f = regression coeff. for region/max elevation</i>		<i>c</i>	<i>f</i>	sSSY tons/km²/yr
Max elev >3,000m	Faga'alu UPPER = 0.88 TOTAL = 1.78	280	-0.54	UPPER = 296 TOTAL = 205
Max elev 1000-3000m (Oceania)		65	-0.46	UPPER = 68 TOTAL = 50
Max elev 500-1,000m		12	-0.59	UPPER = 13 TOTAL = 9